

**EFFECTS OF NANOPARTICLE AGGREGATION,
PARTICLE SIZE AND TEMPERATURE OF NANOFLUIDS
USING MOLECULAR DYNAMICS SIMULATION**

LEE SOON LI

**FACULTY OF ENGINEERING
UNIVERSITY OF MALAYA
KUALA LUMPUR**

2016

**EFFECTS OF NANOPARTICLE AGGREGATION,
PARTICLE SIZE AND TEMPERATURE OF
NANOFLUIDS USING MOLECULAR DYNAMICS
SIMULATION**

LEE SOON LI

**THESIS SUBMITTED IN FULFILMENT OF THE
REQUIREMENTS FOR THE DEGREE OF DOCTOR OF
PHILOSOPHY**

**FACULTY OF ENGINEERING
UNIVERSITY OF MALAYA
KUALA LUMPUR**

2016

UNIVERSITY OF MALAYA
ORIGINAL LITERARY WORK DECLARATION

Name of Candidate: Lee Soon Li

Registration/Matric No: KHA110014

Name of Degree: PhD Engineering

Title of Project Paper/Research Report/Dissertation/Thesis (“this Work”): EFFECTS OF NANOPARTICLE AGGREGATION, PARTICLE SIZE AND TEMPERATURE OF NANOFLUIDS USING MOLECULAR DYNAMICS SIMULATION

Field of Study: Heat transfer

I do solemnly and sincerely declare that:

- (1) I am the sole author/writer of this Work;
- (2) This Work is original;
- (3) Any use of any work in which copyright exists was done by way of fair dealing and for permitted purposes and any excerpt or extract from, or reference to or reproduction of any copyright work has been disclosed expressly and sufficiently and the title of the Work and its authorship have been acknowledged in this Work;
- (4) I do not have any actual knowledge nor do I ought reasonably to know that the making of this work constitutes an infringement of any copyright work;
- (5) I hereby assign all and every rights in the copyright to this Work to the University of Malaya (“UM”), who henceforth shall be owner of the copyright in this Work and that any reproduction or use in any form or by any means whatsoever is prohibited without the written consent of UM having been first had and obtained;
- (6) I am fully aware that if in the course of making this Work I have infringed any copyright whether intentionally or otherwise, I may be subject to legal action or any other action as may be determined by UM.

Candidate’s Signature

Date:

Subscribed and solemnly declared before,

Witness’s Signature

Date:

Name:

Designation:

ABSTRACT

Nanofluids have emerged as potential alternative for next generation of heat transfer fluids by suspending 1-100nm sized nanoparticles into conventional heat transfer fluids to enhance its inherent poor thermal conductivity. Consequently, the main concern of this novel exploitation is based on the fact that there is no established physical fundamental to explain the observed enhanced thermal conductivity and there are controversial laboratories results reported. To make matters worse, the enhanced thermal conductivity in nanofluids is always accompanied by an increase in viscosity. In order to fill the research gap, the objective of this thesis is to study potential mechanisms in enhancing thermal transport of nanofluids, namely Brownian motion of nanoparticles, Brownian motion induced micro-convection in base fluids and effects of nanoparticle aggregation. Apart from this, efficiency of nanofluids (ratio of thermal conductivity and viscosity enhancement) against particle size and temperature effects was also investigated. Several reasons that contributed to the conflicting reported data on thermal conductivity and viscosity include the poor characterisation on nanofluids especially sample polydispersity and difficult-to-measure hydrodynamic particle size distribution. For that reason, molecular dynamics simulation using Green Kubo method was employed in this research to perform an ideal experiment with controlled dispersity of copper-argon nanofluids. The roles of Brownian motion of nanoparticles and its induced micro-convection in base fluid were determined by studying the effects of particle size on the thermal conductivity and diffusion coefficient. Results showed that the Brownian motion and induced micro-convection had insignificant effects to enhance thermal conductivity. Based on microscopic analysis, the hydrodynamic effect was restricted by amorphous-like interfacial fluid structure at the vicinity of nanoparticle due to its higher specific surface area. Apart from this, nanoparticle aggregation was identified as the key mechanism in governing thermal conductivity enhancement. It was

observed that the thermal conductivity enhancement of aggregated nanofluids is higher compared to non-aggregated nanofluids by up to 35%. Based on the decomposition of thermal conductivity that is divided into three modes, namely collision, potential and kinetic; the greater enhancement in aggregated nanofluids was attributed to both higher collision amongst particles and increase in potential energy of nanoparticles to allow effective heat conduction along the backbone of aggregation. Consequently, based on the examination on thermal conductivity and viscosity enhancement, the efficiency of nanofluids was improved by increasing particle size and temperature. The thermal conductivity enhancement increases with increasing particle size but independent of temperature; whereas the viscosity enhancement decreases with increasing particle size and temperature. The particle size variation was therefore shown to be more effective than temperature control.

ABSTRAK

Bendalir nano muncul sebagai bendalir pemindah haba yang berpotensi untuk menggantikan bendalir pemindah haba konvensional. Bendalir-nano terdiri daripada partikel nano dengan saiz 1-100nm yang terampai di dalam bendalir pemindah haba konvensional untuk meningkatkan konduktiviti habanya. Walau bagaimanapun, kebimbangan utama untuk eksploitasi yang murni ini ialah ketiadaan asas fizik yang dapat menerangkan peningkatan konduktiviti haba ini. Tambahan pula terdapat keputusan makmal yang kontroversial dilaporkan mengenai perkara ini. Eksploitasi bendalir nano ini walau bagaimanapun terjejas apabila peningkatan konduktiviti haba sentiasa diiringi oleh peningkatan kelikatan. Dalam usaha untuk mengisi jurang penyelidikan, tesis ini menetapkan objektif untuk mengkaji mekanisme yang berpotensi untuk meningkatkan konduktiviti haba di dalam bendalir nano, iaitu gerakan Brownian dalam partikel nano, perolakan mikro dalam bendalir yang dipengaruhi oleh gerakan Brownian dalam partikel nano dan kesan agregat oleh partikel nano. Selain itu, kesan saiz partikel dan suhu terhadap kecekapan bendalir nano (nisbah peningkatan konduktiviti haba dan peningkatan kelikatan) juga dikaji. Salah satu punca utama yang menyebabkan konflik dalam data konduktiviti dan kelikatan bendalir nano yang dilaporkan adalah kesulitan dalam pencirian bendalir nano terutamanya poli-penyerakan di dalam sampel dan taburan hidrodinamik saiz untuk partikel nano. Oleh sebab itu, simulasi dinamika molekul dengan kaedah Green Kubo telah digunakan dalam tesis ini untuk menjalankan eksperimen dengan penyerakan partikel nano yang terkawal di dalam bendalir nano. Di dalam simulasi ini, bendalir nano yang dikaji terdiri daripada bendalir argon dan penyerakan partikel nano kuprum. Peranan gerakan Brownian dan perolakan mikro di dalam bendalir nano ditentukan dengan mengkaji kesan saiz partikel nano terhadap konduktiviti haba dan pekali resapan. Hasil kajian ini menunjukkan bahawa gerakan Brownian dan perolakan mikro yang dipengaruhi oleh gerakan

Brownian tidak menghasilkan kesan yang ketara untuk meningkatkan kekonduksian haba di dalam bendalir nano. Berdasarkan analisis mikroskopik, kesan hidrodinamik yang dipengaruhi oleh gerakan Brownian dihadkan oleh struktur cecair yang menyerupai amorfus di permukaan partikel nano yang mempunyai luas permukaan tentu yang lebih tinggi. Selain itu, peranan agregat partikel nano dikenalpasti sebagai mekanisme yang penting untuk meningkatkan kekonduksian haba di dalam bendalir nano. Simulasi ini menunjukkan bahawa konduktiviti haba oleh bendalir nano dalam keadaan agregat adalah lebih tinggi berbanding keadaan tak agregat sebanyak 35%. Untuk analisis yang lebih mendalam, konduktiviti haba dalam bendalir nano dipecahkan kepada tiga komponen iaitu perlanggaran antara partikel, tenaga keupayaan dan tenaga kinetik partikel. Ini membuktikan bahawa peningkatan kekonduksian haba yang lebih tinggi di dalam bendalir nano agregat adalah disebabkan oleh dua komponen iaitu perlanggaran yang lebih kerap di antara partikel dan peningkatan tenaga keupayaan pada partikel nano untuk membolehkan pemindahan haba yang berkesan di sepanjang tulang belakang agregat. Akhirnya, berdasarkan pemeriksaan ke atas peningkatan konduktiviti haba dan kelikatan, kecekapan bendalir nano dapat diperbaiki dengan pertambahan saiz partikel nano dan suhu. Peningkatan konduktiviti haba adalah berkadar terus dengan pertambahan saiz partikel nano tetapi tidak dipengaruhi oleh suhu, manakala peningkatan kelikatan berkurangan dengan pertambahan saiz partikel nano dan suhu. Oleh itu, manipulasi saiz partikel nano adalah lebih berkesan daripada kawalan suhu.

ACKNOWLEDGEMENTS

First and foremost, I would like to express my appreciation to my supervisor, Associate Professor Dr. Mohd Faizul Mohd Sabri and ex-supervisor, Professor Dr. Saidur Rahman (now in King Fahd University of Petroleum & Minerals, KFUPM) for their enthusiastic and insightful guidance throughout my postgraduate life in University of Malaya. I am very thankful for the confidence and constant encouragement they have showed in me. I feel extremely fortunate to have them as my mentors in this research.

I would also like to thank the Ministry of Higher Education (MoHE) for the financial support. My graduate study was under MyBrain15, MyPhD scheme whereas the works of this research were supported by UM-MoHE High Impact Research Grant Scheme (HIRG) (Project No.: UM.C/625/1/HIR/MOHE/ENG/29 and UM.C/HIR/MOHE/ENG/40).

I would like to express my gratitude to Dr. Yoon Tiem Leong and Mr. Min Tjun Kit from Universiti Sains Malaysia (USM) for providing me insightful ideas and resources in using the LAMMPS molecular dynamics simulator. This research was conducted in the USM School of Physics using computer clusters in the computer lab.

I have benefited greatly from my interactions with my senior, Dr. Leong Kin Yuen. I will always cherish the stimulating discussions with him on this research. Thank you for sharing knowledge and experiences as they have greatly improved my work.

I would like to convey my heartiest gratitude to my family for their love, prayers and caring. I am grateful to my husband, Sam, for always encouraging me when I am ready to give up. Also, I am thankful to Xiao Xiong for her companion that keeps me going.

Last but not least, I would like to thank God for giving power to believe in my passion and pursue my dreams.

TABLE OF CONTENTS

Abstract	iii
Abstrak	v
Acknowledgements	vii
Table of Contents	viii
List of Figures	xii
List of Tables.....	xvi
List of Symbols and Abbreviations.....	xvii
List of Appendices	xxi
CHAPTER 1: INTRODUCTION.....	1
1.1 Nanofluids.....	1
1.2 Problem Statement.....	3
1.3 Statement of Objectives.....	7
1.4 Scope of the Thesis.....	8
1.5 Outline of the Thesis.....	9
CHAPTER 2: LITERATURE REVIEW.....	10
2.1 Thermal Conductivity in Nanofluids	10
2.1.1 Particle Size Dependence on Thermal Conductivity.....	15
2.1.2 Temperature Dependence on Thermal Conductivity	17
2.2 Potential Mechanisms of Thermal Conductivity Enhancement	20
2.2.1 Brownian Motion of Nanoparticles	20
2.2.2 Brownian Motion Induced Micro-convection.....	23
2.2.3 Effects of Nanoparticle Aggregation.....	25
2.3 Viscosity in Nanofluids	30

2.3.1	Particle Size Dependence on Viscosity	32
2.3.2	Temperature Dependence on Viscosity.....	36
2.4	Efficiency of Nanofluids.....	39
2.5	Applications of Nanofluids.....	39
2.5.1	Transportation	40
2.5.2	Electronics Cooling	41
2.5.3	Nuclear Reactor Application	42
2.5.4	Other Applications	43
2.6	Summary.....	43
 CHAPTER 3: METHODOLOGY		45
3.1	Molecular Dynamics Simulation	45
3.2	Methodology of Equilibrium Molecular Dynamics Simulation.....	47
3.2.1	Geometry Setup.....	49
3.2.2	Inter-atomic Potential Definition.....	53
3.2.3	Energy Minimisation	54
3.2.4	Velocity Initialisation	55
3.2.5	Equilibration.....	56
3.2.6	Data Production	57
	3.2.6.1 Transport Properties	57
	3.2.6.2 Structural Property	60
3.3	Validation	60
3.3.1	Validation on Simulation Method and Employed Potential.....	60
3.3.2	Validation on Equilibrium State.....	62
3.3.3	Validation on Data Collection – Thermal Conductivity	66
3.3.4	Validation on Data Collection – Shear Viscosity.....	67
3.4	Summary.....	71

CHAPTER 4: RESULTS AND DISCUSSIONS	72
4.1 Effects of Brownian Motion and Induced Micro-Convection in Thermal Conductivity of Nanofluids	72
4.1.1 Design of Model	72
4.1.2 Investigation on Brownian Motion of Nanoparticle.....	73
4.1.3 Investigation on Brownian Motion Induced Micro-convection	74
4.1.4 Microscopic Analysis on Brownian Motion and Induced Micro-convection	76
4.1.5 Summary	82
4.2 Effects of Nanoparticle Aggregation in Thermal Conductivity of Nanofluids	83
4.2.1 Design of Model	83
4.2.2 Calculation of Thermal Conductivity	85
4.2.3 Decomposition of Thermal Conductivity	88
4.2.4 Summary	93
4.3 Effects of Particle Size and Temperature on Efficiency of Nanofluids	95
4.3.1 Design of Model	95
4.3.2 Effect of Particle Size on Thermal Conductivity	96
4.3.3 Effect of Temperature on Thermal Conductivity	98
4.3.4 Effect of Particle Size on Viscosity	100
4.3.5 Effect of Temperature on Viscosity	102
4.3.6 Cooling Efficiency of Nanofluids	104
4.3.7 Summary	108
 CHAPTER 5: CONCLUSIONS.....	 110
5.1 Conclusions	110
5.2 Recommendations.....	115
References	116

List of Publications and Papers Presented	134
Appendix A: lammgs input code-properties calculation.....	138
Appendix B: lammgs input code-enthalpy calculation	142

University of Malaya

LIST OF FIGURES

Figure 2.1: Thermal conductivity of oil is enhanced up to 157% at about 1 vol% carbon nanotubes. Measured data are greater than classical prediction where line A = Hamilton Crosser, line B=Bonnecaze and Brady and line C = Maxwell model (Choi et al., 2001).	12
Figure 2.2: For 0.5 vol% Al ₇₀ Cu ₃₀ -ethylene glycol nanofluids, thermal conductivity enhancement decreases with increasing particle size (Chopkar et al., 2006).	16
Figure 2.3: For Al ₂ O ₃ -water nanofluids, thermal conductivity enhancement increases with the increase of particle size below 50nm (Beck et al., 2009).....	17
Figure 2.4: For Al ₂ O ₃ -water nanofluids, thermal conductivity enhancement increases with increasing temperature (Das et al., 2003).	18
Figure 2.5: For suspension of 40nm Al ₂ O ₃ in water and ethylene glycol based nanofluids, thermal conductivity enhancement is independent with temperature (Timofeeva et al., 2007).	19
Figure 2.6: Three potential mechanisms in enhancing thermal conductivity in nanofluids.....	21
Figure 2.7: TEM photograph in nanofluids. (a) Cu-ethylene glycol nanofluids (Eastman et al., 2001); (b) TiO ₂ -deionized water nanofluids (Murshed et al., 2005).....	26
Figure 2.8: Aggregated nanoparticles consist of backbone and dead end particles (Pang et al., 2014).....	26
Figure 2.9: TEM photograph in Al ₂ O ₃ nanofluids (Gao et al., 2009). (a) Animal oil based nanofluids before freezing; (b) animal oil based nanofluids after freezing; (c) hexadecane based nanofluids before freezing; (d) hexadecane based nanofluids after freezing.....	28
Figure 2.10: For suspension of Al ₂ O ₃ -water nanofluids, viscosity enhancement increases with increasing particle volume fraction and particle size (Nguyen et al., 2007).....	32
Figure 2.11: For SiC-water nanofluids, viscosity increases with decrease in particle size (Timofeeva et al., 2010).	36
Figure 2.12: For CuO-ethylene glycol/water nanofluids, viscosity enhancement decreases with increasing temperature (Namburu et al., 2007).	38
Figure 2.13: For TiO ₂ -ethylene glycol nanofluids, the temperature dependence trend in viscosity of nanofluids simply tracks the trend of that base fluid (Chen et al., 2007b)..	38

Figure 3.1: Working principle of MD.	46
Figure 3.2: Flowchart of MD simulation integrated with Green Kubo method.....	48
Figure 3.3: Periodic boundary condition (PBC), the simulation box of interest (marked as yellow) is surrounded identical images of itself.	49
Figure 3.4: Snapshot of four different nanofluids systems.	52
Figure 3.5: Lennard Jones potential for Ar-Ar, Cu-Cu and Ar-Cu interactions.	54
Figure 3.6: Velocity Verlet algorithm (Allen & Tildesley, 1987).	57
Figure 3.7: Validation on methodology and employed inter-atomic potential for structural property of pure liquid argon, RDF comparison against experimental data. ..	61
Figure 3.8: Temperature during equilibration process for system #1- 2.24 vol% nanofluids with single nanoparticle in well-dispersed state.....	62
Figure 3.9: Temperature during equilibration process for system #2- nanofluids with multi-nanoparticle in well-dispersed state, with particle diameter of 15 Å.	63
Figure 3.10: Temperature during equilibration process for system #3- nanofluids with multi-nanoparticle in well-dispersed state, with particle diameter of 20 Å.	63
Figure 3.11: Temperature during equilibration process for system #4- nanofluids with multi-nanoparticle in aggregated state, with particle diameter of 20 Å.....	64
Figure 3.12: Total energy in system during equilibration process for system #1- 2.24 vol% nanofluids with single nanoparticle in well-dispersed state.	64
Figure 3.13: Total energy in system during equilibration process for system #2- nanofluids with multi-nanoparticle in well-dispersed state, with particle diameter of 15 Å.....	65
Figure 3.14: Total energy in system during equilibration process for system #3- nanofluids with multi-nanoparticle in well-dispersed state, with particle diameter of 20 Å.....	65
Figure 3.15: Total energy in system during equilibration process for system #4- nanofluids with multi-nanoparticle in aggregated state, with particle diameter of 20 Å.	66
Figure 3.16: HCACF for thermal conductivity calculation, system #1- 2.24 vol% nanofluids with single nanoparticle in well-dispersed state.....	68

Figure 3.17: HCACF for thermal conductivity calculation, system #2- nanofluids with multi-nanoparticle in well-dispersed state, with particle diameter of 15 Å.	68
Figure 3.18: HCACF for thermal conductivity calculation, system #3- nanofluids with multi-nanoparticle in well-dispersed state, with particle diameter of 20 Å.	69
Figure 3.19: HCACF for thermal conductivity calculation, system #4- nanofluids with multi-nanoparticle in aggregated state, with particle diameter of 20 Å.	69
Figure 3.20: SACF for shear viscosity calculation, system #2- nanofluids with multi-nanoparticle in well-dispersed state, with particle diameter of 15 Å.	70
Figure 3.21: SACF for shear viscosity calculation, system #3- nanofluids with multi-nanoparticle in well-dispersed state, with particle diameter of 20 Å.	70
Figure 4.1: Relative thermal conductivity of 2.24 vol% nanofluids with respect to particle diameter varied from 16 Å to 36 Å at 86 K, comparing with prediction by Maxwell model.	73
Figure 4.2: MSD of liquid atoms in nanofluids as a function of diffusing time.	75
Figure 4.3: Diffusion coefficient of liquid in nanofluids as a function of particle diameter.	75
Figure 4.4: Relative diffusion coefficient of liquid in nanofluids with respect to particle diameter, comparing with prediction by excluded volume model.	77
Figure 4.5: RDF of liquid structure for interaction between liquid-liquid in 2.24 vol% nanofluids as a function of radial distant from reference atom.	79
Figure 4.6: RDF of liquid structure for interaction between solid-liquid in 2.24 vol% nanofluids as a function of radial distant from reference atom.	79
Figure 4.7: VACF of solid atom in 2.24 vol% nanofluids with particle diameter from 16 Å to 36 Å at 86 K.	81
Figure 4.8: Thermal conductivity of non-aggregated and aggregated nanofluids as a function of particle volume fraction, comparing with prediction by Maxwell model. ...	86
Figure 4.9: Comparison of thermal conductivity enhancement of nanofluids in aggregated and non-aggregated states with HS mean field theory.	86
Figure 4.10: HS mean field theory: (a) lower bound corresponds to well-dispersed nanoparticles; (b) upper bound corresponds to large pockets of fluid separated by chain formation or aggregated nanoparticles.	87

Figure 4.11: Thermal conductivity of nanofluids as a function of particle volume fraction. (a) Total thermal conductivity contributed by collision and convective correlations; (b) thermal conductivity contributed by collision correlation; (c) thermal conductivity contributed by convective correlation.	89
Figure 4.12: Decomposition of convective correlation into kinetic energy in aggregated and non-aggregated states as a function of particle volume fraction. (a) Average kinetic energy of Cu; (b) average kinetic energy of Ar.	91
Figure 4.13: Decomposition of convective correlation into potential energy in aggregated and non-aggregated states as a function of particle volume fraction. (a) Average potential energy of Cu; (b) average potential energy of Ar.....	92
Figure 4.14: Relative thermal conductivity as a function of particle volume fraction for nanofluids with particle diameter of 15 Å and 20 Å at temperature 86 K, comparing with prediction by Maxwell model.	97
Figure 4.15: RDF for bulk liquid and 7.65-7.77 vol% nanofluids with particle diameter of 15 Å and 20 Å as a function of radial distant from reference atom.....	98
Figure 4.16: (a) Thermal conductivity and (b) relative thermal conductivity as a function of temperature for nanofluids with particle diameter of 20 Å.	99
Figure 4.17: Relative viscosity as a function of particle volume fraction for nanofluids with particle diameter of 15 Å and 20 Å at temperature 86 K, comparing with prediction by Einstein model and Batchelor model.	101
Figure 4.18: (a) Viscosity and (b) relative viscosity as a function of temperature for nanofluids with particle diameter of 20 Å.....	103
Figure 4.19: Relative thermal conductivity and viscosity as a function of particle volume fraction for (a) nanofluids with particle diameter of 15 Å and (b) nanofluids with particle diameter of 20 Å.	104
Figure 4.20: C_{η}/C_k as a function of particle size and particle volume fraction for nanofluids at 86 K.	105
Figure 4.21: Relative thermal conductivity and viscosity as a function of temperature for (a) 2.59 vol% nanofluids and (b) 7.77 vol% nanofluids with particle diameter of 20 Å.	106
Figure 4.22: C_{η}/C_k as a function of temperature and particle volume fraction for nanofluids with particle diameter of 20 Å.....	107

LIST OF TABLES

Table 1.1: Room-temperature thermal conductivity for solids and liquids (Eastman, Phillpot, Choi, & Keblinski, 2004).	2
Table 2.1: Experimental works on studying thermal conductivity enhancement of nanofluids with respect to particle volume fraction.	13
Table 2.2: Experimental works on studying viscosity enhancement of nanofluids with respect to particle volume fraction (Mahbubul, Saidur, & Amalina, 2012).	33
Table 3.1: Four different nanofluids systems were modelled.	50
Table 3.2: System #1- Nanofluids with single nanoparticle in well-dispersed state.	51
Table 3.3: System #2- Nanofluids with multi-nanoparticle in well-dispersed state, with particle diameter of 15 Å.	51
Table 3.4: System #3 & #4- Nanofluids with multi-nanoparticle in well-dispersed and aggregated state, with particle diameter of 20 Å.	51
Table 3.5: L-J potential parameters for copper-argon nanofluids.	54
Table 3.6: Validation on methodology and employed potential for transport properties of pure liquid argon.	61
Table 4.1: Analysis on Brownian motion and its induced micro-convection effects.	81
Table 4.2: Configurations of aggregated and non-aggregated nanofluids.	84
Table 4.3: Summary on decomposition of thermal conductivity of nanofluids.	93
Table 4.4: Effects of particle size and temperature on thermal conductivity enhancement, viscosity enhancement and efficiency of nanofluids.	107

LIST OF SYMBOLS AND ABBREVIATIONS

SYMBOLS

a	: acceleration (m/s^2)
C	: enhancement coefficient
d	: particle diameter (m)
D	: diffusion coefficient (m^2/s)
E	: per atom energy for kinetic and potential (J)
F	: force (N)
$g(r)$: radial distribution function
h	: average partial enthalpy (J)
J	: heat current ($\text{J}\cdot\text{m}/\text{s}$)
k	: thermal conductivity ($\text{W}/\text{m}\cdot\text{K}$)
k_B	: Boltzmann constant, 1.38×10^{-23} J/K
m	: mass (kg)
n	: empirical shape factor
N	: total number of particles
P	: stress tensor (N/m^2)
r	: displacement (m)
U	: interatomic potential (J)
t	: time (s)
T	: temperature (K)
v	: velocity (m/s)
V	: volume (m^3)
ψ	: sphericity
Φ	: L-J potential (J)

ε	: interaction strength (J)
σ	: interatomic length scale (m)
η	: shear viscosity (Pa.s)
ϕ	: nanoparticles volume fraction (vol%)
ρ	: mean number density (m^{-3})

ABBREVIATIONS

BD	: Brownian dynamics
BET	: Brunauer-Emmett-Teller
CFD	: computational fluid dynamics
CHF	: critical heat flux
CNT	: carbon nanotubes
DIW	: deionised water
DW	: distilled water
EAM	: embedded atom potential
EG	: ethylene glycol
EMD	: equilibrium molecular dynamics
FCC	: face-centered cubic
HC	: Hamilton & Crosser
HCACF	: heat current autocorrelation function
HS	: Hashin-Shtrikman
IVR	: in-vessel retention
LAMMPS	: Large-scale Atomic/Molecular Massively Parallel Simulator
LB	: Lorentz Berthelot
L-J	: Lennard-Jones
MD	: molecular dynamics
MSD	: mean square displacement

NEMD	: non-equilibrium molecular dynamics
NVE	: micro-canonical ensemble
NVT	: canonical ensemble
PBC	: periodic boundary condition
PWR	: pressurized water reactor
PG	: propylene glycol
RDF	: radial distribution function
SACF	: stress autocorrelation function
SAXS	: small-angle X-ray scattering
TNT	: titanate nanotubes
TEM	: transmission electron microscope
VACF	: velocity autocorrelation function
VMD	: Visual Molecular Dynamics
XRD	: X-ray diffraction

SUBSCRIPTS

ar	: argon
B	: Brownian
cu	: copper
f	: base fluid
i	: particle i
j	: particle j
k	: thermal conductivity
nf	: nanofluid
p	: nanoparticle
x	: x axis
y	: y axis

z : z axis
 α : species α
 η : shear viscosity

SUPERSCRIPTS

o : initial

University of Malaya

LIST OF APPENDICES

Appendix A: lammgs input code-properties calculation.....	138
Appendix B: lammgs input code-enthalpy calculation.....	142

University of Malaya

CHAPTER 1: INTRODUCTION

Cooling is a major technical challenge in many industries especially micro-electronics, transportation, manufacturing and nuclear reactor applications. In order to achieve better cooling performance, one of the conventional methods is to extend heat transfer area of the heat exchanger such as fins and micro-channel. However, the extended area has led to undesired increase in size and weight of the heat exchanger, which is against the trend of product miniaturisation. Consequently, in the attempts of improving cooling performance, researchers shift their focus on heat transfer properties of the heat transfer fluid. Water, ethylene glycol and engine oil are common heat transfer fluids used in many diverse industries. From Table 1.1, it can be seen that water possesses the highest thermal conductivity amongst those heat transfer fluids. However, it is only two to three orders of magnitude lower than metals and metal oxides. It is therefore proposed that a potential heat transfer fluid produced by dispersing nanometer size solid particles into liquid to elevate its inherent poor thermal conductivity, namely nanofluids be explored. The exploitation of nanofluids with enhanced thermal conductivity requires understanding the properties at the fundamental level. This thesis addresses the thermal transport of nanofluids at nanoscale level. This chapter presents an introduction to nanofluids and states the problem statement of the recent research. Towards the end of this chapter, the objectives of this thesis are spelt out and the scope of this research is highlighted.

1.1 Nanofluids

Nanofluids are engineered by suspending solid nanoparticles or nanofibers with size of 1-100nm into conventional heat transfer fluids (Choi, 1995). The idea of increasing thermal conductivity of liquid by dispersing small solid particles was first presented by Maxwell (1954) more than a century ago. Initially, the idea was intended for electrical

conductivity and later extended to thermal conductivity. This process starts by suspension of millimeter or micrometer size particles in liquids but it causes several problems such as clogging, erosion to the heat exchanger and sedimentation despite the improved thermal conductivity. On the other hand, nanofluids, in which the nanoparticles suspension behaves like molecules of liquid, have successfully avoid the above-mentioned problems while at the same time improve thermal conductivity. In addition, nanofluids have better stability because of the larger surface-area-to-volume ratio of nanoparticles which overcome differences in density. Therefore, the exploitation of nanofluids opens up the possibilities to improve the efficiency of thermal system while maintaining the existing footprint. Alternatively nanofluids can provide the same efficiency of the cooling system at smaller and lighter footprint as reduced inventory of heat transfer fluids. Eventually, improved cooling performance and lower manufacturing or operating cost in thermal system are the major advantage derived from the application of nanofluids.

Table 1.1: Room-temperature thermal conductivity for solids and liquids (Eastman, Phillpot, Choi, & Koblinski, 2004).

Material		Thermal conductivity at room temperature (W/m.K)
Metallic solids	Silver	429
	Copper	401
	Aluminium	237
Nonmetallic solids	Diamond	3300
	Carbon nanotubes	3000
	Silicon	148
	Alumina (Al ₂ O ₃)	40
Metallic liquids	Sodium at 644K	72.3
Nonmetallic liquids	Water	0.613
	Ethylene glycol	0.253
	Engine oil	0.145

Owing to this stimulating benefits, a large number of research in the scientific community are being carried out with the goal of realising various applications of nanofluids. Initial research focused mainly on thermal conductivity, only recently that subsequently researchers delved into other area of interest such as viscosity, specific heat, density, critical heat flux, heat transfer coefficient, entropy and wear resistance. In existing experimental works, nanofluids can be produced by two methods, namely the two-step process and the one-step process. In a typical two-step process, the nanoparticles are first produced in dry powder form and then mixed with the heat transfer fluids. However, these nanofluids are not stable even though the stability could be enhanced by pH control and surfactant addition. In the one-step process, the synthesis and dispersion of nanoparticles are done at the same time. These nanofluids have better stability due to the weakened Van der Waals force between nanoparticles. Nevertheless, the two-step process is always preferred by the majority of researchers owing to its low setup cost.

1.2 Problem Statement

The applications of nanofluids appear promising in heat transfer industry but the development of this field is hindered by:

- (a) Thermal conductivity enhancement cannot be explained by classical theories
- (b) Lack of agreement between results obtained in different laboratories
- (c) Thermal conductivity enhancement is always accompanied by higher viscosity

Thermal conductivity enhancement cannot be explained by classical theories. There are reports on thermal conductivity enhancement of nanofluids that increases with particle volume fraction but it does not conform to the prediction of classical medium theories such as Maxwell (1954) and Hamilton and Crosser (1962). In the majority of studies, classical medium theories have underestimated the enhancement in nanofluids

(Choi, Zhang, Yu, Lockwood, & Grulke, 2001; Chopkar, Das, & Manna, 2006; Chopkar, Kumar, Bhandari, Das, & Manna, 2007; Eastman, Choi, Li, Yu, & Thompson, 2001). Furthermore, literatures show that the thermal conductivity enhancement is not confined to particle volume fraction and particle shape only as suggested by classical medium theories, but also depends on other parameters such as temperature (Chon, Kihm, Lee, & Choi, 2005; Das, Putra, Thiesen, & Roetzel, 2003; Esfe et al., 2015; Kole & Dey, 2013; Lee, Lee, & Jang, 2014; Li & Peterson, 2006; Mehrali et al., 2014; Mintsu, Roy, Nguyen, & Doucet, 2009; Murshed, Leong, & Yang, 2008; Patel et al., 2003; Sundar, Ramana, Singh, & Sousa, 2014; Wen & Ding, 2004), particle size (Angayarkanni, Sunny, & Philip, 2015; Beck, Yuan, Warriar, & Teja, 2009; Chen, Yu, Singh, Cookson, & Routbort, 2008a; Chon et al., 2005; Chopkar et al., 2006; Chopkar et al., 2007; He et al., 2007; Kim, Choi, & Kim, 2007; Lee et al., 2014; Lee, Choi, Li, & Eastman, 1999; Mintsu et al., 2009; Teng, Hung, Teng, Mo, & Hsu, 2010; Timofeeva et al., 2010; Warriar & Teja, 2011), pH (Lee, Kim, & Kim, 2006) and type of base fluid (Timofeeva, Yu, France, Singh, & Routbort, 2011a). Due to the inadequacy of the classical models, various potential mechanisms have been proposed to explain the enhanced thermal transport, for example Brownian motion of nanoparticles (Kebllinski, Phillpot, Choi, & Eastman, 2002; Kumar et al., 2004; Murshed, Leong, & Yang, 2009; Xuan, Li, & Hu, 2003), molecular liquid layering at solid-liquid interface (Kebllinski et al., 2002; Xie, Fujii, & Zhang, 2005; Xue, 2003), effects of nanoparticle aggregation (Evans et al., 2008; Feng, Yu, Xu, & Zou, 2007; Kebllinski et al., 2002; Pang, Jung, & Kang, 2014; Pang, Lee, & Kang, 2015; Prasher et al., 2006b; Prasher, Phelan, & Bhattacharya, 2006c; Xuan et al., 2003), micro-convection in base fluid induced by Brownian motion of nanoparticles (Jang & Choi, 2004, 2007; Koo & Kleinstreuer, 2004; Krishnamurthy, Bhattacharya, Phelan, & Prasher, 2006; Patel, Anoop, Sundararajan, & Das, 2006; Patel, Sundararajan, & Das, 2008; Prasher, Bhattacharya, &

Phelan, 2005, 2006a; Ren, Xie, & Cai, 2005; Xuan, Li, Zhang, & Fujii, 2006) and the nature of heat transport in nanoparticles (Kebllinski et al., 2002). However, to date, there is no consensus reached on the potential mechanisms in nanofluids.

Lack of agreement between results obtained in different laboratories. As mentioned above, classical medium models failed to account for the anomalously high thermal conductivity enhancement in nanofluids, but some experimental data show that the enhanced thermal conductivity are well described by the classical medium models (Chon et al., 2005; Das et al., 2003; Hwang et al., 2007; Lee et al., 1999; Timofeeva et al., 2007). A clear observation can be made that thermal conductivity enhancement of nanofluids increases with increasing particle volume fraction, but the magnitude of enhancement varies in different laboratories. Similar controversy result was also found in the thermal conductivity dependence on nanofluids parameters. For example, in the effects of particle size, thermal conductivity enhancement has shown increases with increasing particle size (Angayarkanni et al., 2015; Beck et al., 2009; Chen et al., 2008a; Timofeeva et al., 2010; Warriar & Teja, 2011; Yu, France, Routbort, & Choi, 2008) but it is also shown enhanced with decreasing particle size (Chon et al., 2005; Chopkar et al., 2006; Chopkar et al., 2007; He et al., 2007; Kim et al., 2007; Lee et al., 2014; Lee et al., 1999; Mintsu et al., 2009; Teng et al., 2010). It is the same for the effect of temperature where thermal conductivity enhancement is shown to increase with increasing temperature (Chon et al., 2005; Das et al., 2003; Esfe et al., 2015; Kole & Dey, 2013; Lee et al., 2014; Li & Peterson, 2006; Mehrali et al., 2014; Mintsu et al., 2009; Murshed et al., 2008; Patel et al., 2003; Sundar et al., 2014; Wen & Ding, 2004) but also found to be independent of temperature (Beck, Sun, & Teja, 2007; Beck, Yuan, Warriar, & Teja, 2010; Pastoriza-Gallego, Lugo, Legido, & Piñeiro, 2011b; Peñas, de Zárate, & Khayet, 2008; Singh et al., 2009; Timofeeva et al., 2007; Venerus, Kabadı, Lee, & Perez-Luna, 2006; Zhang, Gu, & Fujii, 2006b; Zhang, Gu, & Fujii, 2007). One

of the major causes of the conflicting data on thermal conductivity is the poor characterisation of nanofluids such as method of nanofluid preparation (two-step or one-step process), experimental conditions, measurement deviation, difficulties in producing mono-dispersed suspensions, accurate measurement on particle size, particle size distribution and formation of nanoparticle aggregation. The sample polydispersity and hydrodynamic particle size distribution in nanofluids are regarded as major concerns to correctly understand their novel properties. Different nanofluid preparation methods may produce variation in suspension stability and particle size distribution in the actual nanofluids. Furthermore, the average particle size was declared in the majority of experimental works relies on the primary particle size provided by manufacturers, but the exact particle size, particle size distribution and possible aggregation in suspension are always overlooked in the real sample.

Thermal conductivity enhancement is always accompanied by higher viscosity.

Literatures show that the enhancement in thermal conductivity in nanofluids is always accompanied by an increase in viscosity (Anoop, Sundararajan, & Das, 2009b; Chandrasekar, Suresh, & Chandra Bose, 2010; Chen, Ding, He, & Tan, 2007a; Chen, Ding, Lapkin, & Fan, 2009a; Chen, Ding, & Tan, 2007b; Chen, Witharana, Jin, Kim, & Ding, 2009b; Kole & Dey, 2010; Masuda, Ebata, Teramae, & Hishinuma, 1993; Nguyen et al., 2008; Nguyen et al., 2007; Pak & Cho, 1998). If the viscosity is too high, then large amount of electricity is needed to pump the nanofluids through the system, thus, the overall efficiency of the nanofluids is reduced owing to substantially high operating cost. Successful and practical applications of the nanofluids require the nanofluids to be produced with enhanced thermal conductivity without consuming too much pumping power. In view of this, the increase in thermal conductivity and viscosity should be investigated simultaneously in order to optimise the nanofluids' design with best combination of thermal conductivity and viscosity. However, research in this

aspect remains open as the majority of works are focused on thermal conductivity alone while less attention is given on viscosity.

1.3 Statement of Objectives

In general, three approaches have been used in conducting nanofluids research, namely experimental, analytical and numerical approaches. Although experimental works are increasing in number, they are still constrained by the high cost of nanofluids characterisation and also the difficulty to explore the enhanced thermal transport at nanoscale level. Due to insufficient understanding of the basic thermal transport mechanism, the analytical works carried out are seen as merely data fitting the experiments rather than looking for the fundamental understanding. It appears that the numerical method is the only approach to study well characterised nanofluids at low cost and explain the thermal transport mechanisms at atomic level. Molecular dynamics (MD) simulation is recommended as the only method to perform an ideal experiment with mono-dispersed nanofluids (Rudyak & Krasnolutskaa, 2014) and its flexibility allows the effect of parameters or potential mechanisms of nanofluids to be considered separately.

In order to fill the research gaps in the present nanofluids development, MD simulation integrated with Green Kubo method is used to study thermal transport of nanofluids in this thesis. The following three objectives are investigated by using MD simulation:

- (a) Effects of Brownian motion and its induced micro-convection in thermal conductivity of nanofluids
- (b) Effects of nanoparticle aggregation in thermal conductivity of nanofluids, and
- (c) Effects of particle size and temperature on the efficiency (ratio of thermal conductivity and viscosity enhancement) of nanofluids.

1.4 Scope of the Thesis

In this thesis, nanofluids are modelled by suspending copper nanoparticles in liquid argon. The selection of nanofluids materials should be based on the following criteria: accurate inter-atomic potential to provide insightful information and economical. Even though liquid argon is not a real base fluid for nanofluids, it is chosen in this thesis owing to its Lennard-Jones (L-J) potential that matches well with experimental data (Haile, 1992; Jones & Mandadapu, 2012; Sarkar & Selvam, 2007). Therefore, it is expected that using liquid argon in nanofluids should bring similar experimental success. Simulation on real nanofluids such as suspension of copper nanoparticles in water can definitely be conducted but water having a more complex structure with electrostatic charge can hinder physical interpretation of microscopic conduction modes as well as increase computing time sharply.

The inter-atomic potential of copper is described by the L-J potential. It has yielded similar result with embedded atom potential (EAM) (Yu & Amar, 2002). It is noted that the thermal conductivity of copper is not expected to be accurate because MD does not describe the roles of electron; it is only based on phonon contribution in thermal conduction. Results from previous experiments, where high thermal conductivity of nanoparticles does not necessarily produce higher thermal conductivity enhancement compared to low thermal conductivity of nanoparticles (Hong, Yang, & Choi, 2005; Zhu, Zhang, Liu, Tang, & Yin, 2006). In another words, the intrinsic thermal conductivity of the nanoparticles plays a minor role in the thermal conduction process. Therefore, the simple L-J potential is appropriate to describe the interaction of copper.

The primary focus of this thesis is to obtain qualitative results on the thermal conductivity and viscosity of nanofluids. For this reason, suspension of copper nanoparticles in liquid argon is a suitable choice.

1.5 Outline of the Thesis

So far, this chapter has given a general overview on nanofluids, problem statement regarding the present nanofluids development, statement of objectives and also the scope of the thesis. This thesis is presented based on the following outline:

Chapter 2 is a literature review on existing experimental, analytical and numerical works on nanofluids. Thermal conductivity, viscosity as well as three potential thermal conduction mechanisms in nanofluids, namely Brownian motion of nanoparticles, induced micro-convection in base fluids and nanoparticle aggregation are presented. Finally cooling efficiency and potential applications of nanofluids are also discussed in this chapter.

Chapter 3 explains the methodology of MD simulation in detail. A discussion of the modelling, inter-atomic potential, integration method, system equilibration, thermal transport and structural properties calculation are elaborated. Eventually, validations on the MD method, inter-atomic potential, equilibrium state and accuracy of thermal transport properties are presented.

Chapter 4 elaborates the results and discussions on the three research objectives. The data of thermal conductivity, viscosity, mean square displacement, radial distribution function and microscopic conduction modes of nanofluids are presented in pursuing the objectives. The results are critically analysed and compared with existing works and theories.

Chapter 5 provides a conclusion to the contents of this thesis. Apart of this, recommendations for future research work are also presented.

CHAPTER 2: LITERATURE REVIEW

This chapter aims to present a review of the existing experimental, analytical and numerical works related to nanofluids in order to provide a framework for this thesis. First, thermal conductivity of nanofluids are presented and the different potential thermal conduction mechanisms are discussed. Then, viscosity of nanofluids as well as cooling efficiency (ratio of thermal conductivity and viscosity enhancement) are described. An overview of the potential applications of nanofluids is given at the end of the chapter.

2.1 Thermal Conductivity in Nanofluids

The first experimental work on nanofluids was reported in Japan, where nanofluids were formed by suspending nanoparticles of Al_2O_3 , SiO_2 and TiO_2 in water (Masuda et al., 1993). They demonstrated that the thermal conductivity of water is enhanced up to 33% at 4.3 vol% Al_2O_3 nanoparticles. However, such enhancements are beyond the prediction of Maxwell's effective medium theory model, which is given by (Maxwell, 1954):

$$k_{nf} = \frac{k_p + 2k_f + 2\phi(k_p - k_f)}{(k_p + 2k_f) - \phi(k_p - k_f)} k_f \quad (2.1)$$

where k and ϕ are thermal conductivity and particle volume fraction, respectively. The subscripts nf , p and f , represent the nanofluid, nanoparticle and base fluid, respectively. In the Maxwell model, the particles are assumed to be in a stationary state and the heat is diffused through the effective medium of particles and fluid where faster heat conduction is created in the pathways of particle-liquid-particle. Hamilton & Crosser (HC) model extended the Maxwell model by taking into account the particle shape, giving the equation (Hamilton & Crosser, 1962):

$$k_{nf} = \frac{k_p + (n-1)k_f + (n-1)\phi(k_p - k_f)}{k_p + (n-1)k_f - \phi(k_p - k_f)} k_f \quad (2.2)$$

where n is empirical shape factor, which is defined as:

$$n = \frac{3}{\psi} \quad (2.3)$$

where ψ is the sphericity. Sphericity is the ratio of the surface area of the equivalent sphere having the same volume to the actual surface area of the non-spherical particle. Therefore $n = 3$ for a sphere and in that case the HC model becomes identical to the Maxwell model. Significantly, the prediction of classical models only depends on particle volume fraction and particle shape. However, such models can only predict well for millimeter or micrometer sized particles but failed for nanometer sized particles.

A summary of the experimental works on the study of thermal conductivity enhancement of nanofluids with respect to particle volume fraction is shown in Table 2.1. It indicates that thermal conductivity of conventional heat transfer fluids can be enhanced by suspending oxide nanoparticles, metallic nanoparticles or carbon nanotubes. For suspension of oxide nanoparticles, Xie et al. (2002) reported up to 21% enhancement at 5 vol% Al_2O_3 -water nanofluids. Similar successful thermal conductivity enhancements were also reported in the suspension of nanoparticles in ethylene glycol and oil based nanofluids, where 41% enhancement was observed in 8 vol% Al_2O_3 -ethylene glycol nanofluids (Wang, Xu, & Choi, 1999) and 39% enhancement was reported in 5 vol% Al_2O_3 -oil nanofluids (Xie et al., 2002). As for the suspension of metallic nanoparticles, Eastman et al. (2001) reported that thermal conductivity of ethylene glycol was enhanced up to 41% at particle volume fraction as low as 0.28 vol%. Jana, Salehi-Khojin, and Zhong (2007) reported that the thermal conductivity of water was even enhanced to 74% with suspension of 0.3 vol% Cu nanoparticles. In the suspension of carbon nanotubes, Choi et al. (2001) were the first to observe unusual

high thermal conductivity in nanotubes suspension (Fig. 2.1), where the thermal conductivity of oil is enhanced up to 157% at about 1 vol% of nanotubes. Subsequently, high thermal conductivity enhancement result is also reproduced by Shaikh, Lafdi, and Ponnappan (2007) in carbon nanotubes-oil nanofluids.

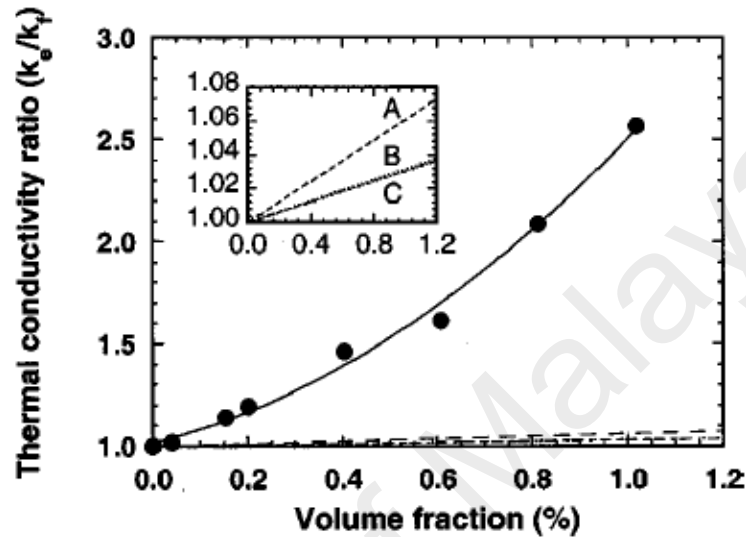


Figure 2.1: Thermal conductivity of oil is enhanced up to 157% at about 1 vol% carbon nanotubes. Measured data are greater than classical prediction where line A = Hamilton Crosser, line B=Bonnecaze and Brady and line C = Maxwell model (Choi et al., 2001).

Significantly, the observed magnitude of enhancement in thermal conductivity varies amongst groups. In majority of cases, the thermal conductivity enhancement is greater than the classical prediction but several experimental works demonstrated the thermal conductivity are well described by classical models (Chon et al., 2005; Das et al., 2003; Hwang et al., 2007; Lee et al., 1999; Timofeeva et al., 2007). Despite the observed variations, the general trend is clear: thermal conductivity of conventional heat transfer fluids is enhanced with the suspension of nanoparticles and thermal conductivity increases with increasing particle volume fraction.

Table 2.1: Experimental works on studying thermal conductivity enhancement of nanofluids with respect to particle volume fraction.

Author	Nanofluids	Particle size (nm)	Particle volume fraction (vol%)	Thermal conductivity enhancement (%)
Masuda et al. (1993)	Al ₂ O ₃ -Water	13	4.3	33
Lee et al. (1999)	Al ₂ O ₃ -Water	38.4	4.3	10
Xie et al. (2002)	Al ₂ O ₃ -Water	60.4	5.0	21
Das et al. (2003)	Al ₂ O ₃ -Water	38.4	4	9
Chon et al. (2005)	Al ₂ O ₃ -Water	47	4	8
Li and Peterson (2007a)	Al ₂ O ₃ -Water	36	10	11
Timofeeva et al. (2007)	Al ₂ O ₃ -Water	40	5	10
Zhang, Gu, and Fujii (2006a)	Al ₂ O ₃ -Water	20	5	15
Wang et al. (1999)	Al ₂ O ₃ -EG	28	8	41
Lee et al. (1999)	Al ₂ O ₃ -EG	38.4	5	18
Xie et al. (2002)	Al ₂ O ₃ -EG	60.4	5	30
Timofeeva et al. (2007)	Al ₂ O ₃ -EG	40	5	13
Wang et al. (1999)	Al ₂ O ₃ - Oil	28	7.4	30
Xie et al. (2002)	Al ₂ O ₃ -Oil	60.4	5	39
Venerus et al. (2006)	Al ₂ O ₃ -Oil	30	2.5	5
Wang et al. (1999)	CuO-Water	23	9.7	34
Lee et al. (1999)	CuO-Water	23.6	3.41	12
Das et al. (2003)	CuO-Water	28.6	4	14
Li and Peterson (2006)	CuO-Water	29	6	36
Wang et al. (1999)	CuO-EG	23	14.8	54
Lee et al. (1999)	CuO-EG	23.6	4	23
Hwang, Park, Lee, and Jung (2006)	CuO-EG	-	1	9
Kang, Kim, and Oh (2006)	SiO ₂ -Water	15-20	4	5

Table 2.1, continued.

Author	Nanofluids	Particle size (nm)	Particle volume fraction (vol%)	Thermal conductivity enhancement (%)
Hwang et al. (2006)	SiO ₂ -Water	-	1	3
Murshed, Leong, and Yang (2005)	TiO ₂ -Water	15 sphere	5	30
Zhang et al. (2007)	TiO ₂ -Water	40	2.5	5
Kang et al. (2006)	Ag-Water	8-15	0.39	11
Patel et al. (2003)	Ag-Water	60-70	0.001	3
Patel et al. (2003)	Au-Water	10-20	0.00026	5
Kumar et al. (2004)	Au-Water	4	0.01	8
Putnam, Cahill, Braun, Ge, and Shimmin (2006)	Au-Ethanol	4	0.07	1.3
Xuan and Li (2000)	Cu-Water	100	2.50	22
Liu, Lin, Tsai, and Wang (2006)	Cu-Water	50-100	0.1	24
Jana et al. (2007)	Cu-Water	10	0.3	74
Eastman et al. (2001)	Cu-EG	<10	0.28	41
Assael, Metaxa, Kakosimos, and Constantinou (2006)	Cu-EG	-	0.48	3
Xuan and Li (2000)	Cu-Oil	100	7.5	43
Xie, Lee, Youn, and Choi (2003)	CNT-Water	15×30000	1	7
Assael, Chen, Metaxa, and Wakeham (2004)	CNT-Water	100×>50000	0.6	38
Hwang et al. (2007)	CNT-Water	10-30×10000-50000	1	7
Xie et al. (2003)	CNT-EG	15×30000	1	13
Choi et al. (2001)	CNT-Oil	25×50000	1	157
Hwang et al. (2007)	CNT-Oil	10-30×10000-50000	0.5	9

Remarks: EG- ethylene glycol

2.1.1 Particle Size Dependence on Thermal Conductivity

Choi (1995) analysed the unusual enhancement in heat transfer fluids attributed to extremely large specific surface area of nanoparticles in which the effect is not addressed in the classical theory prediction. As heat transfer takes place at the surface of nanoparticles, smaller particles with higher specific surface area is expected to produce higher thermal conductivity enhancement compared to larger particles with lower specific surface area. Accordingly, literatures have shown that particle size has significant effects on thermal conductivity enhancement of nanofluids. However, this influence due to particle size dependence has always been controversial.

A group of researchers reported that thermal conductivity increases with decreasing particle size (Chon et al., 2005; Chopkar et al., 2006; Chopkar et al., 2007; He et al., 2007; Kim et al., 2007; Lee et al., 2014; Lee et al., 1999; Mintsa et al., 2009; Teng et al., 2010). Chopkar et al. (2006) measured the thermal conductivity of 0.5 vol% Al₇₀Cu₃₀-ethylene glycol nanofluids. The nanofluids were prepared using the two-steps process and characterised by X-ray diffraction (XRD) and transmission electron microscope (TEM). The result is shown in Figure 2.2 and indicates that thermal conductivity enhancement decreases from 38% to 3% by increasing the particle size from 9nm to 83nm. In another study, Chopkar et al. (2007) further investigated the particle size effects on ethylene glycol and water based nanofluids containing 0.5 vol% Al₂Cu with particle size ranging from 8 nm to 80 nm. Again, it is confirmed that thermal conductivity enhancement decreases with increasing particle size for both water and ethylene glycol based nanofluids. Recently, Lee et al. (2014) measured the thermal conductivity enhancement for 0.51 vol% Al₂O₃-water nanofluids with particle size of 71.6 nm, 114.5 nm and 136.8 nm. The nanofluids were produced without using surfactant or dispersant. A significant decrease in thermal conductivity with increasing particle size was observed.

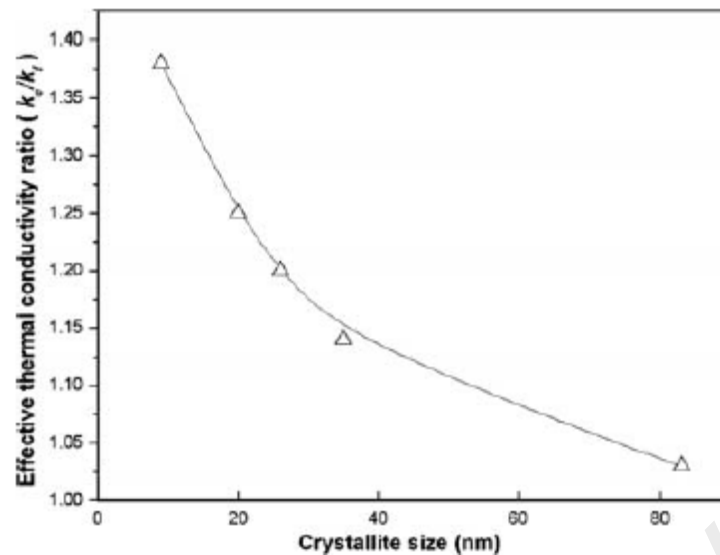


Figure 2.2: For 0.5 vol% Al₇₀Cu₃₀-ethylene glycol nanofluids, thermal conductivity enhancement decreases with increasing particle size (Chopkar et al., 2006).

However, another group of researchers reported an opposite trend on particle size dependence in which thermal conductivity of nanofluids increases with increasing particle size (Angayarkanni et al., 2015; Beck et al., 2009; Chen et al., 2008a; Timofeeva et al., 2010; Warriar & Teja, 2011; Yu et al., 2008). Beck et al. (2009) demonstrated that thermal conductivity enhancement in nanofluids decreases as the particle size decreases below 50nm for suspension of Al₂O₃ in water and ethylene glycol with particle diameter varied from 8nm to 28nm at particle volume fraction 2 vol%, 3 vol% and 4 vol% (Fig. 2.3). In their studies, the average particle sizes were determined using Brunauer-Emmett-Teller (BET) surface area measurement, in which the average particle sizes obtained after evaporating the base fluid from the nanofluids. Similarly, BET was also used by Timofeeva et al. (2010) to study the particle size effects in 4.1 vol% water based α -SiC nanofluids. Again, they showed that thermal conductivity enhancement of nanofluids increases from 7.0% to 12.5% for particle size range of 16nm to 90nm. Chen et al. (2008a) characterised particle size distribution by using small-angle X-ray scattering (SAXS) and found that thermal conductivity

enhancement increases from 6% to 16% for particle size from 10nm to 30nm at 16 vol% SiO₂-water nanofluids.

In contrast to the reported trend of monotonic increases or decreases in the thermal conductivity enhancement with decreasing particle size, Xie et al. (2002) demonstrated that an increase followed by a decrease in thermal conductivity enhancement with decreasing particle size of Al₂O₃ in oil and ethylene glycol based nanofluids.

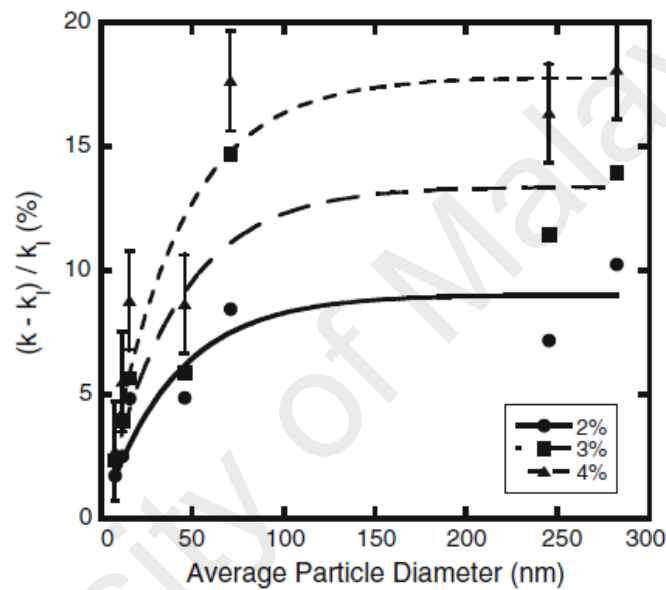


Figure 2.3: For Al₂O₃-water nanofluids, thermal conductivity enhancement increases with the increase of particle size below 50nm (Beck et al., 2009).

2.1.2 Temperature Dependence on Thermal Conductivity

One of the interesting findings in nanofluids is the temperature dependence of thermal conductivity enhancement, which is also not taken into account in the classical theories. Such temperature behaviour has made nanofluids to be a more attractive heat transfer fluid for device with high energy density in order to provide immediate cooling to avoid hot spots.

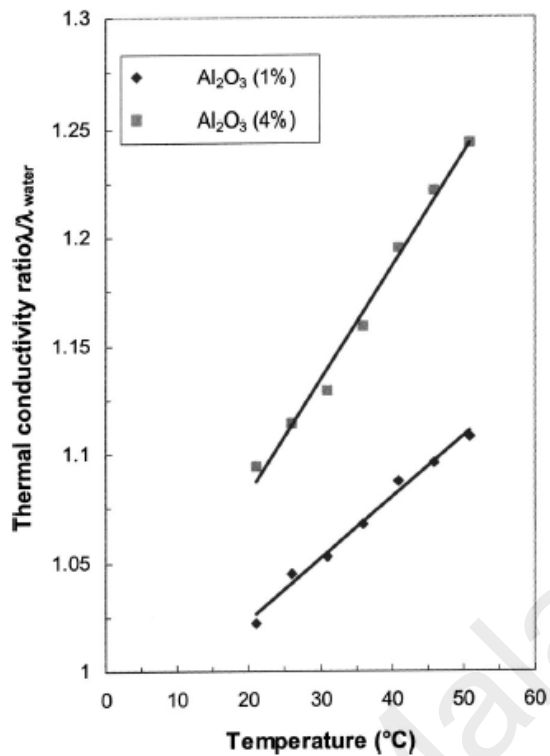


Figure 2.4: For Al₂O₃-water nanofluids, thermal conductivity enhancement increases with increasing temperature (Das et al., 2003).

Das et al. (2003) was the first group to discover that thermal conductivity enhancement increases with increasing temperature. Their results are shown in Figure 2.4, for 1 vol% Al₂O₃ suspension, the enhancement of water increased from 2% to 10.8% with temperature rising from 21°C to 51°C, more interesting features were even observed in higher particle volume fraction, for example 4 vol%, the enhancement of water increases from 9.4% to 24.4% at the same temperature range. Such temperature dependence was also observed by Li and Peterson (2006), the enhancement of water increased about 3 times in the temperature range of 27.5°C to 34.7°C at particle volume fraction of 2 vol%, 5 vol% and 10 vol%. They also demonstrated that such temperature dependence is more pronounced in higher particle volume fraction compared to lower particle volume fraction. Furthermore, Lee et al. (2014) added that the temperature dependence is not only noticeable on particle volume fraction but also particle size. The observation was obtained from their experimental works on 0.51 vol% Al₂O₃-water

nanofluids with average particle diameter of 71.6 nm, 114.5 nm and 136.8 nm in temperature range of 21°C to 51°C. Such temperature dependence of thermal conductivity enhancement are concurrent with other experimental studies (Chon et al., 2005; Esfe et al., 2015; Kole & Dey, 2013; Mehrali et al., 2014; Mintsa et al., 2009; Murshed et al., 2008; Patel et al., 2003; Sundar et al., 2014; Wen & Ding, 2004).

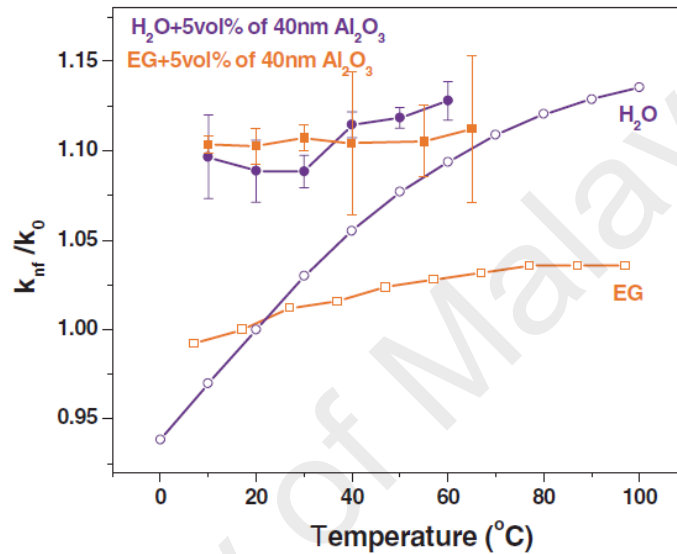


Figure 2.5: For suspension of 40nm Al₂O₃ in water and ethylene glycol based nanofluids, thermal conductivity enhancement is independent with temperature (Timofeeva et al., 2007).

Nevertheless, the opposite trend was also reported in which the temperature dependence is absent in thermal conductivity enhancement of nanofluids (Beck et al., 2007; Beck et al., 2010; Pastoriza-Gallego et al., 2011b; Peñas et al., 2008; Singh et al., 2009; Timofeeva et al., 2007; Venerus et al., 2006; Zhang et al., 2006b; Zhang et al., 2007). Timofeeva et al. (2007) studied the temperature dependence of the thermal conductivity of water and ethylene glycol nanofluids with 5 vol% Al₂O₃ nanoparticles (Fig. 2.5). They found that the absolute thermal conductivity increases with increasing temperature in the range of 10°C to 65°C. However, the temperature dependence simply tracked the temperature dependence of the base fluid rather than the behaviour related to

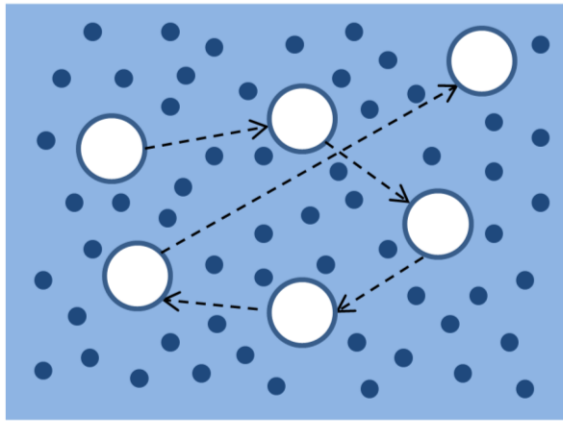
the nanoparticles. Thus, they concluded that the thermal conductivity enhancement is independent of temperature. Wider temperature ranged has been studied by Beck et al. (2010) for suspension of Al_2O_3 nanoparticles in ethylene glycol, water and mixtures of ethylene glycol and water. In the temperature range of 296K to 410K, the temperature dependence behaviour of thermal conductivity follows closely to that of base fluid. All these findings confirmed that the thermal conductivity enhancement is not influenced by the temperature effect, which is consistent with the classical theories.

2.2 Potential Mechanisms of Thermal Conductivity Enhancement

Several potential mechanisms have been proposed to explain the thermal conductivity enhancement owing to the inadequacy found in classical theories, namely Brownian motion of nanoparticles, molecular liquid layering on solid-liquid interface, effects of nanoparticle aggregation, the nature of heat transport in nanoparticles, interfacial thermal resistance and Brownian motion induced micro-convection in base fluids. In this thesis, the focus will be on the investigation of three hotly debating mechanisms which are Brownian motion of nanoparticles, Brownian motion induced micro-convection in base fluids, and effects of nanoparticle aggregation. The mechanisms are illustrated in Figure 2.6 and discussed in detail.

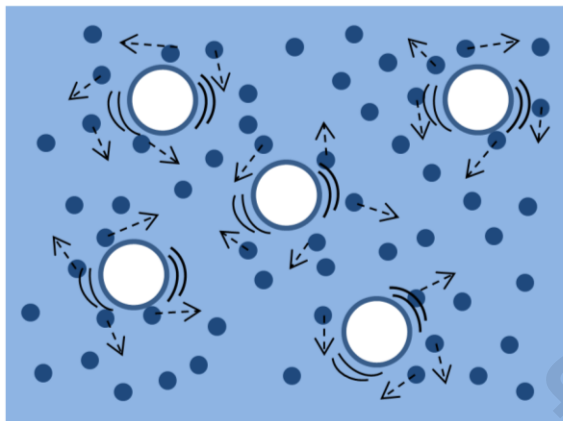
2.2.1 Brownian Motion of Nanoparticles

The thermal conductivity enhancement in nanofluids is believed to be attributed to the Brownian motion of nanoparticles (Kumar et al., 2004; Murshed et al., 2009; Xuan et al., 2003) because of the observed particle size and temperature dependence. As nanofluids are a dynamic system in which nanoparticles are constantly in motion, the Brownian motion could allow the nanoparticle to absorb the heat from surrounding base fluid and moves at greater distant to release the thermal energy to colder region of surrounding base fluid. It further enhances the thermal transport when two nanoparticles



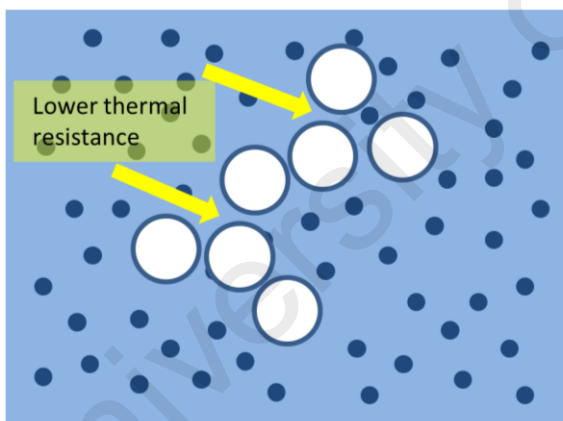
Brownian Motion

Nanoparticle to absorb the heat from surrounding base fluid and moves at greater distant to release the thermal energy to colder region of surrounding base fluid, causing an increase in thermal conductivity.



Brownian Motion Induced Micro-convection

Nanoparticles moving in Brownian motion could set up the convection current in fluid molecules at immediate vicinity to the nanoparticles, causing an increase in thermal conductivity.



Nanoparticle Aggregation

Aggregated nanoparticle form linear chains or percolating networks embedded in large pockets of base fluids, could create a path of lower thermal resistance and enhance the thermal conductivity in nanofluids

Figure 2.6: Three potential mechanisms in enhancing thermal conductivity in nanofluids.

collide and enables direct solid-solid transport of heat from one nanoparticle to another.

The Brownian motion is characterised by particle diffusion constant, D_B , given by

Stokes-Einstein formula (Einstein, 1956):

$$D_B = \frac{k_B T}{3\pi\eta d} \tag{2.4}$$

where k_B is Boltzmann constant, η is fluid viscosity, T is fluid temperature and d is particle diameter. It can be seen that, the Brownian motion increases with increasing temperature and decreasing particle size, and hence, this model predicts well for the reported trend of temperature and particle size dependence.

However, the Brownian model proposed by Kumar et al. (2004) received strong criticism by several researchers (Bastea, 2005; Keblinski & Cahill, 2005) due to unphysical assumption of the nanoparticle mean free path on the order of 1 cm. Thus, the model overestimates the contribution of Brownian motion to heat transfer by several orders of magnitude larger. Apart from this, even though the effects of Brownian motion is quantitatively justified in Brownian dynamics (BD) simulation (Bhattacharya, Saha, Yadav, Phelan, & Prasher, 2004), the employed algorithm and inter-particle potential with a range of the order of one light year are questionable (Eapen, Rusconi, Piazza, & Yip, 2010; Keblinski, Eastman, & Cahill, 2005). Keblinski et al. (2002) also added that, based on kinetic theory analysis, the Brownian diffusion is too slow to transport the heat compared to thermal diffusion. Physically, the measured diffusion coefficient of nanoparticle from MD simulation is 1-3 orders of magnitude smaller than the diffusion coefficient in fluid (Sarkar & Selvam, 2007; Vladkov & Barrat, 2006). The insignificant role of Brownian motion was also determined in MD simulations by showing that the heat transfer rate for nanofluids with free moving nanoparticle is similar with “frozen” or static nanoparticle (Keblinski et al., 2002; Vladkov & Barrat, 2006).

Although the role of Brownian motion is debatable, it could have an indirect role to induce micro-convection in base fluid or enable nanoparticle aggregation to enhance the overall thermal conductivity in nanofluids.

2.2.2 Brownian Motion Induced Micro-convection

Jang and Choi (2004, 2007) were the first to propose that the Brownian motion induced micro-convection is the principal mechanism to enhance the thermal transport of nanofluids. They hypothesised that large number of nanoparticles moving in Brownian motion could set up the convection current in fluid molecules in the immediate vicinity of the nanoparticles. In turn, it enhances the heat transfer between nanoparticles and base fluid, and causing an increase in thermal conductivity of nanofluids. In their model, they considered four modes of energy transport: collisions between base fluid, thermal diffusion in nanoparticles, collision in nanoparticles due to Brownian motion (neglected) and micro-convection in base fluid. Subsequently, the micro-convection based model was developed by different of groups of researchers (Koo & Kleinstreuer, 2004; Patel et al., 2006; Patel et al., 2008; Prasher et al., 2005, 2006a; Ren et al., 2005; Xuan et al., 2006). These models are in good agreement with reported experimental data and correctly predict the observed trend in particle size and temperature. The importance of induced micro-convection in base fluid is further supported in experiments (Krishnamurthy et al., 2006) and simulation studies (Li & Peterson, 2007b; Sarkar & Selvam, 2007). Li and Peterson (2007b) employed CFD and analysed the flow velocity gradient around the nanoparticles which is more apparent than bulk fluid. Krishnamurthy et al. (2006) observed that the diffusion coefficient of fluorescent dye in water based nanofluids is greater than water; because convection and mass transfer are similar processes, they exhibited that the convection in nanofluids is enhanced. However, it was pointed out that the enhancement in dye diffusion was incorrectly determined from the complexation interaction between dye and nanoparticles (Ozturk, Hassan, & Ugaz, 2010). Such experimental method is inappropriate since the diffusion between free dye and complexation of dye-nanoparticles cannot be differentiated.

In contrast, several other groups had questioned the role of micro-convection in nanofluids. To estimate the contribution of Brownian motion induced micro-convection in base fluids, the entire volume of fluid was assumed to diffuse together with the Brownian motion of nanoparticles, the velocity of fluid is the same as the Brownian velocity of nanoparticles; this assumption was integrated into the kinetic theory, where it showed that the contribution of induced micro-convection to the effective thermal conductivity is less than 1% (Evans, Fish, & Keblinski, 2006). This results was also confirmed by the calculation from the integral of heat flux autocorrelation function in Green Kubo method (Nie, Marlow, & Hassan, 2008) and indicated that thermal conductivity contributed by hydrodynamic effects of Brownian motion is only $\approx 10^{-15}$ W/m.K for water based nanofluids at 320 K, such contribution is negligible if compared to thermal conductivity of water. Eapen et al. (2007b) examined the micro-convection model proposed by Prasher et al. (2005) in conducting direct experimental investigation on suspended silica and perfluorinated particles. Their results were in agreement with effective medium theory of Maxwell but not with the micro-convection model. They commented that the micro-convection velocities can only be the order of the thermophoretic velocities. They measured thermophoretic velocities as low as 1 nm/s while the assumed convection velocities in Prasher et al. (2005) and Jang and Choi (2004) models are O(1) m/s and O(0.1) m/s, respectively. Thus, the several orders of larger magnitude in the convection velocities had overestimated the role of micro-convection mechanism.

The insignificant role of micro-convection are further supported by experimental works (Gerardi, Cory, Buongiorno, Hu, & McKrell, 2009; Shima, Philip, & Raj, 2009) and MD simulations (Babaei, Keblinski, & Khodadadi, 2013; Ghosh, Roy, Pabi, & Ghosh, 2011; Keblinski & Thomin, 2006). In experimental works, Gerardi et al. (2009) demonstrated that the diffusion coefficient of water decreases with increasing Al₂O₃

nanoparticles, which is in opposite trend of aforementioned observation. In MD simulation, Koblinski and Thomin (2006) pointed out that the amplitude of the velocity field around a Brownian particle decay much faster than the velocity field around constant a moving particle. In turn, micro-convection mechanism is not pronounced due to the quicker decay of the hydrodynamic field around the Brownian particle.

2.2.3 Effects of Nanoparticle Aggregation

Ideally nanofluids have well-dispersed nanoparticles in the base fluids, but it is experimentally proven that nanofluids are in aggregated state (Eastman et al., 2001; Murshed et al., 2005; Pastoriza-Gallego, Casanova, Legido, & Piñeiro, 2011a; Zhu et al., 2006), as shown in Figure 2.7. This is because nanoparticles suspended in base fluid are under the influence of Brownian and Van der Waals forces. Thus, nanoparticles tend to aggregate under these forces to minimise surface energy. Koblinski et al. (2002) were the first to propose that aggregated nanoparticles form linear chains or percolating networks embedded in large pockets of base fluids which create a path of lower thermal resistance, and hence, enhance the thermal conductivity in nanofluids. Since then, several nanoparticle aggregation-based models have been developed to explain the conduction enhancement in nanofluids (Evans et al., 2008; Feng et al., 2007; Pang et al., 2014; Pang et al., 2015; Prasher et al., 2006b; Prasher et al., 2006c; Xuan et al., 2003).

The most recognised aggregation-based model is the three level homogenisation model (Evans et al., 2008; Prasher et al., 2006b). It is hypothesised that a fractal aggregate is embedded within a sphere which consists of a few approximately linear chains, which span the whole aggregate and side chains, as depicted in Figure 2.8. The linear chains which span the whole cluster are called the backbone. The chains on the other side, which do not span the whole aggregate, are called dead ends. The effective thermal conductivity contributed by the backbone is crucial, so it is incorporated in the

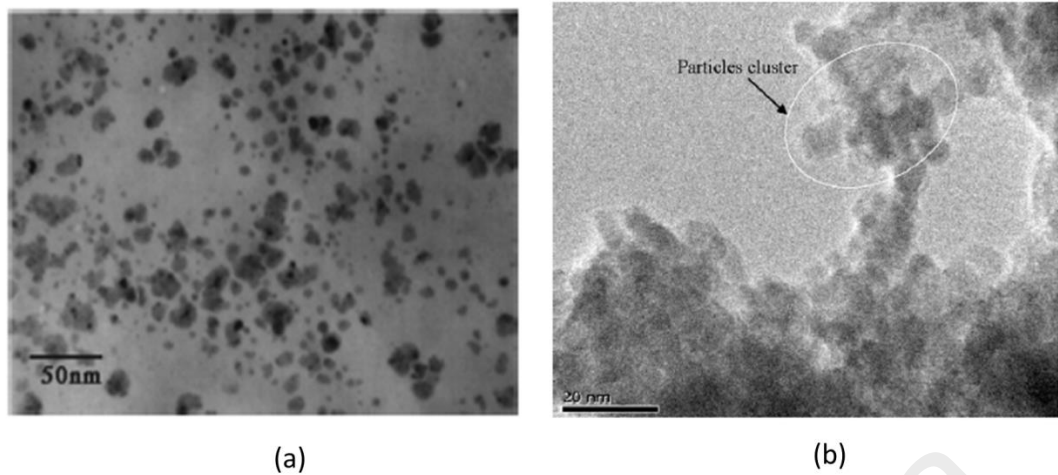


Figure 2.7: TEM photograph in nanofluids. (a) Cu-ethylene glycol nanofluids (Eastman et al., 2001); (b) TiO₂-deionized water nanofluids (Murshed et al., 2005).

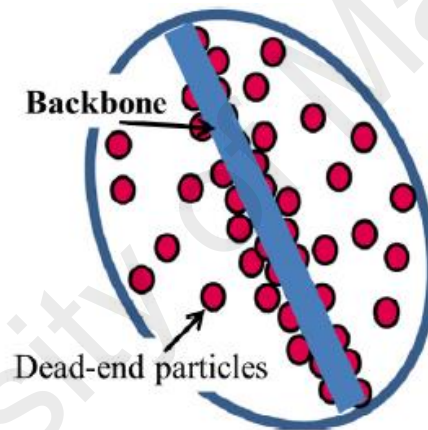


Figure 2.8: Aggregated nanoparticles consist of backbone and dead end particles (Pang et al., 2014).

effective medium theory for conduction prediction owing to its high aspect ratio to allow for rapid heat flow over large distance and also diminish thermal resistance on thermal transport. The studies proved that the thermal conductivity is a strong function of aggregation, in which the enhancement due to aggregation is higher than well-dispersed nanoparticles. Prediction of this three level homogenisation model is in agreement with the Monte Carlo simulation of heat conduction on modelling fractal aggregates (Evans et al., 2008; Prasher et al., 2006b). Experimentally, it has been

observed that thermal conductivity has strong correlation with nanoparticle aggregation (Gao, Zheng, Ohtani, Zhu, & Chen, 2009; Gharagozloo, Eaton, & Goodson, 2008; Hong & Kim, 2012; Philip, Shima, & Raj, 2007; Philip, Shima, & Raj, 2008; Shalkevich, Shalkevich, & Bürgi, 2010; Shima et al., 2009; Timofeeva et al., 2007). Gao et al. (2009) carried out a structural analysis in solid and liquid states for Al_2O_3 nanofluids using two different base fluids: animal oil and hexadecane. For the animal oil based nanofluids, the thermal conductivity enhancement in the solid state is slightly lower than the liquid state. On the contrary, for the hexadecane based nanofluids, the thermal conductivity enhancement in the solid state where the Brownian motion is frozen; is higher than the liquid state. Morphology from transmission electron microscope (Fig. 2.9) showed that when in solid state, Al_2O_3 nanoparticles in hexadecane base fluid formed linear chain and pushed into grain boundaries but this did not happen in animal oil based nanofluids. Therefore, they concluded that the forming of chain like nanoparticle aggregation is the key to govern thermal conductivity enhancement in nanofluids, rather than Brownian motion. A similar conclusion was also drawn by observing the thermal conductivity of a gelled sample, formed with interconnected nanoparticles higher than fluidic sample which consists of fully moving nanoparticles in suspension (Hong & Kim, 2012; Shalkevich et al., 2010). The positive role of nanoparticle aggregation is also supported by MD simulations, in which the nanofluids with aggregated nanoparticles have obviously higher thermal conductivity than well-dispersed nanofluids, the level of thermal conductivity enhancement is strongly dependent on the configuration of nanoparticle aggregation (Kang, Zhang, Yang, & Li, 2012; Vladkov & Barrat, 2008). Although these studies successfully demonstrated that nanoparticle aggregation induces higher thermal conductivity in nanofluids, no further microscopic details were revealed in their works.

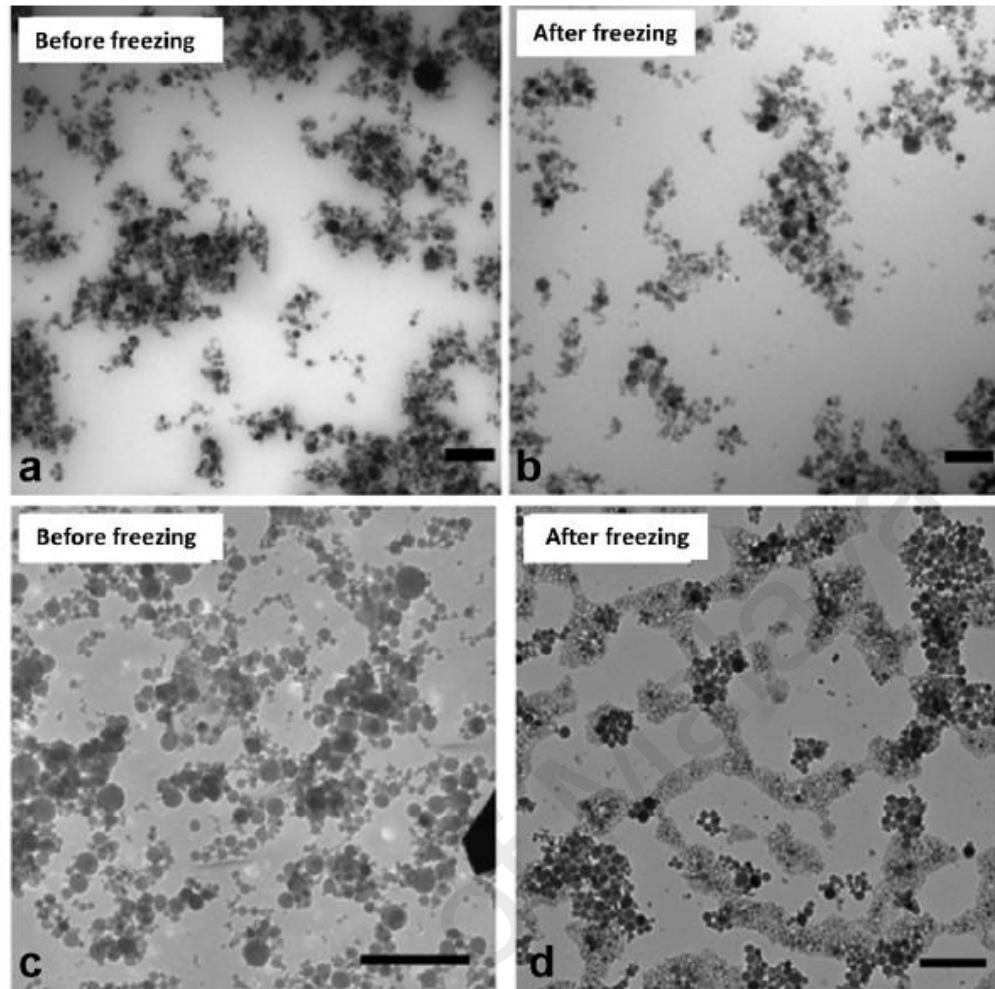


Figure 2.9: TEM photograph in Al_2O_3 nanofluids (Gao et al., 2009). (a) Animal oil based nanofluids before freezing; (b) animal oil based nanofluids after freezing; (c) hexadecane based nanofluids before freezing; (d) hexadecane based nanofluids after freezing.

It has been noticed that the thermal conductivity is a time dependent process or aging process (Angayarkanni & Philip, 2014; Hong, Hong, & Yang, 2006; Karthikeyan, Philip, & Raj, 2008; Shima, Philip, & Raj, 2010; Timofeeva et al., 2007). Most recently, Angayarkanni and Philip (2014) observed that over some time after sonication process for oxide water based nanofluids, there is an increase in thermal conductivity enhancement and reach a peak value followed by a decrease. This may be due to the fact that the nanoparticles are in well-dispersed state right after sonication process, as time elapse, the nanoparticles get closer and start to form aggregation, leading to a

greater thermal conductivity. As time increases, the nanoparticle aggregation is bigger and eventually settles down due to gravity force, resulting in the decrease in thermal conductivity. However, it differs from the trend observed by other groups (Hong et al., 2006; Karthikeyan et al., 2008). In Fe nanofluids (Hong et al., 2006) and CuO nanofluids (Karthikeyan et al., 2008), it was observed that the aggregation size increases as a function of time after the sonication process stopped, but the thermal conductivity decreases right after the sonication process and further decreases with the elapsed time due to the increasing aggregation size. Therefore, the researchers concluded that stability of suspension of well-dispersed nanoparticles is one of the key parameter to improve thermal conductivity. Significantly, the above experimental results failed to conclude the trend of thermal conductivity with respect to the effect of nanoparticle aggregation. In spite of that, one thing proven is the aggregation state is the main variable in controlling thermal conductivity enhancement in nanofluids.

One should bear in mind that, the clumping of large aggregation of nanoparticles not only leads to abrasion and clogging of the thermal devices but also decreases the thermal conductivity enhancement as reported in aforementioned experimental works (Angayarkanni & Philip, 2014). Eastman et al. (2004) commented that such clumping of aggregation would most likely settle out of the fluid due to gravity, especially at low volume fraction, and create large region of particle free base fluid with higher thermal resistance and lead to lower thermal conductivity. As the rate of aggregation is proportional with particle volume fraction, consequently, it may offset the thermal conductivity enhancement caused by the increasing particle volume fractions, resulting in non-linear increases in thermal conductivity against particle volume fraction (Zhu et al., 2006). Therefore, it is important to differentiate between percolating nanoparticle aggregation and clumping of large nanoparticle aggregation, the former can generate additional conduction path while the latter cannot. In view of this, it is believed that

different aggregation state has led the aforementioned controversies on the data of thermal conductivity. Remarkably, how well the control of nanoparticle aggregation is the key parameter to determine the thermal conductivity in nanofluids. Several techniques have been practiced to control the aggregation state, including controlling the electrical double layer of nanoparticles by inserting additives (to form aggregated or well-dispersed state), changing the pH of base fluid or using sonication process to excite the nanoparticles.

2.3 Viscosity in Nanofluids

Shear viscosity describes the internal resistance of fluid flow. In fact, the significance of viscosity is as important as thermal conductivity especially for energy system that employs fluid flow. In convection heat transfer of nanofluids, the heat transfer coefficient not only depends on the thermal conductivity but also on viscosity, density and specific heat of nanofluids. Thus, the viscosity of nanofluids has direct correlation with pressure drop and pumping power.

The Einstein model (Einstein, 1956) is a pioneer theory in describing effective viscosity of fluids with suspended particles. Einstein assumed that spherical particles are well suspended into the fluid without any interaction between the particles and the flow field perturbations are caused by the suspended small particles. The Einstein model is given by:

$$\eta_{nf} = (1 + 2.5\phi)\eta_f \quad (2.5)$$

where η and ϕ is viscosity and particle volume fraction, respectively. The subscripts nf and f represent the nanofluid and base fluid, respectively. The majority of viscosity correlations have been established based on this extension. As the Brownian motion of particles becomes more significant for smaller particles, Batchelor (1977) proposed a

viscosity correlation which includes the Brownian motion of nanoparticles and interaction between particles. Batchelor model is given below:

$$\eta_{nf} = (1 + 2.5\phi + 6.5\phi^2)\eta_f \quad (2.6)$$

However, similar with the prediction of thermal conductivity, the above classical theories of viscosity only describe well for suspension of microparticles instead of nanoparticles. It has been observed that the classical theories which are only dependent on particle volume fractions always underestimate the effective viscosity of nanofluids. A summary of the experimental works on the study of viscosity enhancement of nanofluids with respect to particle volume fraction is shown in Table 2.2.

It can be seen in Table 2.2 that even though the magnitude of viscosity enhancement varies with respect to particle volume fraction, one significant trend can be observed, viscosity of nanofluids increases with increasing particle volume fraction. For example, Nguyen et al. (2007) measured viscosity for Al₂O₃-water nanofluids with particle volume fraction from 0.15 vol% to 13 vol%. The results is shown in Figure 2.10, for 47 nm Al₂O₃ nanoparticle, the viscosity enhancement is 12%, 60%, 200% and 430% corresponding to particle volume fraction of 1 vol%, 4 vol%, 9 vol% and 12 vol%, respectively. Similar behaviour is also found in 36 nm Al₂O₃ nanoparticle, the viscosity enhancement increases from 10% to 40%, then to 100% and finally to 210% corresponding to particle volume fraction of 2.1 vol% to 4.3 vol%, to 8.5 vol% and then 12.2 vol%. In another study, Chen et al. (2009a) reported that viscosity of titanate nanotubes in ethylene glycol increases with increasing particle volume fraction. It showed that the viscosity enhancement are 3.30%, 7.00%, 16.22%, 26.34% and 70.96% corresponding to particle volume fraction of 0.5 vol%, 1.0 vol%, 2.0 vol% 4.0 vol% and 8.0 vol%.

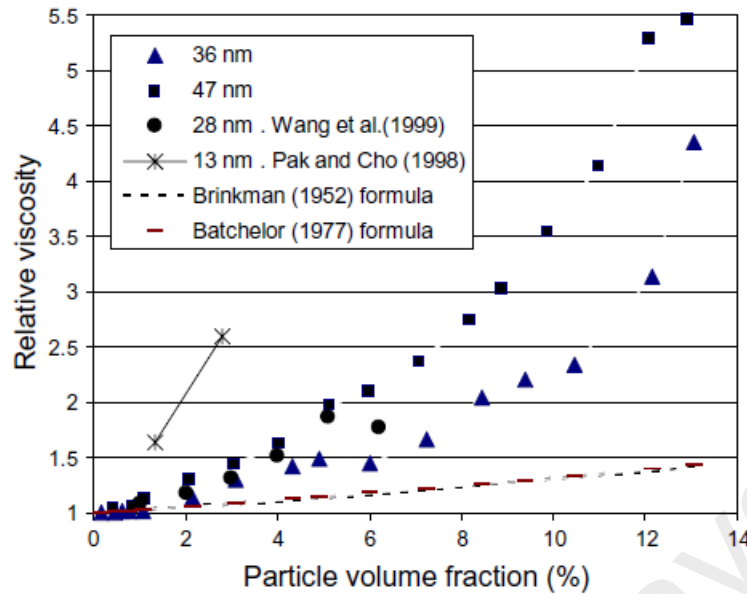


Figure 2.10: For suspension of Al₂O₃-water nanofluids, viscosity enhancement increases with increasing particle volume fraction and particle size (Nguyen et al., 2007).

2.3.1 Particle Size Dependence on Viscosity

Even though particle size dependence is not included in the classical theories for viscosity prediction, literatures showed particle size dependence on viscosity of nanofluids. Unlike the observed monotonic increase in viscosity with increasing particle volume fraction, the particle size dependence on viscosity is always in contradiction. The viscosity is not only shown to increase and decrease with increasing particle size but also shown to be independent of particle size.

A group of researchers observed that viscosity decreases with increasing particle size (Anoop et al., 2009b; Chang et al., 2005; Chevalier et al., 2007; Pastoriza-Gallego et al., 2011a; Rudyak, Dimov, Kuznetsov, & Bardakhanov, 2013; Timofeeva et al., 2010; Timofeeva et al., 2011a). Pastoriza-Gallego et al. (2011a) investigated particle size effects on viscosity by dispersing CuO nanoparticle with particle size of 33 nm and 11 nm into water. Both nanofluids have the same particle volume fraction of 1-10 wt%

Table 2.2: Experimental works on studying viscosity enhancement of nanofluids with respect to particle volume fraction (Mahbubul, Saidur, & Amalina, 2012).

Author	Nanofluid	Particle size (nm)	Particle volume fraction	Viscosity enhancement (%)
Chandrasekar et al. (2010)	Al ₂ O ₃ -Water	43	1-5 vol%	14-136
Nguyen et al. (2008), Nguyen et al. (2007)	Al ₂ O ₃ -Water	36	2.1-12 vol%	10-210
Nguyen et al. (2008), Nguyen et al. (2007)	Al ₂ O ₃ -Water	47	1-12 vol%	12-430
Pak and Cho (1998)	Al ₂ O ₃ -Water	13	1-3 vol%	60-300
Kole and Dey (2010)	Al ₂ O ₃ -car engine coolant	<50	0.1-1.5 vol%	4-136
Wang et al. (1999)	Al ₂ O ₃ -DW	28	1-6 vol%	9-86
Wang et al. (1999)	Al ₂ O ₃ -EG	28	1.2-3.5 vol%	7-39
Prasher, Song, Wang, and Phelan (2006d)	Al ₂ O ₃ -PG	27	0.5-3 vol%	7-29
Prasher et al. (2006d)	Al ₂ O ₃ -PG	40	0.5-3 vol%	6-36
Prasher et al. (2006d)	Al ₂ O ₃ -PG	50	0.5-3 vol%	5.5-24
Murshed et al. (2008)	Al ₂ O ₃ -DIW	80	1-5 vol%	4-82
Anoop et al. (2009b)	Al ₂ O ₃ -Water	45	2-8 wt%	1-6
Anoop et al. (2009b)	Al ₂ O ₃ -Water	150	2-8 wt%	1-3
Anoop, Kabelac, Sundararajan, and Das (2009a)	Al ₂ O ₃ -Water	95	0.5-6 vol%	3-77
Anoop et al. (2009a)	Al ₂ O ₃ -Water	100	0.5-6 vol%	3-57
Anoop et al. (2009a)	Al ₂ O ₃ -EG	100	0.5-6 vol%	5.5-30
Masuda et al. (1993)	TiO ₂ -Water	27	1-4.3 vol%	11-60
Masuda et al. (1993)	TiO ₂ -DIW	15	1-5 vol%	24-86
Chen et al. (2007a), Chen et al. (2007b)	TiO ₂ -EG	25	0.1-1.86 vol%	0.5-23
He et al. (2007)	TiO ₂ -DW	95, 145, 210	0.024-1.18 vol%	4-11
Chen et al. (2009b)	TiO ₂ -Water	25	0.25-1.2 vol%	3-11

Table 2.2, continued.

Author	Nanofluid	Particle size (nm)	Particle volume fraction	Viscosity enhancement (%)
Duangthongsuk and Wongwises (2009)	TiO ₂ -Water	21	0.2-2 vol%	4-15
Turgut et al. (2009)	TiO ₂ -DW	21	0.2-3 vol%	4-135
Anoop et al. (2009a)	CuO-EG	152	0.5-6 vol%	8-32
Pastoriza-Gallego et al. (2011a)	CuO-water	23-37	1-10 wt%	0.5-11.5
Pastoriza-Gallego et al. (2011a)	CuO-water	11±3	1-10 wt%	2.5-73
Chevalier, Tillement, and Ayela (2007)	SiO ₂ -Ethanol	35	1.2-5 vol%	15-95
Chevalier et al. (2007)	SiO ₂ -Ethanol	94	1.4-7 vol%	12-85
Chevalier et al. (2007)	SiO ₂ -Ethanol	190	1-5.6 vol%	5-44
Chen et al. (2009a), Chen et al. (2009b)	TNT-EG	~10, L=100nm	0.1-1.86 vol%	3.3-70.96
Chen et al. (2009b), Chen et al. (2008b)	TNT-Water	~10, L=100nm	0.12-0.6 vol%	3.5-82
Garg et al. (2008)	Cu-EG	200	0.4-2 vol%	5-24
Zhu, Li, Wu, Zhang, and Yin (2010)	CaCO ₃ -DW	20-50	0.12-4.11 vol%	1-69
Lee, Park, Kang, Bang, and Kim (2011)	SiC-DW	<100	0.001-3 vol%	1-102

Remarks: DW-distilled water; EG- ethylene glycol; PG- propylene glycol; DIW-deionised water

and temperature range of 283.15-323.15 K. The results however, showed that nanofluids with smaller particle size have higher viscosity than that larger particle size. The results indicated that the differences in particle size, aggregation state and particle size distribution have determining influence on viscosity. Timofeeva et al. (2010) studied the viscosity of 4.1 vol% SiC-water nanofluids with four different particle sizes, 16 nm, 29 nm, 66 nm and 90 nm at controlled pH of 9.4. The result shown in Figure 2.11 demonstrates that viscosity increases with decreasing particle size. Maximum viscosity was observed for nanofluids with particle size of 16 nm while minimum viscosity for nanofluids with particle size of 90 nm, which correspond to enhancement of 85% and 30%, respectively. Such behaviour on particle size dependence on viscosity is also supported by MD simulation (Lu & Fan, 2008; Rudyak, Belkin, & Egorov, 2009; Rudyak & Krasnolutskii, 2014).

In contrast, several studies (He et al., 2007; Nguyen et al., 2008; Nguyen et al., 2007) showed that viscosity of nanofluids increases with increasing particle size. He et al. (2007) measured the viscosity for 0.6 vol% TiO₂ nanofluids at three different average particle sizes of 95 nm, 145 nm and 210 nm. The results showed that the viscosity increases with increasing particle size. Nguyen et al. (2007) measured the viscosity for water-based nanofluids with 36 nm and 47 nm Al₂O₃ nanoparticles. The results is shown in Figure 2.10 demonstrates that for particle volume fractions lower than 4 vol%, viscosity for both particle size alumina-water nanofluids are similar. For higher particle volume fraction, viscosity of 47 nm particle size nanofluids is significantly higher than those of 36 nm particle size. Nevertheless, such finding is questionable owing to the absence of control over the actual particle size and the suspension pH in the experimental works, hence, it is impossible to identify the true effect of the particle size on viscosity (Timofeeva et al., 2010).

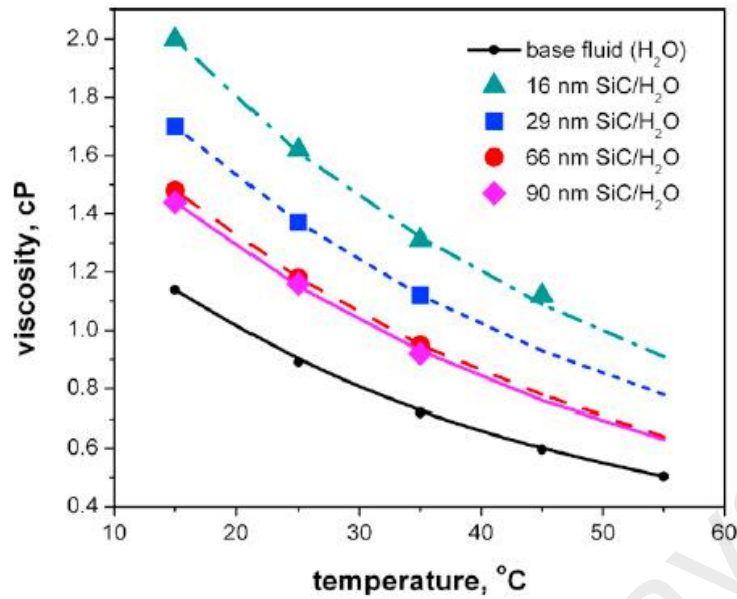


Figure 2.11: For SiC-water nanofluids, viscosity increases with decrease in particle size (Timofeeva et al., 2010).

Instead of showing monotonic decrease and increase in viscosity with increasing particle size, Prasher et al. (2006d) showed that viscosity enhancement is largely independent of particle size, which is well in agreement of classical theories in viscosity prediction.

2.3.2 Temperature Dependence on Viscosity

Similar with the effect of particle size, the temperature dependence is not taken into account in classical theories of viscosity prediction. However, the temperature is found to have strong influence on the viscosity of nanofluids. Most experimental works observed a non-linear decrease in viscosity and viscosity enhancement of nanofluids with increasing temperature (Kole & Dey, 2013; Murshed, Santos, & Nieto de Castro, 2013; Namburu, Kulkarni, Misra, & Das, 2007; Nguyen et al., 2008; Nguyen et al., 2007; Pastoriza-Gallego et al., 2011b; Sundar et al., 2014; Tavman, Turgut, Chirtoc, Schuchmann, & Tavman, 2008; Timofeeva et al., 2010; Timofeeva et al., 2011a). Such decreasing nature in viscosity with temperatures makes nanofluids to be more promising

for elevated temperature applications. Murshed et al. (2013) studied the viscosity of nanofluids by dispersing TiO_2 and SiO_2 nanoparticles into silicone oil. It showed that, as temperature rises from 21°C to 57°C , the viscosity of 0.05 vol% nanofluids with TiO_2 and SiO_2 nanoparticles decreases about 37% and 42%, respectively. Namburu et al. (2007) also measured the viscosity of nanofluids that consists of CuO dispersed in ethylene glycol and water mixtures over temperature range from 35°C to 50°C . Figure 2.12 depicts the results, which shows viscosity enhancement decreases with increasing temperature; the change in viscosity enhancement over temperature is higher for higher particle volume fraction, for example decrease in viscosity enhancement is higher for 6.12 vol% nanofluids compared to 1 vol% nanofluids. Similar behaviour has also been reported by Nguyen et al. (2008) who dealt with Al_2O_3 -water nanofluids over temperature range from 21°C to 75°C . They reported that the change in viscosity enhancement is higher for temperature around ambient condition, for example from 22°C to 40°C and such temperature dependency is also stronger for 9.4 vol% nanofluids than 1 vol% nanofluids. Furthermore, hysteresis phenomenon was observed in viscosity measurement if the nanofluids are heated beyond a critical temperature.

However, a contradictory result has been reported in which viscosity enhancement is independent of temperature (Chen et al., 2007a; Chen et al., 2007b; Prasher et al., 2006d). Chen et al. (2007b) reported that, for 0.5-8.0 vol% TiO_2 -ethylene glycol nanofluids as shown in Figure 2.13, viscosity is a strong function of temperature in range of 20°C to 60°C . Nevertheless, the temperature dependence trend in viscosity of nanofluids simply tracks the trend of that base fluid. Such temperature-independent nature could be hypothesised that nanofluids have negligible Brownian diffusion compared with convection in high shear flows.

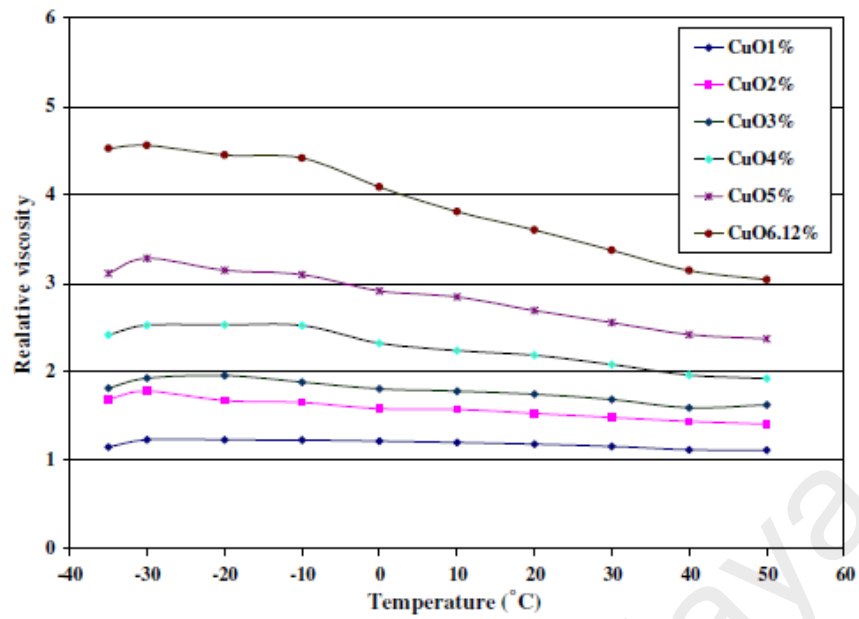


Figure 2.12: For CuO-ethylene glycol/water nanofluids, viscosity enhancement decreases with increasing temperature (Namburu et al., 2007).

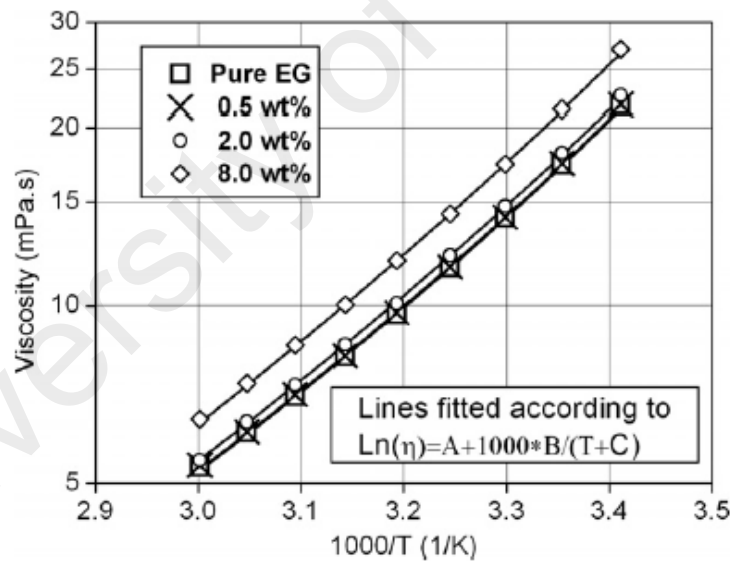


Figure 2.13: For TiO₂-ethylene glycol nanofluids, the temperature dependence trend in viscosity of nanofluids simply tracks the trend of that base fluid (Chen et al., 2007b).

2.4 Efficiency of Nanofluids

From the literature on thermal conductivity and viscosity of nanofluids, it can be seen that thermal conductivity enhancement is always accompanied by viscosity enhancement. Therefore, the benefit of nanofluids application becomes questionable owing to the increased viscosity and pumping power in energy system. In order to predict the potential of nanofluids in actual application, Prasher et al. (2006d) suggested a convenient way to estimate the efficiency of nanofluids in laminar flow by comparing viscosity enhancement coefficient and thermal conductivity enhancement coefficient, which is given by:

$$\frac{\eta_{nf}}{\eta_f} = 1 + C_\eta \phi ; \frac{k_{nf}}{k_f} = 1 + C_k \phi ; \frac{C_\eta}{C_k} < 4 \quad (2.7)$$

where C_η and C_k are viscosity and thermal conductivity enhancement coefficient, respectively. To make the nanofluids more efficient than the base fluid, the ratio of enhancement coefficient should be less than 4. If the ratio of enhancement coefficient is greater than or equal to 4, the efficiency of nanofluids is lower than the base fluid due to the enhanced higher thermal conductivity negated by the increase in pumping power and pressure drop in the energy system. It implies that either the viscosity need to be reduced or the thermal conductivity at the same particle volume fraction has to be improved.

2.5 Applications of Nanofluids

Nanofluids with enhanced thermal conductivity can be used to improve heat transfer and energy efficiency in energy system. In this section, some examples for potential application of nanofluids in the fields of transportation, electronics, nuclear reactor system and other applications will be presented.

2.5.1 Transportation

In a heavy duty diesel engine, only one-third of total energy produced from fuel combustion is used to move the vehicle, while one-third of total energy is converted into heat and removed by exhaust system and the remaining one-third is converted as heat and remain in the engine. To ensure the engine operates properly, a proper cooling system is necessary to absorb the heat in the engine and transport it to the radiator and dissipates to the environment. Mixture of ethylene glycol and water is commonly used as heat transfer fluid in engine cooling systems. Water is used to provide the heat transfer function while ethylene glycol is used to provide freeze protection in the cooling system. Suspension of nanoparticles in the standard engine heat transfer fluid enhances the thermal conductivity and heat transfer; it has the ability to reduce the size, weight and number of heat exchanger in engine cooling, and eventually results in smaller cooling system and lighter vehicles.

Physically, two cooling systems are used for hybrid electric vehicles, namely higher temperature system for cooling the combustion engine and lower temperature system for cooling the power electronics. Related research (Dileep, Timofeeva, Yu, & France, 2013) showed that thermal conductivity enhancement of graphitic nanofluids in 50/50 mixture of ethylene glycol and water is in the range of 50%-130% at 5 vol% nanoparticles compared to standard engine base fluid at room temperature; thus, nanofluids are promising option to eliminate the lower temperature cooling system so that all cooling is done with a single higher temperature cooling system.

Another nanofluids application in the transportation industry can be found in lubrication. Dispersion of nanoparticles of molybdenum disulfide (MoS_2) into poly-alpha-olefin (PAO) has been shown to reduce friction and wear in lubricant and thus increasing the lifetime and fuel efficiency of vehicle components (Demas, Timofeeva,

Routbort, & Fenske, 2012). Using Raman spectroscopy, they showed that the existence of a thin film between the nanoparticles and rubbing surface is responsible for the improved properties.

2.5.2 Electronics Cooling

Industry trend that is moving towards miniaturisation and higher operating speed is driving the need for more advanced cooling technology in electronics industry. For example, proper cooling system is necessary to ensure smart phone or tablet computer can run for hours with small batteries and stay cool to human touch. However, current air cooling technology for heat removal has been stretched to the limit owing to poor heat transfer property. One alternative for heat control is liquid cooling which has higher heat transfer property compared to air cooling. In view of this, nanofluids with enhanced thermal conductivity have emerged as the alternative heat transfer fluid over water in electronic cooling technology.

Tsai et al. (2004) used water based nanofluids as heat transfer fluid for conventional circular heat pipe and it was designed as a heat spreader for the central processing unit (CPU) in a computer. The result indicated that there is a remarkable decrease in the thermal resistance of the heat pipe filled with nanofluids, which is 20%-37% lower than that of using deionised water. Later, Ma et al. (2006) developed nanofluids based oscillating heat pipe, where experimental results showed that the heat transport capability noticeably increases; for example, at the input power of 80W, 1 vol% nanofluids can reduce the temperature difference between the evaporator and the condenser from 40.9°C to 24.3°C. Similar success has also been reported in conventional water block cooling for CPU (Roberts & Walker, 2010; Turgut & Elbasan, 2014), in which an enhancement of approximately 20% in the conductance was

observed in water block system using Al_2O_3 nanofluids over deionised water (Roberts & Walker, 2010).

Microchannel heat sink has emerged as one of the effective cooling technologies for electronics cooling. Recently, there is growing interest in employing nanofluids in the microchannel heat sinks. Results showed that thermal performance of nanofluids outperformed water, having significantly higher average heat transfer coefficient and hence lower thermal resistance (Ho, Wei, & Li, 2010; Kuppusamy, Mohammed, & Lim, 2014; Mohammed, Gunnasegaran, & Shuaib, 2011).

2.5.3 Nuclear Reactor Application

Nuclear reactors generate electricity by starting a chain reaction in the uranium fuel. This chain reaction causes the fission of uranium atoms into other radioactive elements, and releasing very large amount of heat. This heat needs to be transferred away from the reactor and converted into electricity. However, it is not physically feasible to convert all the heat generated in the nuclear reactor into electricity. A cooling system is necessary to ensure nuclear reactors operate in a safe mode by removing heat from the reactors during normal operation as well as during shut down. Two physical parameters are important in nuclear reactor coolant, namely enhanced critical heat flux (CHF) and rapid quenching process (Buongiorno & Hu, 2010).

Nanofluids are reported to enhance critical heat flux up to 200% than the base fluid (You, Kim, & Kim, 2003) and have been proposed as nuclear coolant for waste heat removal system and standby safety system for emergency. Buongiorno et al. (2008) explored the potential use of nanofluids as main reactor coolant in pressurised water reactor (PWR). It indicated that the use of nanofluids with at least 32% higher CHF could enable a 20% power density uprate in current plants without changing the fuel assembly design. Consequently, the potential use of nanofluids has also been

investigated in the enhancement of in-vessel retention (IVR) capability in the severe accident management strategy implemented by certain light-water reactors (Buongiorno et al., 2009). It showed that the nanofluids system enables 40% decay heat removal enhancement for a given margin of CHF.

2.5.4 Other Applications

Other than the aforementioned potential applications, nanofluids are good alternatives to improve heat transfer performance in many situations. For example, nanofluids have a potential application in the biomedical industry in producing effective cooling around the surgical region. Thus, it enhances the chance of survival for patients and reduces the risk of organ damage. In the renewable energy industry, nanofluids with enhanced heat transfer properties have the potential to improve the efficiency of solar system, substantially reducing compactness of solar devices to achieve energy saving. Nanofluids have also other potential applications in many major industries for example defence, space, chemical, laser, oil and gas, printing and textiles. More details of the potential application of nanofluids are presented in recent review papers (Saidur, Leong, & Mohammad, 2011; Taylor et al., 2013; Yu et al., 2008).

2.6 Summary

This chapter furnished literature review on the present development of nanofluids. It has shown that classical theories failed to explain the enhanced thermal conductivity and viscosity of nanofluids compared to that of base fluids. Experimental works showed that the thermal conductivity and viscosity enhancement are not only dependent on particle volume fraction as mentioned in classical theories but also depend on particle size and temperature. In order to explain the unusual thermal transport of nanofluids, three potential thermal conduction mechanisms were discussed, namely Brownian motion of nanoparticles, Brownian induced micro-convection in base fluid and

nanoparticle aggregation. However, the evaluation showed that large contradictions were reported on the significance of the above-mentioned nanofluids parameters on thermal conductivity and viscosity as well as potential thermal conduction mechanisms. As stated in Section 1.2, the major causes on the conflicting data on thermal conductivity and viscosity are mainly attributed to poor characterisation of nanofluids especially sample polydispersity and hydrodynamic particle size measurement. As thermal conductivity enhancement is always accompanied by viscosity enhancement, the nanofluids efficiency evaluation by comparing both enhancements was presented. At the end of the chapter, potential applications of nanofluids in the fields of transportation, electronics, nuclear reactor and others were reviewed. Nanofluids have proven its capability of making breakthrough in cooling technology.

CHAPTER 3: METHODOLOGY

In this chapter, the methodology of molecular dynamics simulation used in this thesis is presented. This chapter begins with an introduction on molecular dynamics simulation. Then, the main focus of this chapter that is the process of equilibrium molecular dynamics simulation integrated with the Green Kubo is explained in detail. Finally, the validation on the simulation method against experimental results and analytical theories are discussed.

3.1 Molecular Dynamics Simulation

Molecular dynamics (MD) simulation is a computer simulation where the atomic positions are obtained by numerically solving differential equations of motion; the positions are connected in time and provide information on the dynamics of individual atoms as in a motion picture (Allen & Tildesley, 1987). The basic working principle of MD is purely based on classical mechanics without relying on any underlying assumptions. In MD simulation, the force acting on a particle can be determined from the knowledge of inter-atomic potential between atoms, which is given by:

$$\mathbf{F}_i = -\nabla_i U \quad (3.1)$$

where \mathbf{F}_i is the force exerted on the particle i ; U is the inter-atomic potential between atoms. Based on the information of force, acceleration of atom of particle i can be calculated from Newton's second law of motion, given by:

$$\mathbf{F}_i = m\mathbf{a}_i \quad (3.2)$$

where m is the mass of particle i and \mathbf{a}_i is its acceleration. Therefore, the velocity and position of particle i can be updated from the information on acceleration, they are given by:

$$\mathbf{v}_i = \mathbf{v}_i^o + \mathbf{a}_i t \quad (3.3)$$

$$\mathbf{r}_i = \mathbf{r}_i^o + \mathbf{v}_i t + \frac{1}{2} \mathbf{a}_i t^2 \quad (3.4)$$

where \mathbf{v}_i and \mathbf{r}_i are velocity and position of particle i at time t , respectively; superscript o is the initial value for particle i . After the updates on atomic velocity and position are done, Equation 3.1 to Equation 3.4 is repeated for time $t + \Delta t$ for N particles in the system. The working principle of MD is shown in Figure 3.1. Based on the trajectories of large collection of particles in the system, the average values of properties such as structural and thermal transport properties can be determined via statistical mechanics.

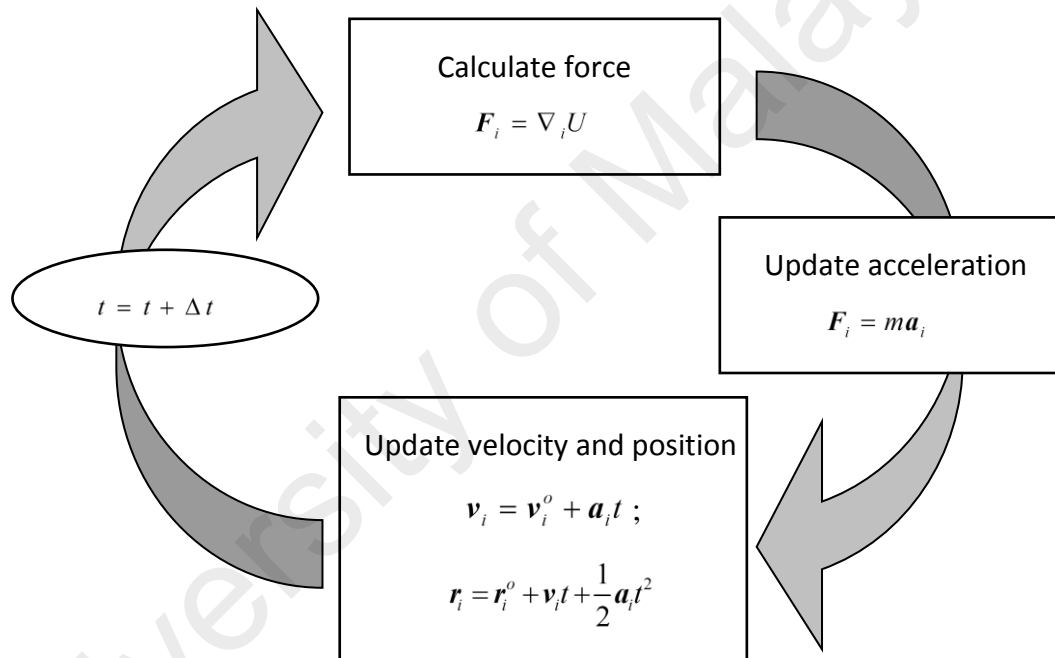


Figure 3.1: Working principle of MD.

MD simulation can be used for dynamic phenomena in equilibrium (EMD) or non-equilibrium (NEMD) state. NEMD method is used to measure the response of macroscopic properties to the gradient of external fields such as force, temperature or chemical potential. For example, if temperature gradient is applied, the response is heat flow; the thermal conductivity can be determined from the amount of heat flow. However, no gradient of external fields is applied in EMD method, it only describes the

reaction of an equilibrium system to a small external perturbation via linear response theory (Hansen & McDonald, 1986; McQuarrie, 2000). Green Kubo formulas (Kubo, Yokota, & Nakajima, 1957) is the results of linear response theory in statistical mechanics, transport coefficients such as thermal conductivity, shear viscosity and diffusion coefficient can be expressed as time integral of appropriate time autocorrelation functions.

In this thesis, MD simulation integrated with Green Kubo method was used to investigate the thermal transport of nanofluids. The nanofluids were modelled by dispersing copper nanoparticles into liquid argon. This work was carried out using Large-scale Atomic/Molecular Massively Parallel Simulator (LAMMPS) (Plimpton, 1995) MD software and visualised by Visual Molecular Dynamics (VMD) (Humphrey, Dalke, & Schulten, 1996). EMD method was chosen over NEMD method mainly for two reasons. First, the transport coefficients such as thermal conductivity, shear viscosity and diffusion coefficient can be calculated from a single simulation in EMD method; whereas different sets of simulations are required for NEMD method in order to create different gradient of interest. Furthermore, EMD method computes the transport coefficient in smaller system size compared to NEMD method, hence reducing computational time and amount (Hess, 2002; Jones & Mandadapu, 2012).

3.2 Methodology of Equilibrium Molecular Dynamics Simulation

Figure 3.2 depicts the flowchart of the present simulation which is MD simulation integrated with Green Kubo method. The details of the flowchart will be discussed in the subsequent section. Time step $\Delta t = 4\text{fs}$ was used throughout the simulation. A parallel computing was performed using ten CPUs.

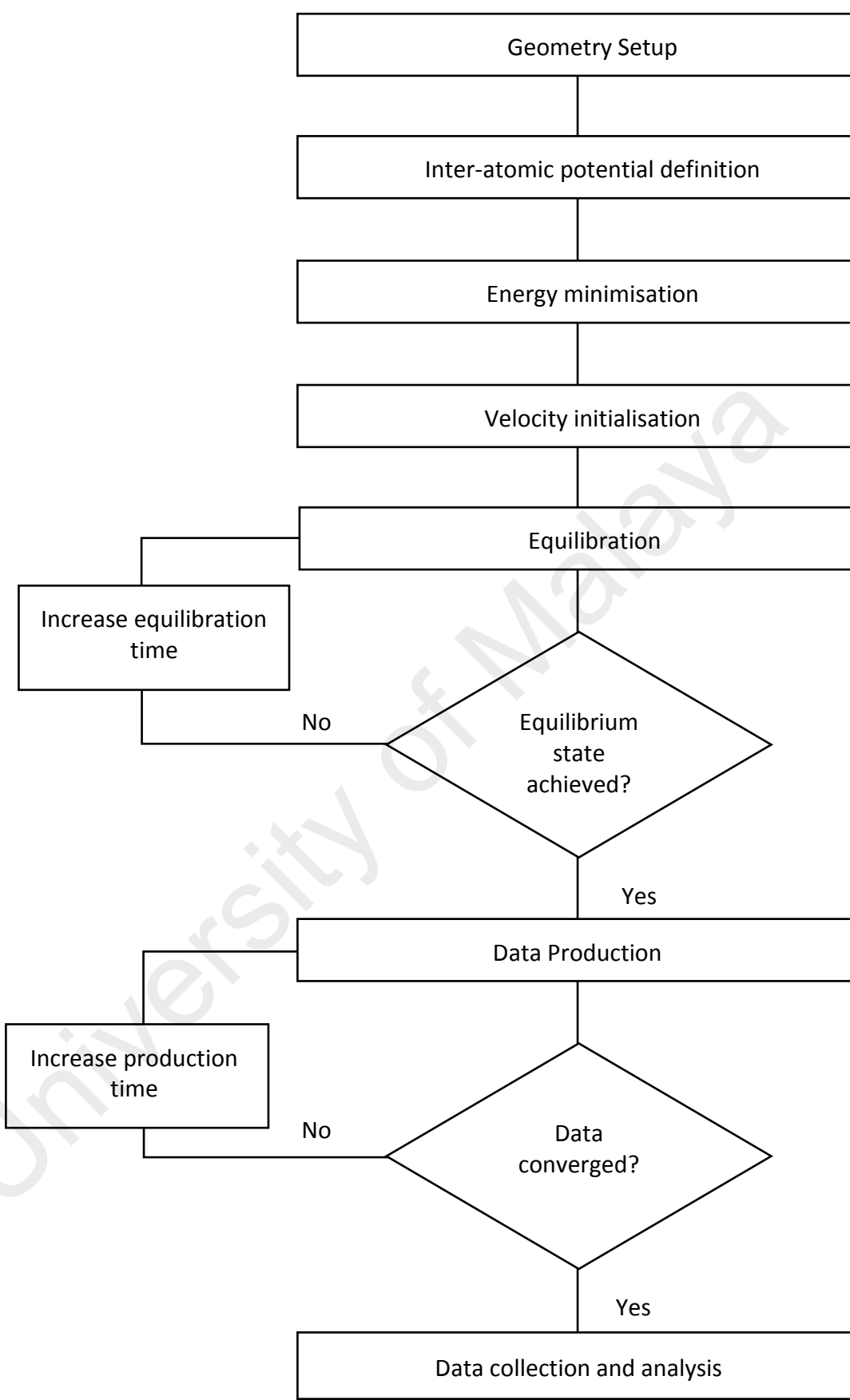


Figure 3.2: Flowchart of MD simulation integrated with Green Kubo method.

3.2.1 Geometry Setup

Nanofluids system was modelled by suspending copper nanoparticles in liquid argon. In this geometry setup, the argon atoms were arranged in face-centered cubic (FCC) with a lattice constant 5.72 \AA and spherical regions were carved out by placing copper atoms with FCC lattice constant 3.6153 \AA . The molecular weight of argon and copper are 39.948 g/mol and 63.55 g/mol , respectively. Periodic boundary condition (PBC) was applied in three dimensional of the simulation system to permit the modelling of very large system, hence overcome differences between molecular microscale and macroscale. In the effect of PBC, the simulation box of interest is surrounded by identical images of itself, as if the simulation box is in the middle of an infinite phase, as illustrated in Figure 3.3.

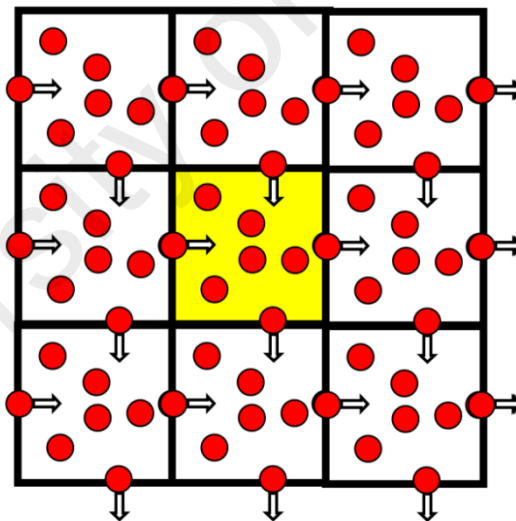


Figure 3.3: Periodic boundary condition (PBC), the simulation box of interest (marked as yellow) is surrounded identical images of itself.

Four different nanofluids systems were modelled to achieve different objectives in this thesis where the details are shown in Table 3.1. In nanofluids modelling, the suspension of nanoparticles can be chosen either single nanoparticle or multi-nanoparticle. The suspension of single nanoparticle as modelled in the system #1

represents well-dispersed state in the base fluid without taking into account effects of collision between nanoparticles. Such assumption is valid for low particle volume fraction in nanofluids. In system #1, the size of the simulation box will be changed proportionally to the particle diameter in order to maintain the fixed particle volume fraction of 2.24 vol%. On the other hand, suspensions of multi-nanoparticle were modelled in system #2, #3 and #4. In such suspensions, effects of interaction between nanoparticles are considered and the particle volume fraction is controlled by varying the number of nanoparticles in a fixed size simulation box. With the effects of interaction between nanoparticles, suspension of nanoparticles can be modelled in well-dispersed state or aggregated state. According to Kang et al. (2012), well-dispersed state can be modelled by placing the nanoparticles at certain distances so that it has insufficient time to aggregate within the time domain; whereas the aggregated state can be modelled by initially placing the nanoparticles close to each other so that it enables aggregation to take place within the time domain. The details of system #1 and #2 are presented in Table 3.2 and Table 3.3, respectively. The details of system #3 and #4 which are identical are shown in Table 3.4 where both systems have the same particle diameter of 20 Å but are different only in dispersing states. In this case, both systems have the same number of atoms in the simulation box but differ in the initial positions of nanoparticles. The snapshots of the four systems are displayed in Figure 3.4.

Table 3.1: Four different nanofluids systems were modelled.

Nanofluids System	Single/multi nanoparticle	Well-dispersed/aggregated	Particle diameter (Å)	Particle volume fraction (vol%)	Temperature (K)
#1	single	well-dispersed	16-36	2.24	86
#2	multi	well-dispersed	15	2.19-7.65	86
#3	multi	well-dispersed	20	2.59-7.77	86-101
#4	multi	aggregated	20	2.59-7.77	86

Table 3.2: System #1- Nanofluids with single nanoparticle in well-dispersed state.

Particle volume fraction (vol%)	Particle diameter (Å)	No. of copper atom	No. of argon atom	Total atom in system	Size of simulation box (Å ³)
2.24	16	177	2,005	2,182	95,820
	20	369	3,913	4,282	187,149
	24	627	6,711	7,398	323,394
	28	959	10,751	11,710	513,538
	32	1,481	16,015	17,496	766,563
	36	2,093	22,797	24,890	1,091,454

Table 3.3: System #2- Nanofluids with multi-nanoparticle in well-dispersed state, with particle diameter of 15 Å.

Particle volume fraction (vol%)	No. of nano-particle	No. of copper atom	No. of argon atom	Total atoms in system	Size of simulation box (Å ³)
2.19	4	600	6,740	7,340	323,393
3.83	7	1,056	6,611	7,667	
5.47	10	1,512	6,482	7,994	
6.56	12	1,816	6,396	8,212	
7.65	14	2,120	6,310	8,430	

Table 3.4: System #3 & #4- Nanofluids with multi-nanoparticle in well-dispersed and aggregated state, with particle diameter of 20 Å.

Particle volume fraction (vol%)	No. of nano-particle	No. of copper atom	No. of argon atom	Total atoms in system	Size of simulation box (Å)
2.59	2	702	6,742	7,444	323,393
3.89	3	1,055	6,651	7,706	
5.18	4	1,412	6,564	7,976	
6.48	5	1,807	6,467	8,274	
7.77	6	2,176	6,380	8,556	

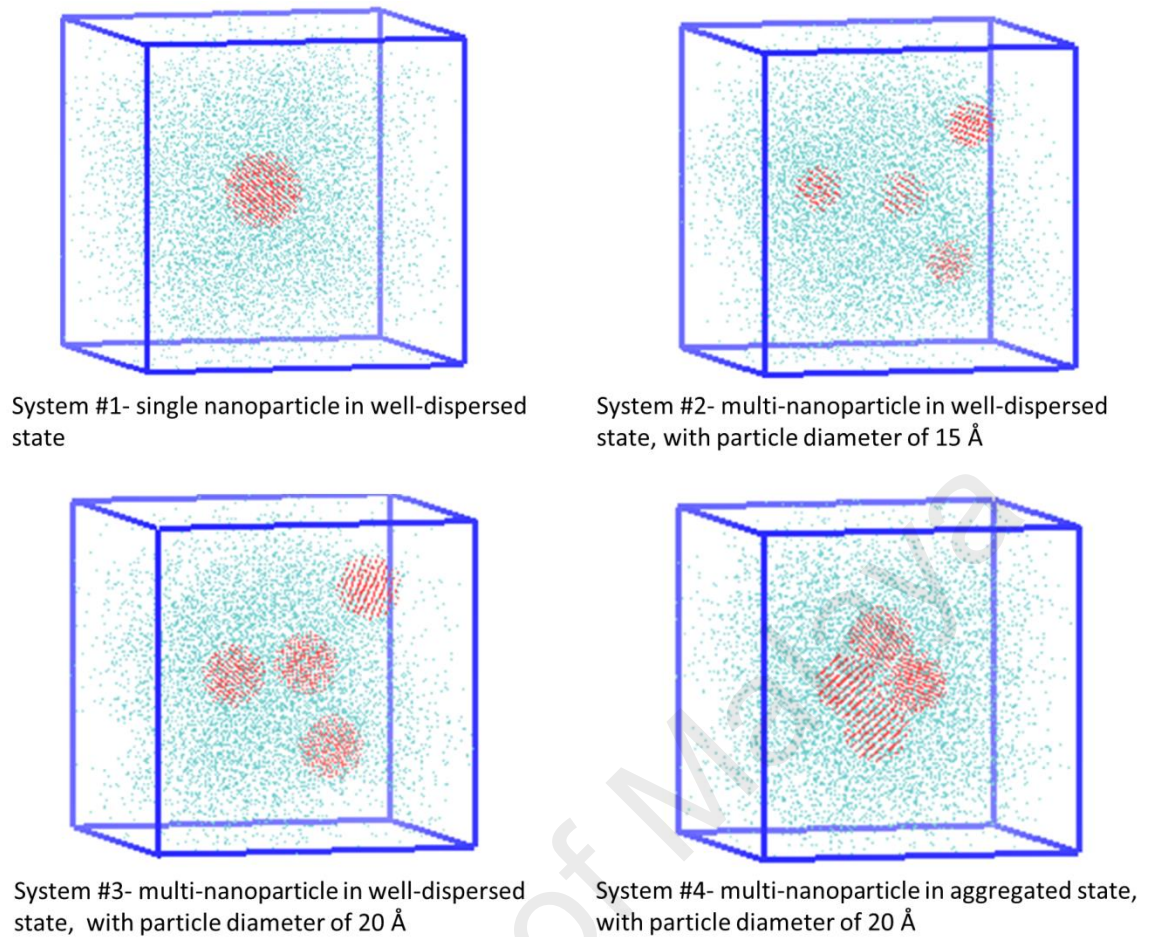


Figure 3.4: Snapshot of four different nanofluids systems.

Other than modelling the nanofluids systems, pure liquid argon was also modelled to validate the present methodology and L-J potential with well-known experimental results. Furthermore, the enhancement on thermal transport properties of nanofluids could be determined by comparing them with liquid argon (base fluid). The simulation box of liquid argon has a volume of $323,393 \text{ \AA}^3$ and contains 6,912 atoms. According to a finite size study reported by Sarkar and Selvam (2007), the simulation result of pure liquid argon was in good agreement with experimental data when the number of argon atoms is more than 500. Therefore, to be on the safe side, the number of argon atoms in the present work was modelled over 2,005 atoms as shown in Table 3.2 to Table 3.4

3.2.2 Inter-atomic Potential Definition

The real input for MD simulation is the inter-atomic potential. For copper-argon nanofluids, there will be three interactions, namely Ar-Ar, Cu-Cu and Ar-Cu. In this work, Lennard-Jones (L-J) potential (Lennard-Jones & Devonshire, 1937) was used to describe the three inter-atomic interactions. The L-J potential, Φ , is defined by:

$$\Phi(r_{ij}) = 4\varepsilon \left[\left(\frac{\sigma}{r_{ij}} \right)^{12} - \left(\frac{\sigma}{r_{ij}} \right)^6 \right] \quad (r_{ij} < r_{cutoff}) \quad (3.5)$$

where r_{ij} is the distance between atom i and j ; ε and σ are L-J potential parameters, representing interaction strength and inter-atomic length scale, respectively. The first term of L-J equation r^{-12} is responsible for the repulsion at short distance and the second term r^{-6} is responsible for the attraction at long distance. The potential parameters for the three interactions are listed in Table 3.5 and the potentials are plotted in Figure 3.5. As shown in Figure 3.5, the L-J potential gets weaker and close to zero at large separation distance between atoms. In order to reduce computational amount in this work, the L-J potential was set at a cut-off radius of $2.8\sigma_{ar}$, which is in the proposed range of $1.6-3.6\sigma_{ar}$ by Vogelsang, Hoheisel, and Ciccotti (1987). When the separation distance of atoms is larger than the cut-off radius, L-J potential is defined by:

$$\Phi(r_{ij}) = 0 \quad (r_{ij} \geq r_{cutoff}) \quad (3.6)$$

The cross-interaction potential of Ar-Cu was calculated using Lorentz Berthelot (LB) mixing rule (Allen & Tildesley, 1987), which is given by:

$$\varepsilon_{ar-cu} = \sqrt{\varepsilon_{ar-ar} * \varepsilon_{cu-cu}} \quad (3.7)$$

$$\sigma_{ar-cu} = \frac{\sigma_{ar-ar} + \sigma_{cu-cu}}{2} \quad (3.8)$$

This LB mixing rules is used to mix the L-J parameters between Ar-Ar and Cu-Cu for the cross interaction L-J parameters.

Table 3.5: L-J potential parameters for copper-argon nanofluids.

	Ar-Ar (Haile, 1992)	Cu-Cu (Yu & Amar, 2002)	Ar-Cu
ϵ (kJ/mol)	0.2381	9.4500	1.5000
σ (Å)	3.4050	2.3377	2.8714

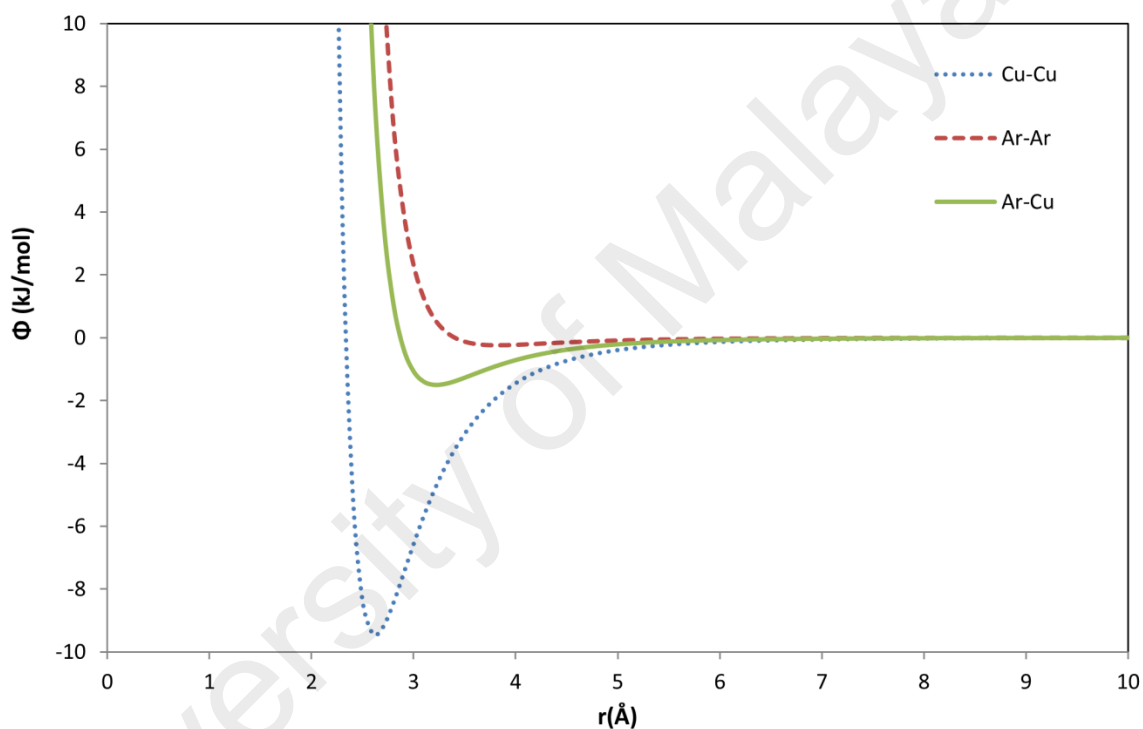


Figure 3.5: Lennard Jones potential for Ar-Ar, Cu-Cu and Ar-Cu interactions.

3.2.3 Energy Minimisation

The initial geometry setup may produce bad contacts that contain higher energy, for example, two atoms are too near to each other and having higher repulsive energy.

Therefore, the process of energy minimisation is required to optimise the geometry setup with minimum energy arrangements to prevent the simulation from “blowing up”.

The MD integrator may fail if the simulation is having atoms or molecules with too

large force. The process of energy minimisation is performed by adjusting the starting positions of atoms to the nearby local energy minimum. Polak-Ribiere of conjugate gradient algorithm was used in this work. In every iteration, the force gradient is combined with previous iteration information to determine the optimum direction for a new search which is perpendicular to the previous search direction. The algorithm requires modest computational amount and time, and hence, is efficient for solving large scale problems. The minimisation process will be terminated if any of the criterions below is fulfilled:

- (a) the change in energy between iteration is less than a certain defined threshold
- (b) the global force vector is less than a certain defined threshold
- (c) the line search fails to reduce the energy during the last iteration
- (d) the number of iterations exceeds defined threshold
- (e) the number of total force evaluation exceeds defined threshold

In this work, the threshold for the change in energy and global force vector were set zero while the maximum number of iterations and total force evaluation were set 10,000 time steps. As a result, zero line search was the stopping criterion in this work. After the process of energy minimisation is terminated, the optimised geometry serves as a starting geometry for the MD simulation run.

3.2.4 Velocity Initialisation

After setting the initial atomic positions, the next step is to initialise the atomic velocities by assigning random initial velocities. Appropriate numerical method is required to predict the trajectories for all the particles in the system by solving the differential equations of motion from Equation 3.1 to Equation 3.4. Velocity Verlet algorithm (Allen & Tildesley, 1987) was employed as the numerical method for this work, which is given by:

$$\mathbf{r}(t + \Delta t) = \mathbf{r}(t) + \mathbf{v}(t)\Delta t + \frac{1}{2}\mathbf{a}(t)\Delta t^2 \quad (3.9)$$

$$\mathbf{v}(t + \Delta t) = \mathbf{v}(t) + \frac{1}{2}[\mathbf{a}(t) + \mathbf{a}(t + \Delta t)]\Delta t \quad (3.10)$$

Firstly, the new positions at time $t + \Delta t$ are calculated based on Equation 3.9. After that, the velocities are calculated at half step using:

$$\mathbf{v}(t + \frac{1}{2}\Delta t) = \mathbf{v}(t) + \frac{1}{2}\mathbf{a}(t)\Delta t \quad (3.11)$$

The forces and accelerations are then calculated at time $t + \Delta t$, and the velocities are calculated at full step:

$$\mathbf{v}(t + \Delta t) = \mathbf{v}(t + \frac{1}{2}\Delta t) + \frac{1}{2}\mathbf{a}(t + \Delta t)\Delta t \quad (3.12)$$

At this point, the positions and velocities at time $t + \Delta t$ are completed, and the system will be advanced to the next time step and repeated. The process of the Velocity Verlet algorithm is shown in Figure 3.6. Velocity Verlet algorithm is seen to require less computational amount as only one set of positions, velocities and forces need to be carried out at one time.

3.2.5 Equilibration

The MD simulation commenced with initial atomic positions and velocities, however, the initial configurations are not representative of the state of equilibrium. Therefore, the equilibration process must be performed for a certain amount of time to relax the initial configurations to equilibrium state prior to data production. In the present work, the system was equilibrated for 100,000 time steps (0.4 ns) under canonical ensemble (NVT) and the equilibration steps were ignored for the data production. The temperature was kept constant using Nose-Hoover thermostat (Hoover, 1985).

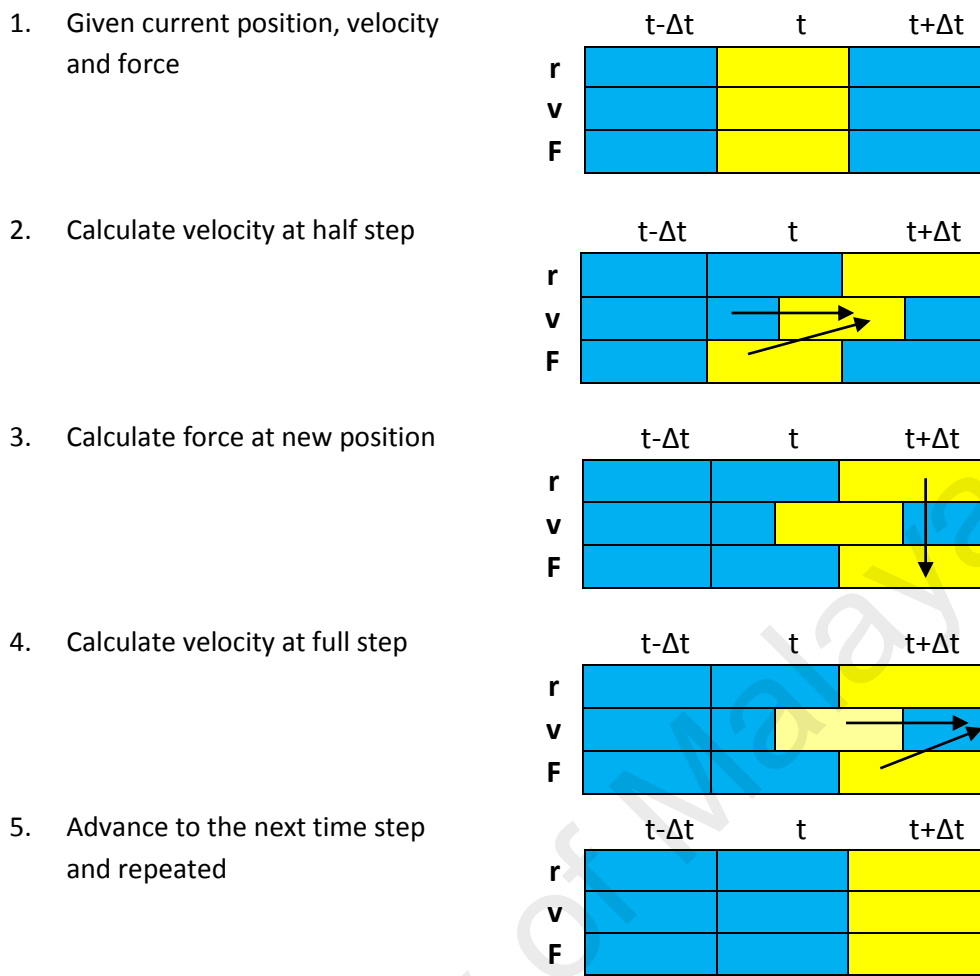


Figure 3.6: Velocity Verlet algorithm (Allen & Tildesley, 1987).

3.2.6 Data Production

Once the system has achieved equilibrium state, data production can be initiated to compute the transport and structural properties. A 1000,000 time step (4 ns) was used for data production under micro-canonical ensemble (NVE). Data of transport properties such as thermal conductivity and shear viscosity were collected in a correlation length of 5,000 time steps (20 ps). To improve the statistics, each transports properties were further averaged over five different initial velocities.

3.2.6.1 Transport Properties

(a) *Thermal Conductivity*

The Green Kubo relation for thermal conductivity, is given by (McQuarrie, 2000):

$$k = \frac{1}{3Vk_B T^2} \int_0^\infty \langle \mathbf{J}_i(0) \mathbf{J}_i(t) \rangle dt \quad (3.13)$$

where k is the thermal conductivity, v is the volume of simulation box, T is the system temperature, k_B is the Boltzmann constant, and $\langle \mathbf{J}(0) \mathbf{J}(t) \rangle$ is the heat current autocorrelation function (HCACF). The heat current, \mathbf{J} , is given by:

$$\mathbf{J} = \left[\sum_{j=1}^N \mathbf{v}_j E_j - \sum_{\alpha=1}^2 h_\alpha \sum_{j=1}^{N_\alpha} \mathbf{v}_{\alpha j} \right] + \frac{1}{2} \left[\sum_{i=1}^N \sum_{j=1, j \neq i}^N \mathbf{r}_{ij} (\mathbf{v}_j \cdot \mathbf{F}_{ij}) \right] \quad (3.14)$$

where \mathbf{v}_j is the velocity of particle j ; E_j is kinetic and potential energy per atom; h_α is average partial enthalpy of species α ; \mathbf{r}_{ij} and \mathbf{F}_{ij} are displacement and interacting force between particle i and j , respectively; and N is total number of particles. The first term is referred as the convection of particles, which is internal energy being the summation of kinetic energy and potential energy. The second term is referred as collision or virial, which is the interaction between particles or the work done by the stress tensor. The average partial enthalpy h_α refers to the average of the sum of kinetic energy, potential energy and average virial per particle, which is given by:

$$h_\alpha = \frac{1}{N_\alpha} \sum_{j=1}^{N_\alpha} (E_j + \mathbf{r}_j \cdot \mathbf{F}_j) \quad (3.15)$$

The average partial enthalpy is critical in determining the thermal conductivity of a multi-component system. Partial enthalpy is always zero for single component system but it is not zero for multi-component system and must be excluded from the convective term. The exclusion of the average partial enthalpy is important since such quantity just moves silently with diffusing particles, but the associated energy is not being exchanged and does not contribute to heat conduction (Babaei, Keblinski, & Khodadadi, 2012).

Thus, a well-defined partial enthalpy is essential in order to avoid anomalous high thermal conductivity in multi-component system.

(b) **Shear Viscosity**

The Green Kubo relation for shear viscosity, is given by (McQuarrie, 2000):

$$\eta_{xy} = \frac{V}{k_B T} \int_0^{\infty} \langle P_{xy}(0) P_{xy}(t) \rangle dt \quad (3.16)$$

where η is the viscosity, and $\langle P(0)P(t) \rangle$ is stress autocorrelation function (SACF). The stress tensor P is given by:

$$P_{xy} = \sum_j m_j v_{xj} v_{yj} + \frac{1}{2} \sum_{i \neq j} r_{xij} F_{yij} \quad (3.17)$$

As $P_{xy} = P_{yx}$, thus only P_{xy} , P_{xz} and P_{yz} were taken into account for autocorrelation function. The SACF is derived from the scalar of off-diagonal components of the stress tensor, whereas the HCACF is calculated from the vector of heat flow in the system.

(c) **Diffusion Coefficient**

The Green Kubo relation for diffusion coefficient, is given by (McQuarrie, 2000):

$$D = \frac{1}{3} \int_0^{\infty} \langle \mathbf{v}_i(0) \mathbf{v}_i(t) \rangle dt \quad (3.18)$$

where D is the diffusion coefficient, and $\langle \mathbf{v}(0) \mathbf{v}(t) \rangle$ is the velocity autocorrelation function (VACF). Meanwhile, the diffusion coefficient of Einstein method is given by:

$$D = \frac{1}{6} \lim_{t \rightarrow \infty} \frac{d}{dt} \langle |\mathbf{r}(t) - \mathbf{r}(0)|^2 \rangle \quad (3.19)$$

where $|\mathbf{r}(t) - \mathbf{r}(0)|^2$ is mean square displacement (MSD), which is the displacement (vector) travelled by the atom over time interval length t , and $\langle \dots \rangle$ is the averaging over

all the atoms. Equation 3.19 can be plotted as MSD versus time, and the diffusion coefficient can be extracted from 1/6 of the limiting slope.

3.2.6.2 Structural Property

(a) *Radial Distribution Function*

The radial distribution function (RDF) is used to study the structure of crystalline solid, liquid and gas. RDF characterises the structure of matter by describing the probability of finding an atom at a given radial location to a reference atom, is given by (McQuarrie, 2000):

$$g(r) = \left(\frac{N(r)}{\Delta V(r)} \right) / \rho \quad (3.20)$$

where $g(r)$ is the RDF; $N(r)$ is number of atoms in the r^{th} ring from the centre of the reference atom; $\Delta V(r)$ is the volume of the r^{th} ring from the centre of reference atom and ρ is mean number density.

3.3 Validation

Before presenting the results for nanofluids, it is necessary to validate the present methodology and employed inter-atomic potential with well-known experimental results. In this work, validations were conducted for (1) simulation method and employed potential, (2) equilibrium state, (3) data collection on thermal conductivity and (4) data collection on viscosity.

3.3.1 Validation on Simulation Method and Employed Potential

To validate the simulation method and employed potential, the transport and structural properties of liquid argon were validated against experimental results at $T = 86 \text{ K}$, $\rho = 1418 \text{ kg/m}^3$ and 6,912 atoms in a simulation box with a size of 12 lattices in three directions. The compared results on thermal conductivity, shear viscosity and diffusion coefficient are given in Table 3.6. It can be seen that MD simulation computed

the thermal transport properties with an error range of 2.3% to 5.9% compared to the experimental results. Thus, the maximum error of the present work is 5.9%. Besides, the structural property of liquid argon via RDF was also compared with experimental values reported by Yarnell, Katz, Wenzel, and Koenig (1973), as shown in Figure 3.7. The comparison on RDF shows good agreement, all peaks and valleys of MD simulation overlap almost exactly over the experimental values. Thus, it can be concluded that the employed methodology and L-J potential are capable to predict good results.

Table 3.6: Validation on methodology and employed potential for transport properties of pure liquid argon.

	MD simulation	Experimental result	Reference	Error
Thermal conductivity (W/m.K)	0.135	0.132	(Müller-Plathe, 1997)	2.3%
Shear viscosity (mPa.s)	0.293	0.280	(Haile, 1992)	4.6%
Diffusion coefficient (m ² /s)	1.828×10 ⁻⁹	1.942×10 ⁻⁹	(Naghizadeh & Rice, 1962)	5.9%

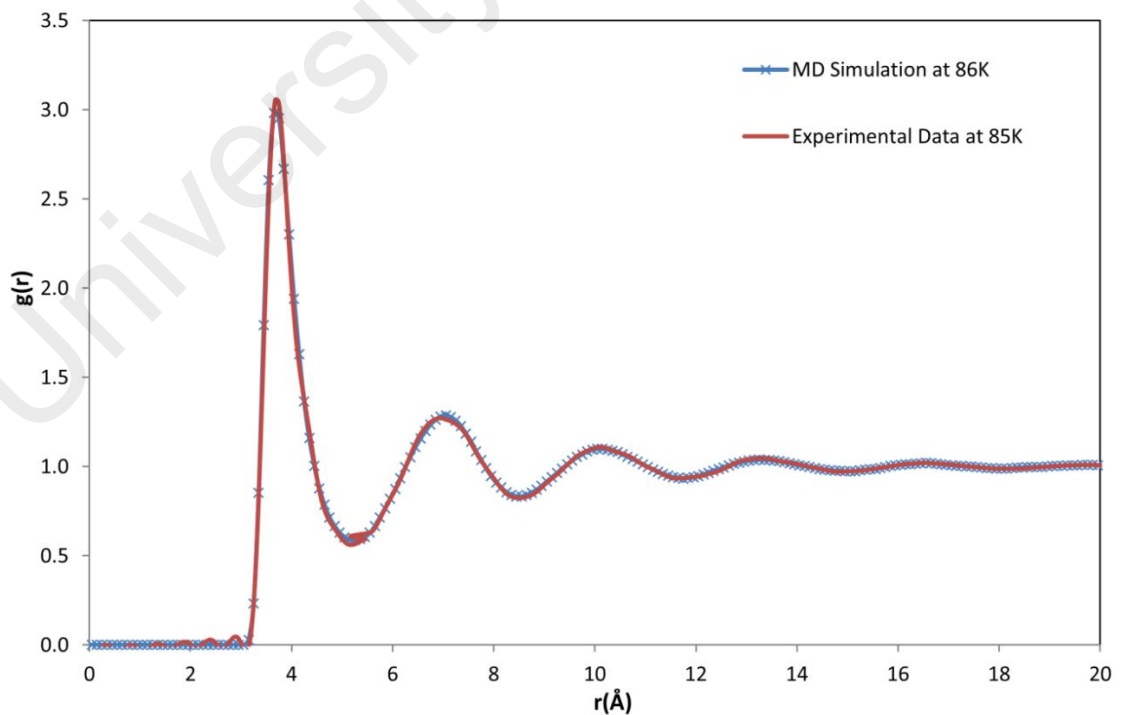


Figure 3.7: Validation on methodology and employed inter-atomic potential for structural property of pure liquid argon, RDF comparison against experimental data.

3.3.2 Validation on Equilibrium State

To check whether equilibrium state has been reached, convergence on temperature and total energy in system as a function of equilibration time was observed. As seen in Figure 3.8 to Figure 3.11, the temperatures of the four nanofluids systems are converged by fluctuating around the setting temperature 86 K. Figure 3.12 to Figure 3.15 show total energy in the systems are converged during equilibration process. It can be seen that the total energy increased with increasing nanoparticle sizes as well as particle volume fractions. The similar trend on particle volume fraction dependence was also reported by Sankar, Mathew, and Sobhan (2008) in a MD simulation for platinum-water nanofluids. The rise in total energy in the system was attributed to the increase in the total number of argon and copper atoms in the system itself. Based on the observed convergences in temperature and total energy, it can be concluded that the four nanofluids system were in equilibrium states.

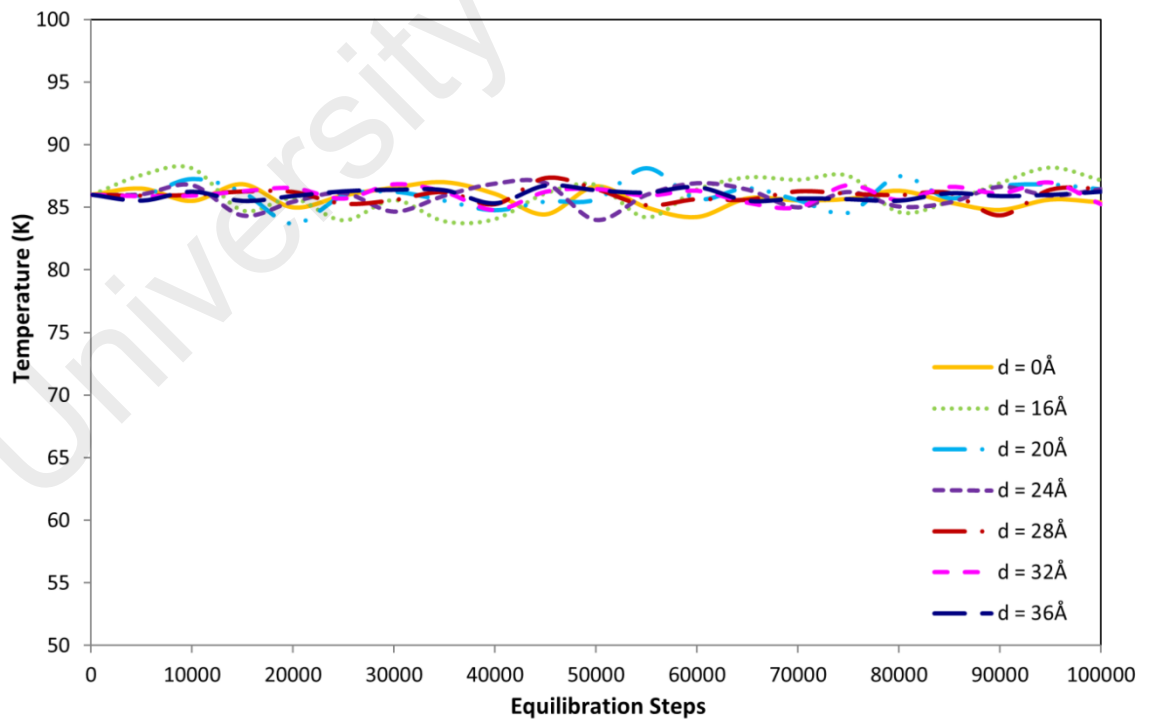


Figure 3.8: Temperature during equilibration process for system #1- 2.24 vol% nanofluids with single nanoparticle in well-dispersed state.

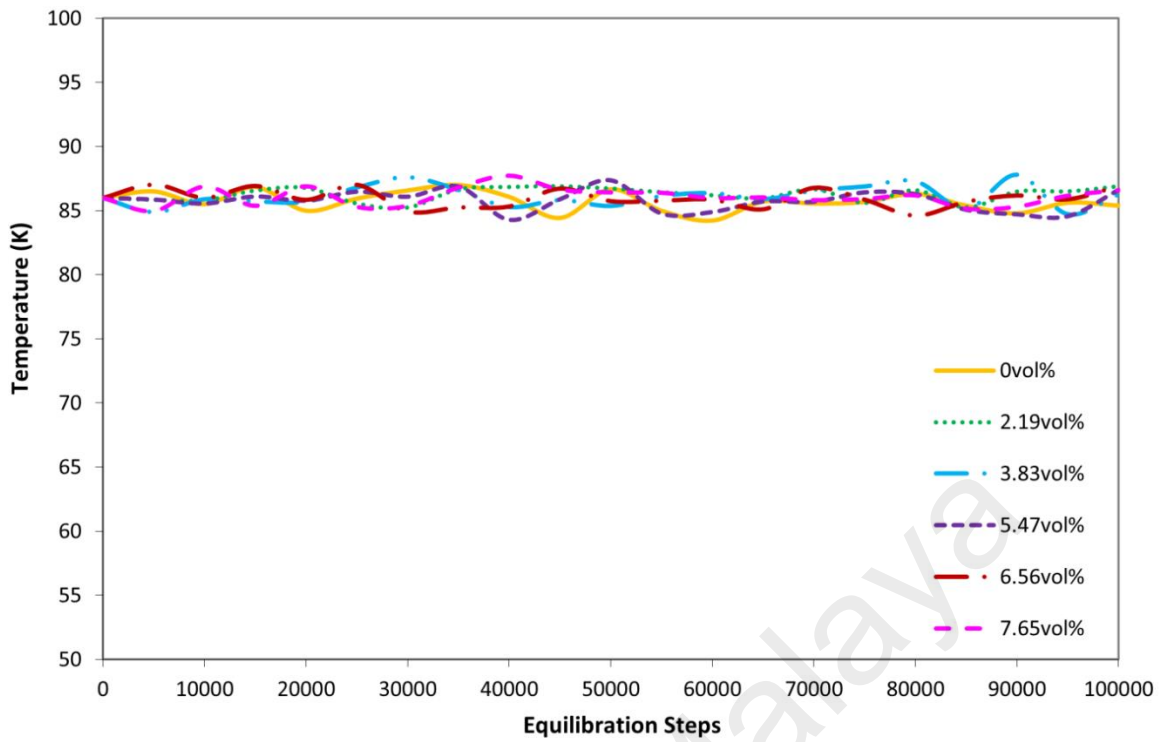


Figure 3.9: Temperature during equilibration process for system #2- nanofluids with multi-nanoparticle in well-dispersed state, with particle diameter of 15 Å.

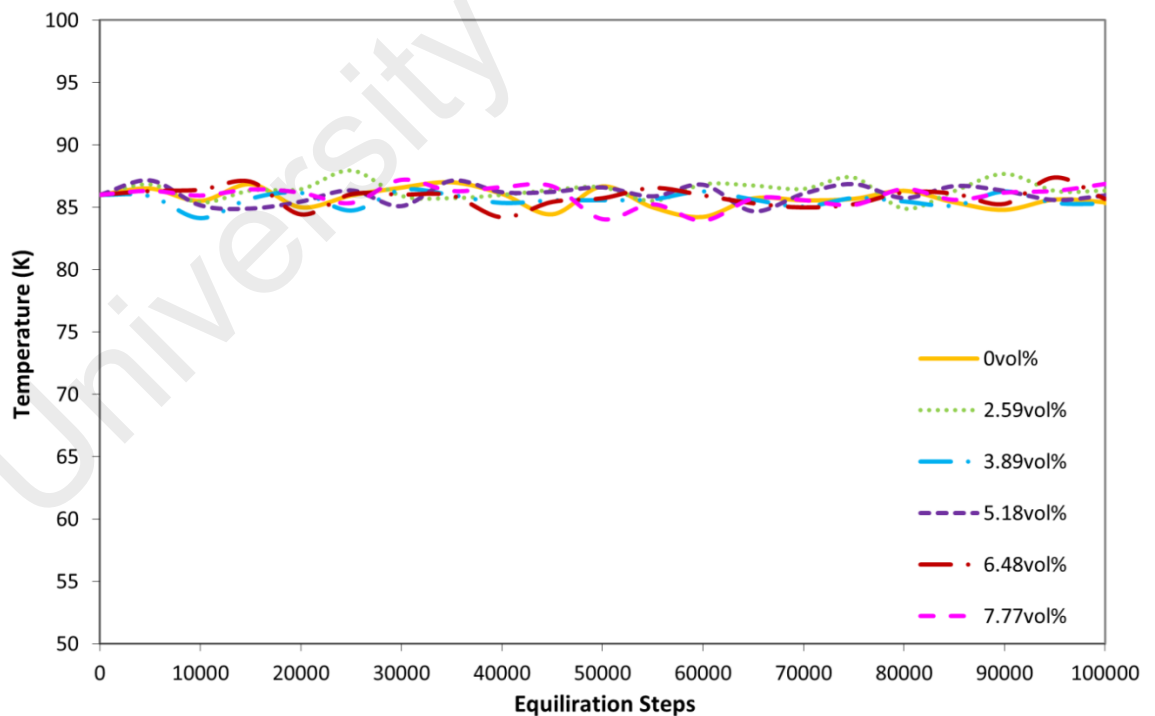


Figure 3.10: Temperature during equilibration process for system #3- nanofluids with multi-nanoparticle in well-dispersed state, with particle diameter of 20 Å.

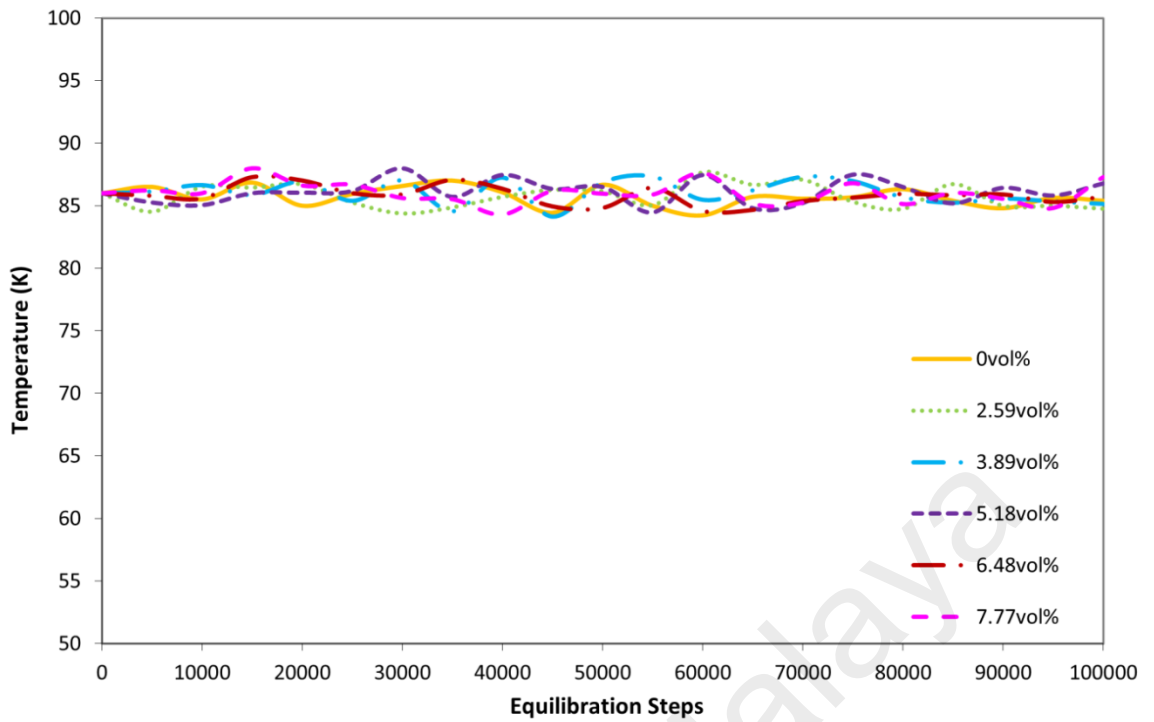


Figure 3.11: Temperature during equilibration process for system #4- nanofluids with multi-nanoparticle in aggregated state, with particle diameter of 20 Å.

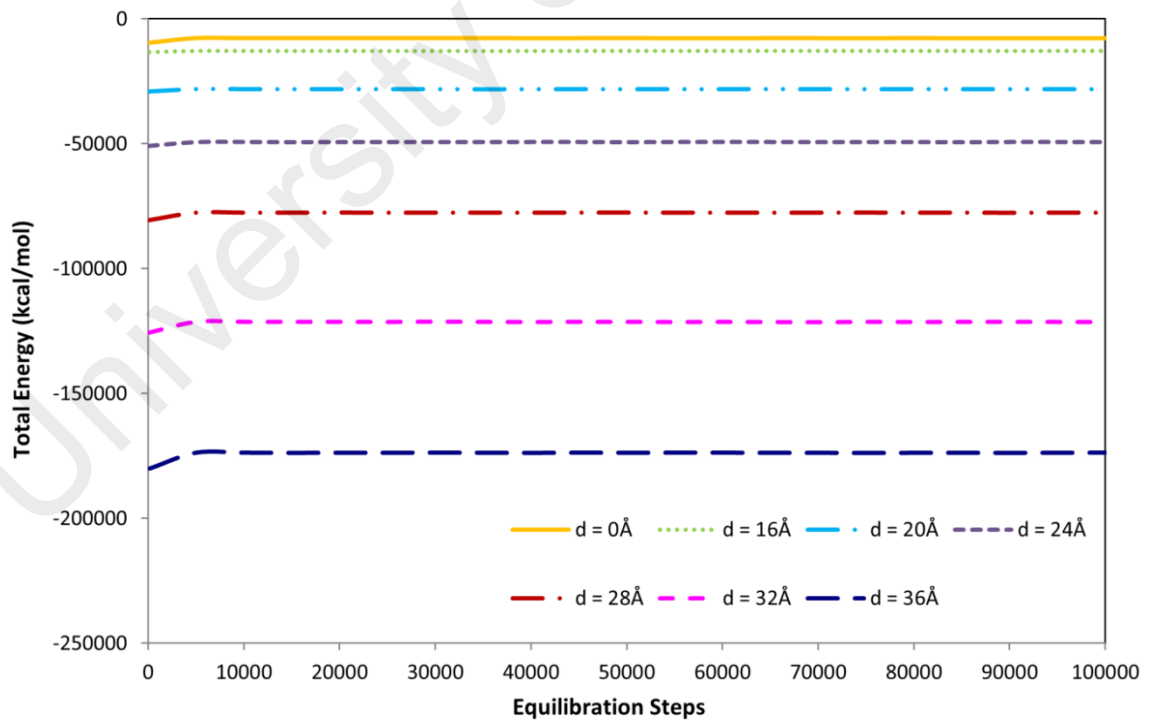


Figure 3.12: Total energy in system during equilibration process for system #1- 2.24 vol% nanofluids with single nanoparticle in well-dispersed state.

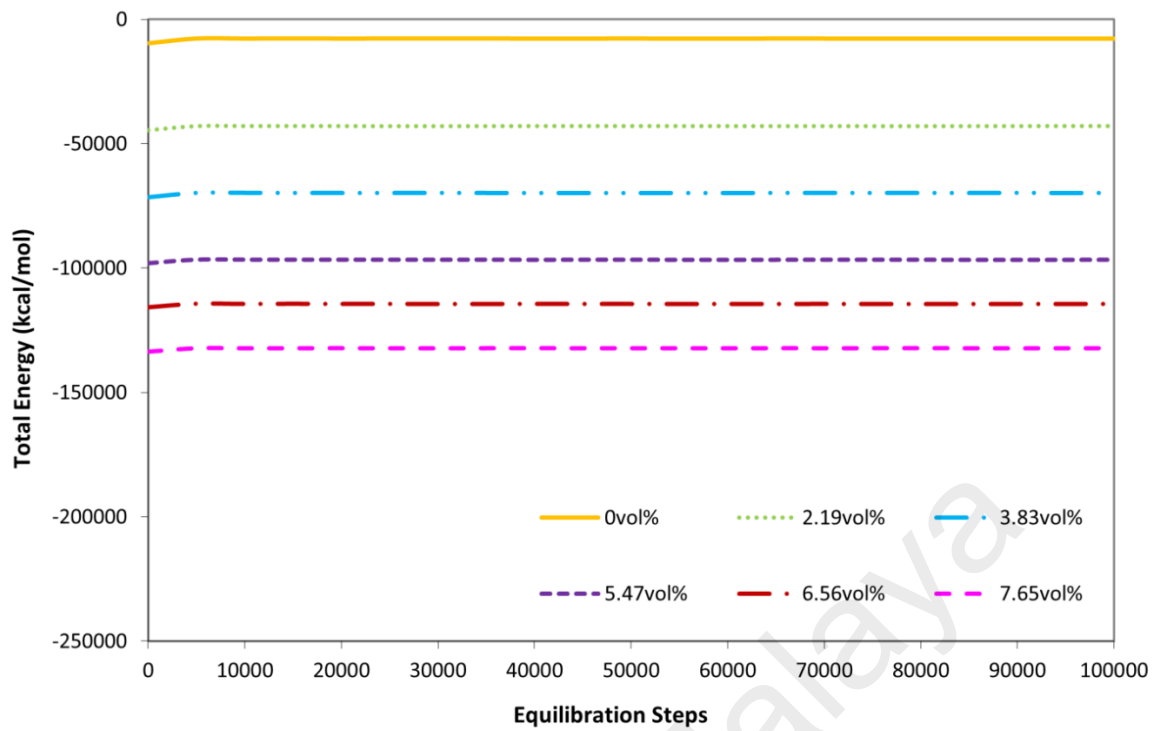


Figure 3.13: Total energy in system during equilibration process for system #2-nanofluids with multi-nanoparticle in well-dispersed state, with particle diameter of 15 Å.

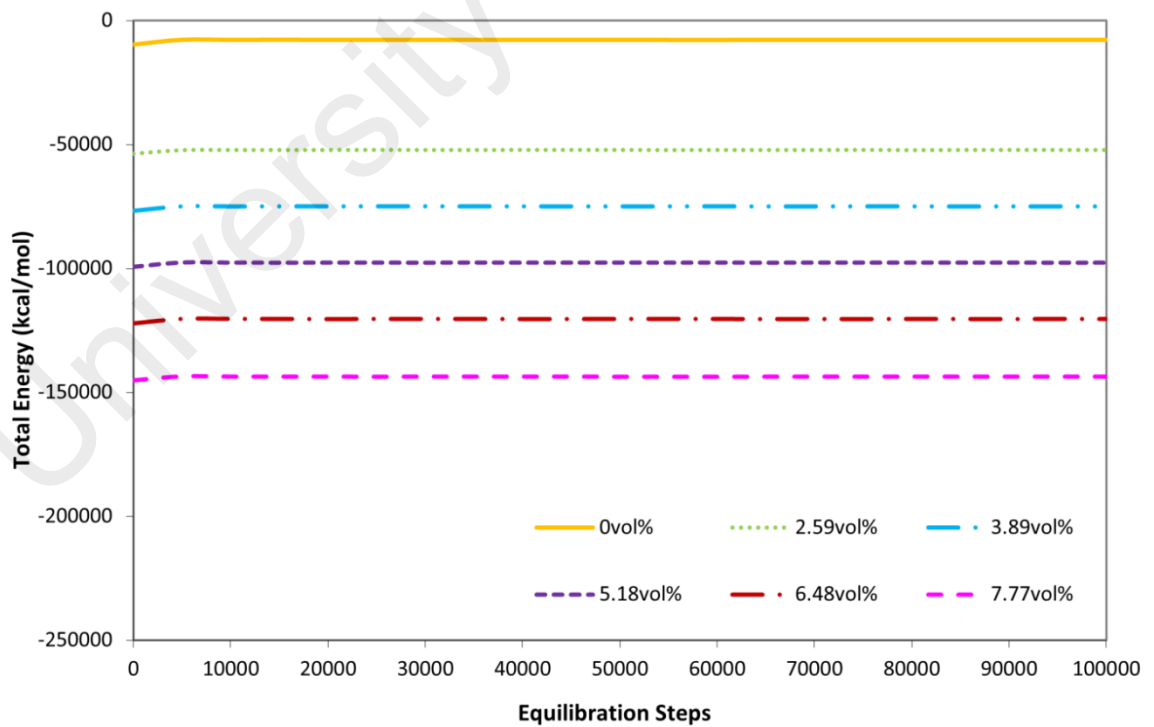


Figure 3.14: Total energy in system during equilibration process for system #3-nanofluids with multi-nanoparticle in well-dispersed state, with particle diameter of 20 Å.

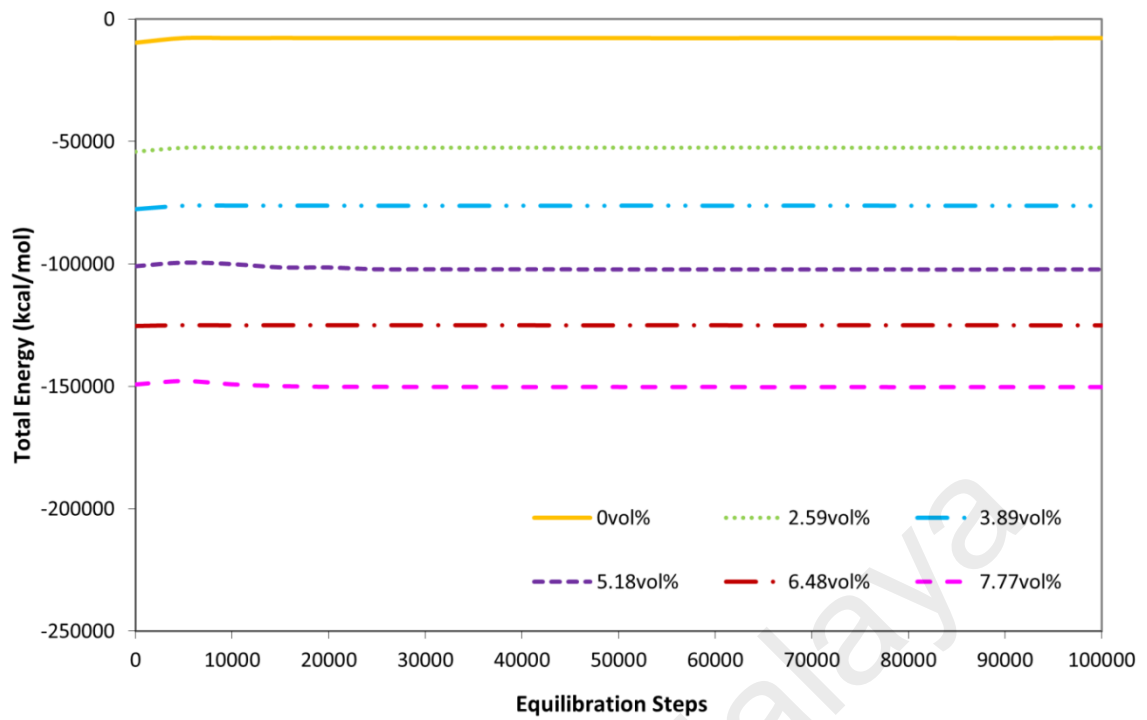


Figure 3.15: Total energy in system during equilibration process for system #4-nanofluids with multi-nanoparticle in aggregated state, with particle diameter of 20 Å.

3.3.3 Validation on Data Collection – Thermal Conductivity

As discussed in Section 3.2.6.1, the area under heat current autocorrelation function (HCACF) is referred as thermal conductivity. The accuracy of thermal conductivity is determined by the convergence of HCACF to plateau within the correlation length. As seen in Figure 3.16 to Figure 3.19, the HCACF of the four nanofluids systems decay well to plateau within the correlation length. Therefore, the correlation length of 20 ps was long enough for the autocorrelation function to be decayed. It was observed that the HCACF of liquid argon decayed to zero exponentially, and this is typical behaviour for a liquid (McGaughey & Kaviany, 2004). The HCACF of nanofluids decayed to zero initially and oscillated between positive and negative before converging to zero. Such oscillation manner was also observed in amorphous phase L-J argon (McGaughey & Kaviany, 2004). Koblinski et al. (2002) pointed out that the negative value of oscillations is attributed to backscattering of atoms, in which the phonons carrying heat

energy are reflected by solid-liquid interface. It is worth noting that when the nanoparticle size and particle volume fraction were increased, the oscillation behaviour became stronger, and hence, resulted in an increase in thermal conductivity of nanofluids. In short, the strong oscillation explained the rather high thermal conductivity in nanofluids compared to pure base fluid.

3.3.4 Validation on Data Collection – Shear Viscosity

As discussed in Section 3.2.6.1, the area under stress autocorrelation function (SACF) is referred as shear viscosity. The accuracy of viscosity is defined by the convergence of SACF to plateau within the correlation length. In this work, viscosity was only calculated for nanofluids systems #2 and #3, which were nanofluids with multi-nanoparticle in well-dispersed state with particle diameter of 15 Å and 20 Å. The SACF of the two systems are presented in Figure 3.20 and Figure 3.21. It was seen that the correlation length of 20 ps was long enough for the autocorrelation function to be decayed. Similar with HCACF, the SACF of argon liquid decayed to zero exponentially and the SACF of nanofluids decayed to zero in an oscillatory behaviour. It was observed that there was a strong effect on particle volume fraction on the oscillation of SACF in nanofluids which could significantly increase the viscosity. Such oscillatory behaviour in nanofluids was also reported by Wang, Wang, Luo, and Cen (2008), where they mentioned that the oscillation of SACF was attributed to the stress wave reflection or scattering at the solid-liquid interface instead of induced by Brownian motion or oscillation of the nanoparticles and liquid. At the solid-liquid interface there will be acoustic impedance mismatch which results in weak transmission and strong reflection or scattering of the stress tensor, and form oscillation between particles.

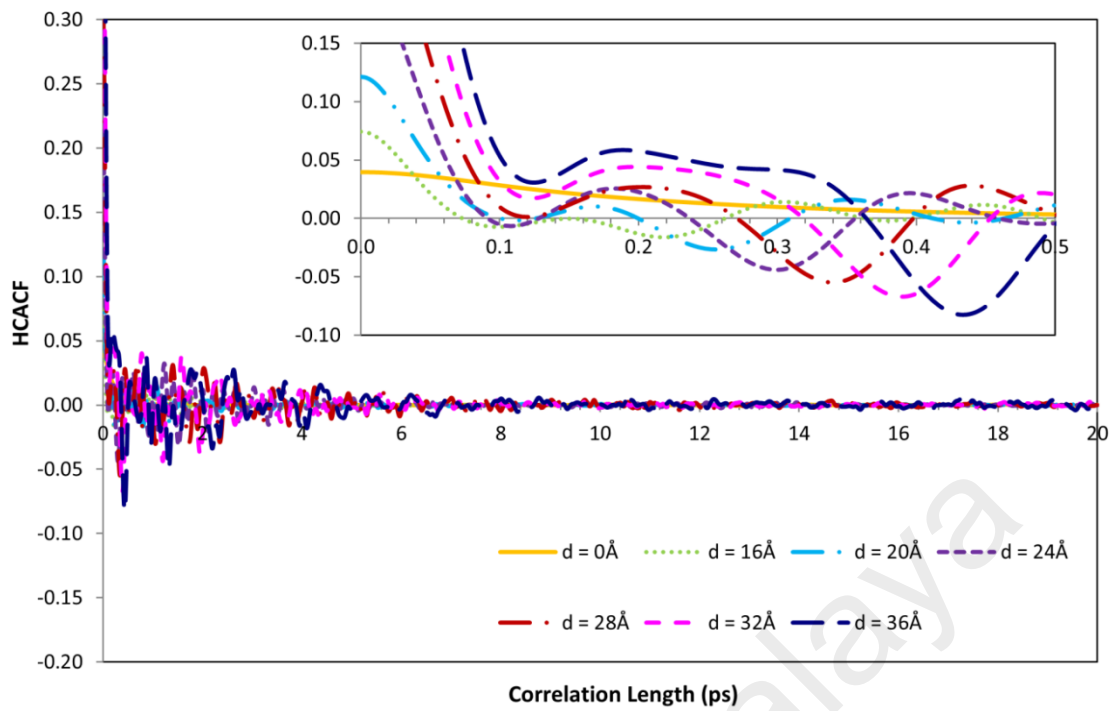


Figure 3.16: HCACF for thermal conductivity calculation, system #1- 2.24 vol% nanofluids with single nanoparticle in well-dispersed state.

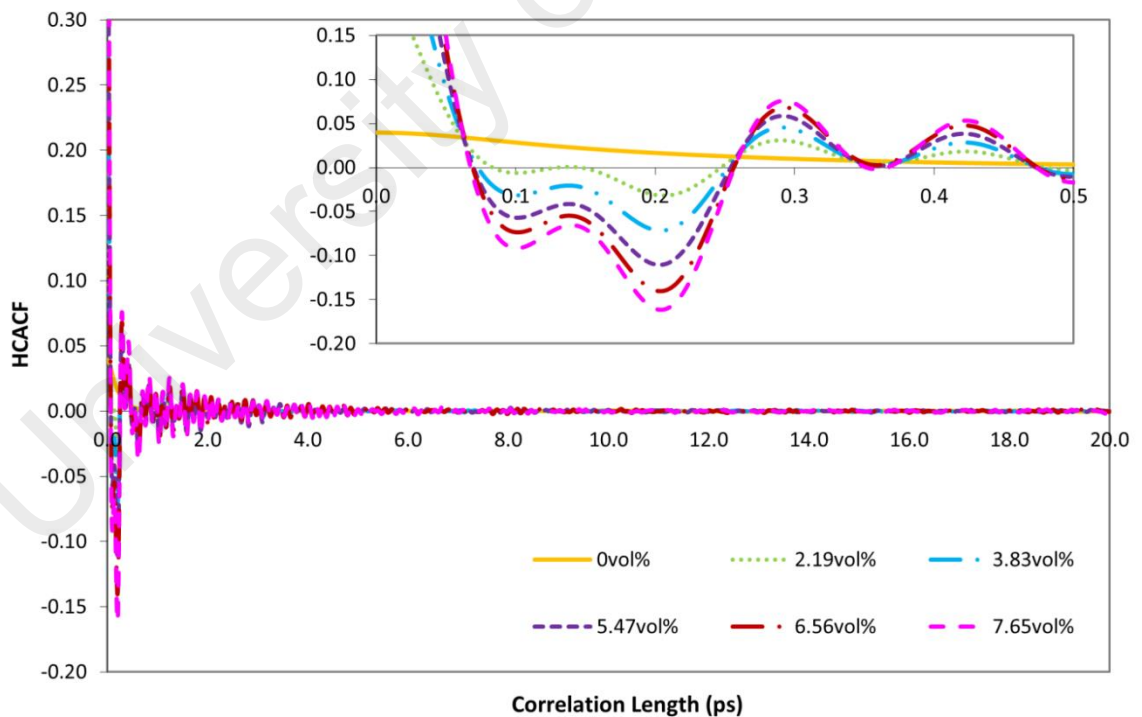


Figure 3.17: HCACF for thermal conductivity calculation, system #2- nanofluids with multi-nanoparticle in well-dispersed state, with particle diameter of 15 Å.

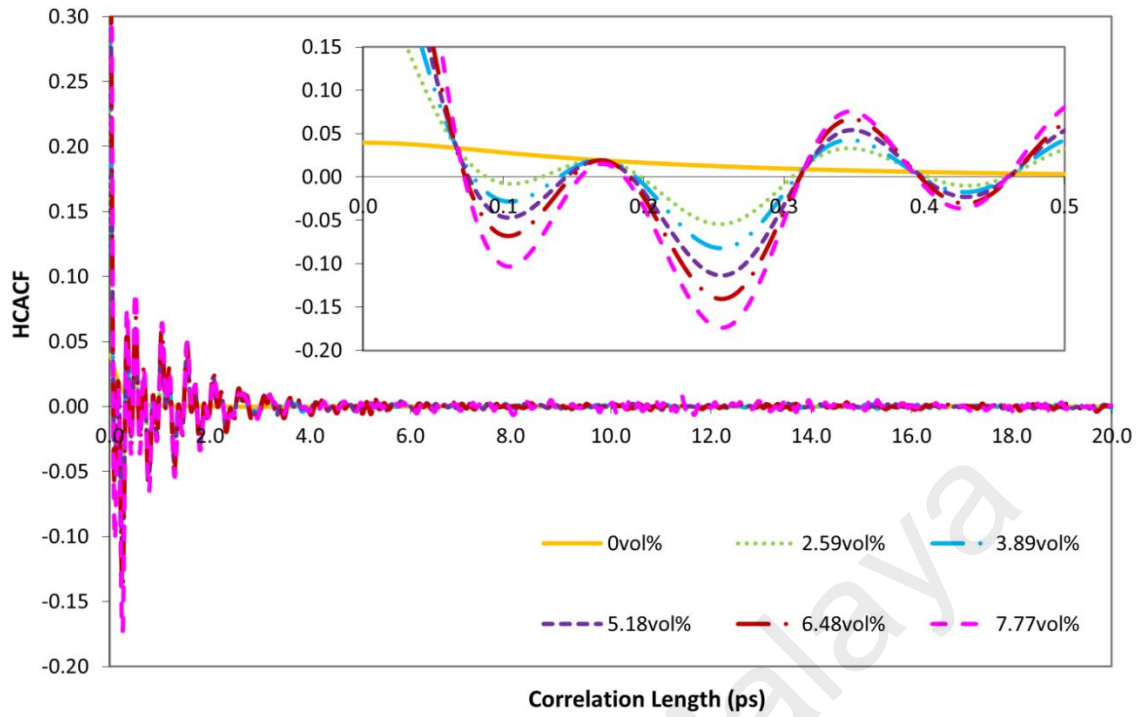


Figure 3.18: HCACF for thermal conductivity calculation, system #3- nanofluids with multi-nanoparticle in well-dispersed state, with particle diameter of 20 Å.

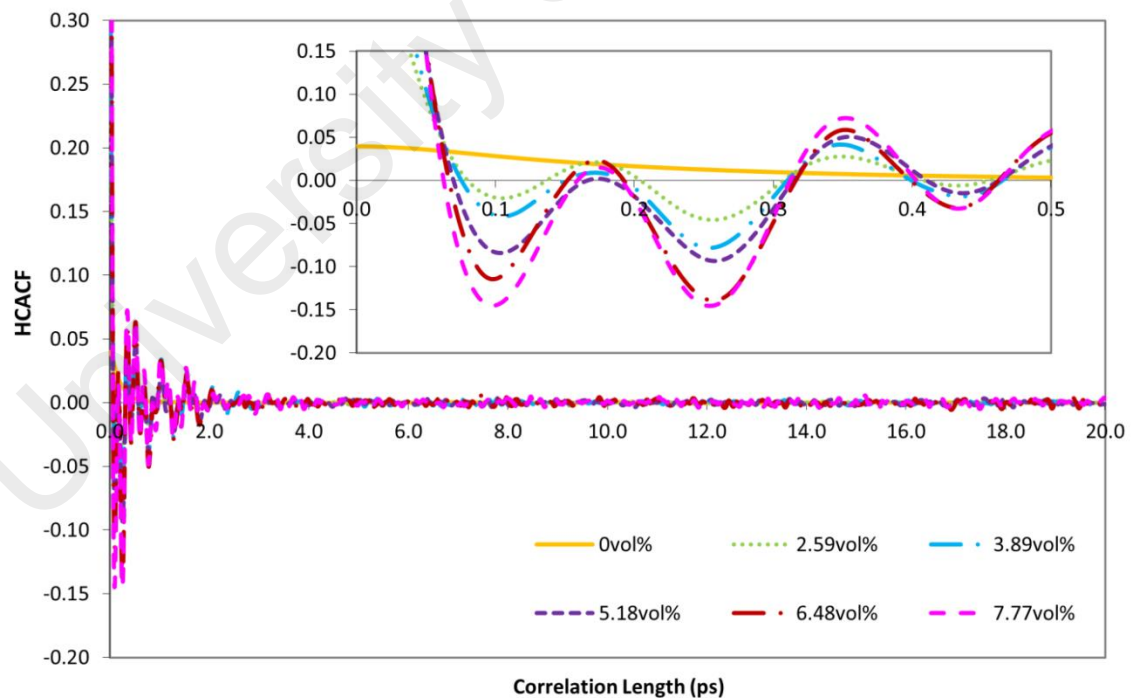


Figure 3.19: HCACF for thermal conductivity calculation, system #4- nanofluids with multi-nanoparticle in aggregated state, with particle diameter of 20 Å.

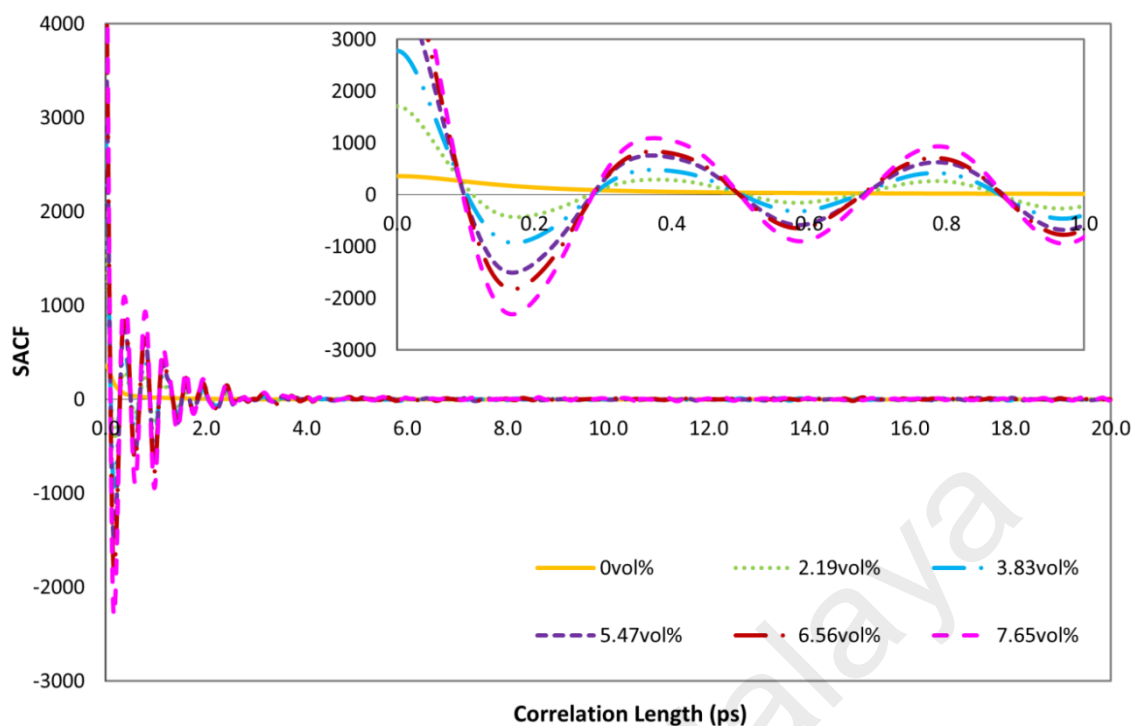


Figure 3.20: SACF for shear viscosity calculation, system #2- nanofluids with multi-nanoparticle in well-dispersed state, with particle diameter of 15 Å.

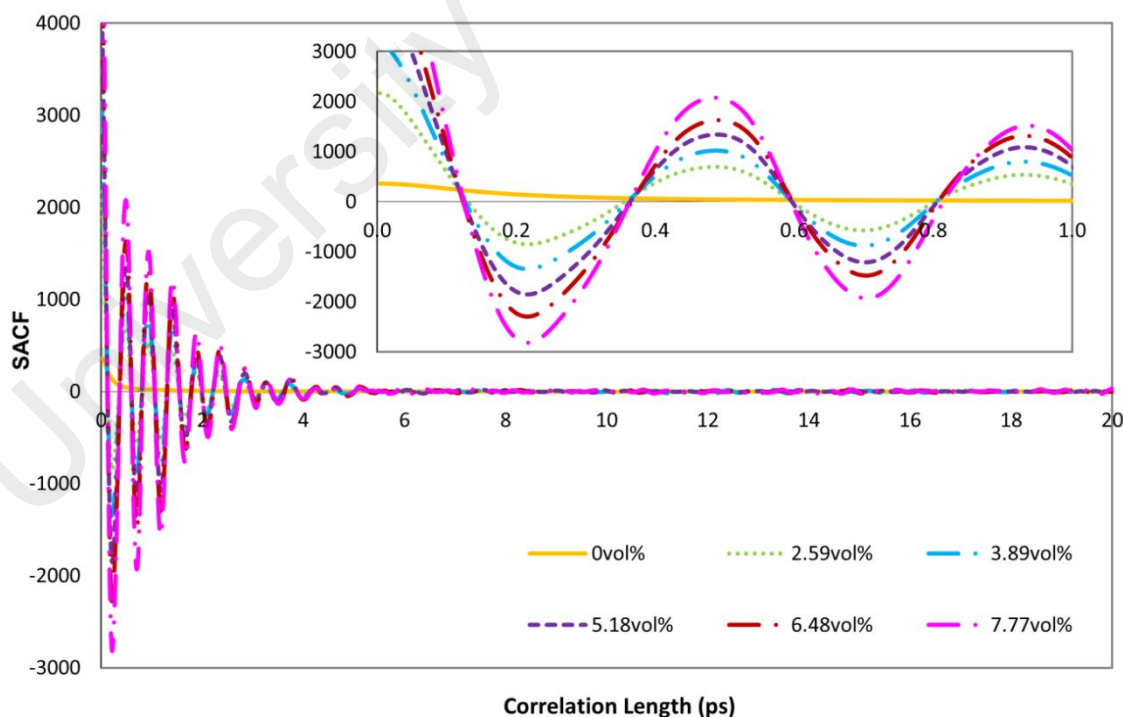


Figure 3.21: SACF for shear viscosity calculation, system #3- nanofluids with multi-nanoparticle in well-dispersed state, with particle diameter of 20 Å.

3.4 Summary

MD simulation integrated with Green Kubo method was employed to calculate thermal conductivity, shear viscosity, diffusion coefficient and radial distribution function. Four different copper-argon nanofluids systems were modelled to achieve different objectives in this thesis. L-J potential was employed to model interaction between Ar-Ar, Cu-Cu and Ar-Cu. The differential equations of motion for particles in the system were solved by using Velocity Verlet algorithm. Time step size of 4 fs was used and 100,000 time steps (0.4 ns) were carried out to achieve equilibrium state in NVT ensemble. Additional 1000,000 time steps (4 ns) were carried out to have data production under NVE ensemble. The thermal conductivity and shear viscosity were collected in a correlation length of 5,000 time steps (20 ps) to allow fluctuation of autocorrelations. The results of validations showed that the employed methodology and L-J potential were able to predict results which are in good agreement with experimental results with maximum error of 5.9%. The equilibrium state was achieved prior to data production by observing convergences in temperature and total energy in the systems during equilibration process. Furthermore, the selected correlation length of 20 ps was sufficient for the autocorrelation function to be decayed well to plateau value, and hence established the accuracy of thermal conductivity and shear viscosity calculation.

CHAPTER 4: RESULTS AND DISCUSSIONS

This chapter aims to present results and discussions on the three objectives of this thesis. First, the investigation on the effects of Brownian motion and its induced micro-convection in enhancing thermal conductivity of nanofluids is featured. Then, the investigation on the effects of nanoparticle aggregation in thermal conductivity enhancement of nanofluids is furnished. Finally, the evaluation on efficiency of nanofluids with the effects of particle size and temperature is discussed.

4.1 Effects of Brownian Motion and Induced Micro-Convection in Thermal Conductivity of Nanofluids

The objective in this section is to investigate the effects of Brownian motion and its induced micro-convection in enhancing thermal conductivity of nanofluids. According to Stokes-Einstein (1905) formula as presented in Equation 2.4, Brownian motion is inversely proportional to particle size. This means that, a smaller nanoparticle size in base fluid can produce higher thermal conductivity in nanofluids. Based on this correlation, the role of Brownian motion and its induced micro-convection can be determined by computing thermal conductivity and diffusion coefficient of nanofluids with effects of different particle size at constant particle volume fraction.

4.1.1 Design of Model

Well-dispersed nanofluids with constant particle volume fraction of 2.24 vol% were modelled by suspending a single nanoparticle into base fluid with six different particle diameters of 16 Å, 20 Å, 24 Å, 28 Å, 32 Å and 36 Å at temperature of 86 K. The system is represented as system #1 which is described clearly in Section 3.2.1. The details of simulation cell and snapshot of the system are presented in Table 3.2 and Figure 3.4, respectively.

4.1.2 Investigation on Brownian Motion of Nanoparticle

Figure 4.1 depicts the relative thermal conductivity (defined as the nanofluid-to-base fluid ratio of thermal conductivity) for 2.24 vol% nanofluids, as a function of particle diameter varying from 16 Å to 36 Å at a temperature of 86 K. The result of MD simulation is compared with the prediction obtained through the Maxwell model. The computed thermal conductivity is higher than the prediction of Maxwell model. The prediction of Maxwell model remains constant at 7% enhancement with increasing particle diameter because its particle effect is not accounted for in the classical prediction. It is interesting to note that the computed thermal conductivity increases with increasing particle diameter, which is at variance with Brownian model (Kumar et al., 2004; Murshed et al., 2009; Xuan et al., 2003). The thermal conductivity enhancement is steeper at very small particle diameter, for example 16 Å and 20 Å, which is up to 13% and 23%, respectively. Later, the thermal conductivity enhancement gradually increases from 24% to 28%, to 26% and then to 31%, corresponding to

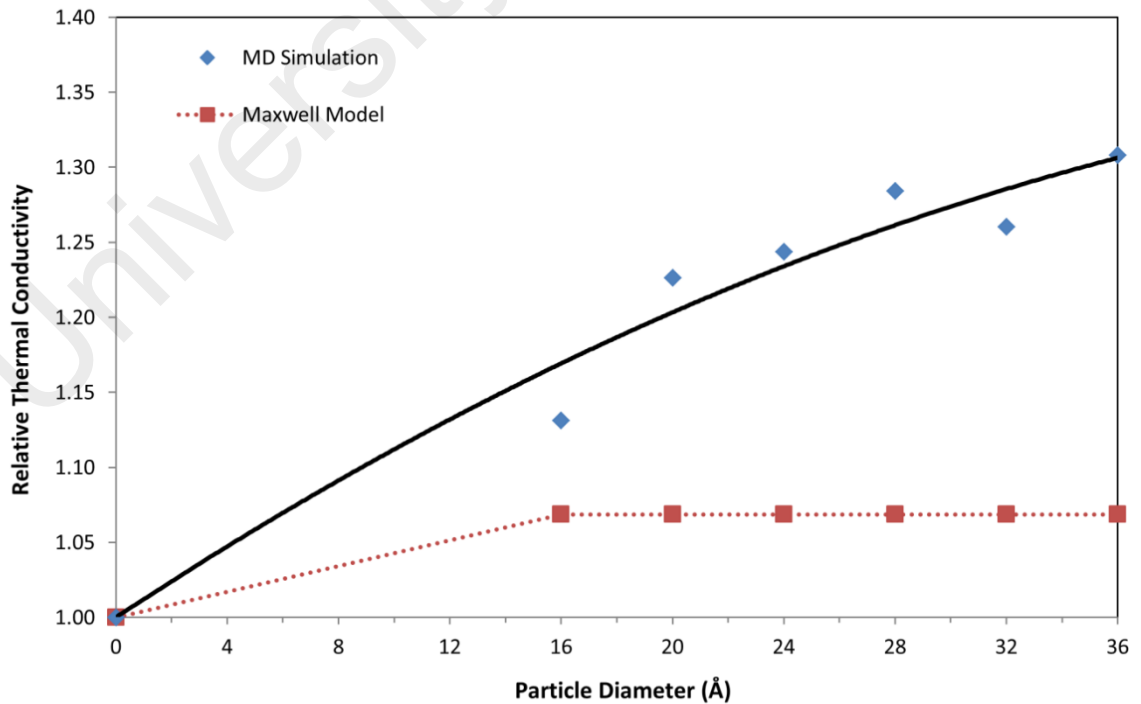


Figure 4.1: Relative thermal conductivity of 2.24 vol% nanofluids with respect to particle diameter varied from 16 Å to 36 Å at 86 K, comparing with prediction by Maxwell model.

particle diameter from 24 Å to 28 Å, to 32 Å and then to 36 Å, respectively. These results are in good agreement with the general trend which were reported in previous experimental works (Angayarkanni et al., 2015; Beck et al., 2009; Chen et al., 2008a; Timofeeva et al., 2010; Warriar & Teja, 2011; Yu et al., 2008). The present simulation indicates that bigger particle size produces higher thermal conductivity compared to smaller particle size, which is in contrast to the trend of Stokes-Einstein formula presented in Equation 2.4. Thus, it is confirmed that Brownian motion of nanoparticle has insignificant effects in enhancing thermal conductivity of nanofluids.

4.1.3 Investigation on Brownian Motion Induced Micro-convection

The previous section, it was demonstrated that Brownian motion of nanoparticle does not contribute to the thermal conductivity enhancement in nanofluids. However, such irregular Brownian motion of nanoparticles may induce micro-convection in base fluid to enable energy transfer between nanoparticle and base fluid, and hence increases the effective thermal conductivity of nanofluids (Jang & Choi, 2004, 2007; Koo & Kleinstreuer, 2004; Patel et al., 2006; Patel et al., 2008; Prasher et al., 2005, 2006a; Ren et al., 2005; Xuan et al., 2006). As convective heat transfer is analogous with mass transfer (Krishnamurthy et al., 2006), the role of induced micro-convection in the base fluid can be identified by computing the diffusion coefficient of base fluid in nanofluids.

The mean square displacement (MSD) of liquid atoms in 2.24 vol% nanofluids with particle diameter varied from 16 Å to 36 Å at 86 K are plotted against the diffusing time, as shown in Figure 4.2. It indicates that the MSD of liquid atoms increases with increasing particle diameter in nanofluids. However, the MSD of liquid atoms in nanofluids is even lower than liquid atoms in a pure base fluid. According to Equation 3.19, diffusion coefficient of liquid atoms can be further extracted from the slope of MSD against diffusing time, where the slope of the linear regression of the data is equal

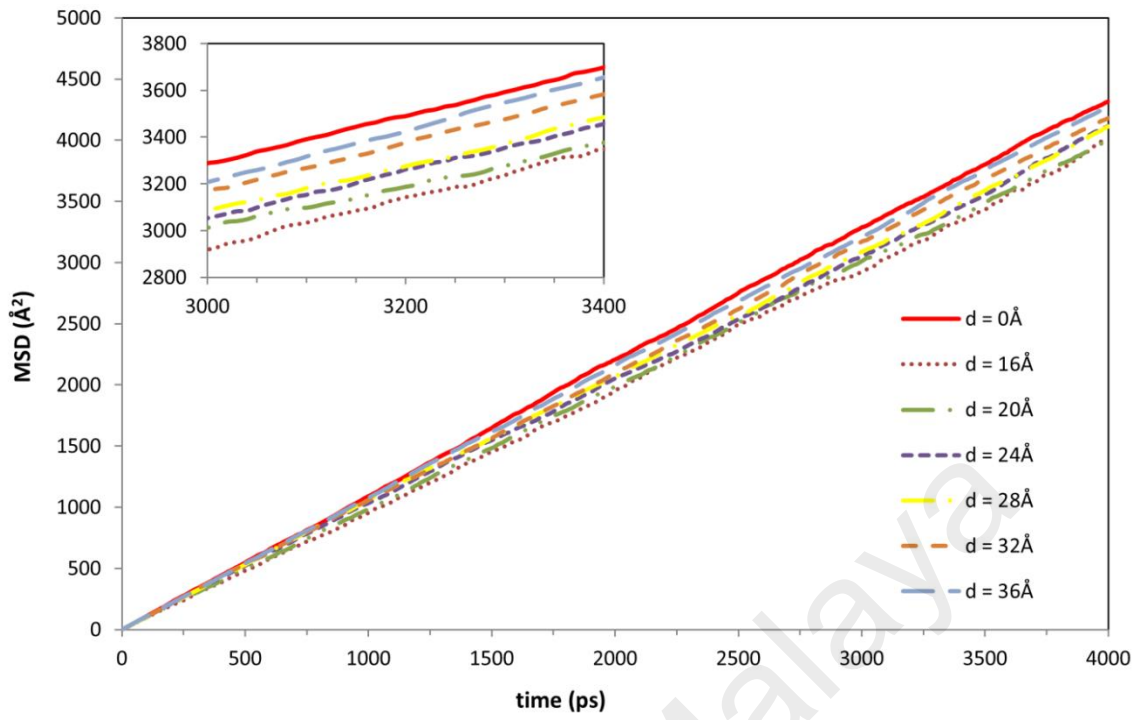


Figure 4.2: MSD of liquid atoms in nanofluids as a function of diffusing time.

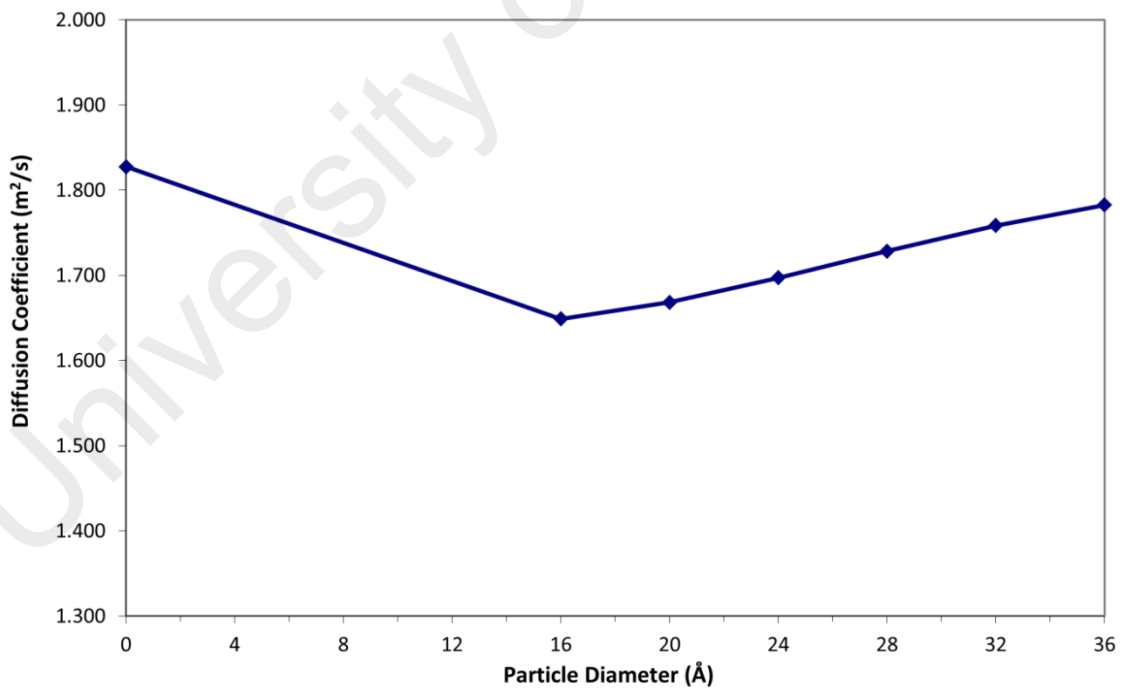


Figure 4.3: Diffusion coefficient of liquid in nanofluids as a function of particle diameter.

to 6 times the diffusion coefficient. The R^2 of the regression lines of liquid atoms in nanofluids are relatively high, which are in the range of 0.9996 to 1.0000. Figure 4.3 presents the diffusion coefficient of liquid in 2.24 vol% nanofluids compared to that of pure base fluid, as a function of particle diameter varying from 16 Å to 36 Å at 86 K. Similar to the trend of MSD, the diffusion coefficient of liquid in nanofluids increases with increasing particle diameter. However, the overall diffusion coefficients of nanofluids are still lower than the pure base fluid. Such difference becomes more pronounced for smaller particle diameter. The reduction trend in diffusion coefficient of liquid in nanofluids was also reported in other experimental works (Feng & Johnson, 2012; Gerardi et al., 2009; Turanov & Tolmachev, 2009). Significantly, the findings in present simulation are in contradiction to the above-mentioned hydrodynamic models. The presence of nanoparticle in base fluid reduces the effect of micro-convection in base fluid of nanofluids instead of enhancing it. For that reason, the role of Brownian motion induced micro-convection is identified to have negligible effects in thermal conductivity enhancement of nanofluids.

4.1.4 Microscopic Analysis on Brownian Motion and Induced Micro-convection

The reduction in diffusion coefficient of liquid in nanofluids is attributed to two effects (Gerardi et al., 2009): (1) the diffusion path of liquid atoms is being obstructed when nanoparticles are in their way; and (2) the liquid atoms are absorbed to the interface of nanoparticle to form an ordered liquid layer, which lowered the diffusion coefficient compared to free moving liquid atoms. The first effect of obstruction in the diffusing path can be further explained using the excluded volume effect given by (Jönsson, Wennerström, Nilsson, & Linse, 1986):

$$D_{nf} = \frac{D_f}{(1+0.5\phi)} \quad (4.1)$$

where D_{nf} is the diffusion coefficient of liquid in nanofluids with volume fraction ϕ , and D_f is the diffusion coefficient of pure base fluid. Conceptually, the liquid atoms give way to the nanoparticle that takes up the space and hence the total volume occupied by the nanoparticle is excluded. Figure 4.4 compares the prediction by excluded volume model and MD simulation for the relative diffusion coefficient (nanofluid-to-base fluid ratio of diffusion coefficient) for 2.24 vol% nanofluids as a function of particle diameter. It clearly shows that the reduction predicted by the excluded volume model is less than the data obtained from the present simulation. For prediction by the excluded volume model, it remains constant as 1% reduction with increasing particle diameter because the particle size effect is not taken into account for the prediction. In contrast, in the computation by MD simulation, the maximum reduction in diffusion coefficient in nanofluid is up to 10% reduction for particle diameter of 16 Å; the reduction is gradually reduced from 9% to 7%, to 5%, and then to 4%, for nanofluids with particle diameter from 20 Å to 24 Å, to 28 Å and then to 32 Å. Eventually, the prediction of the

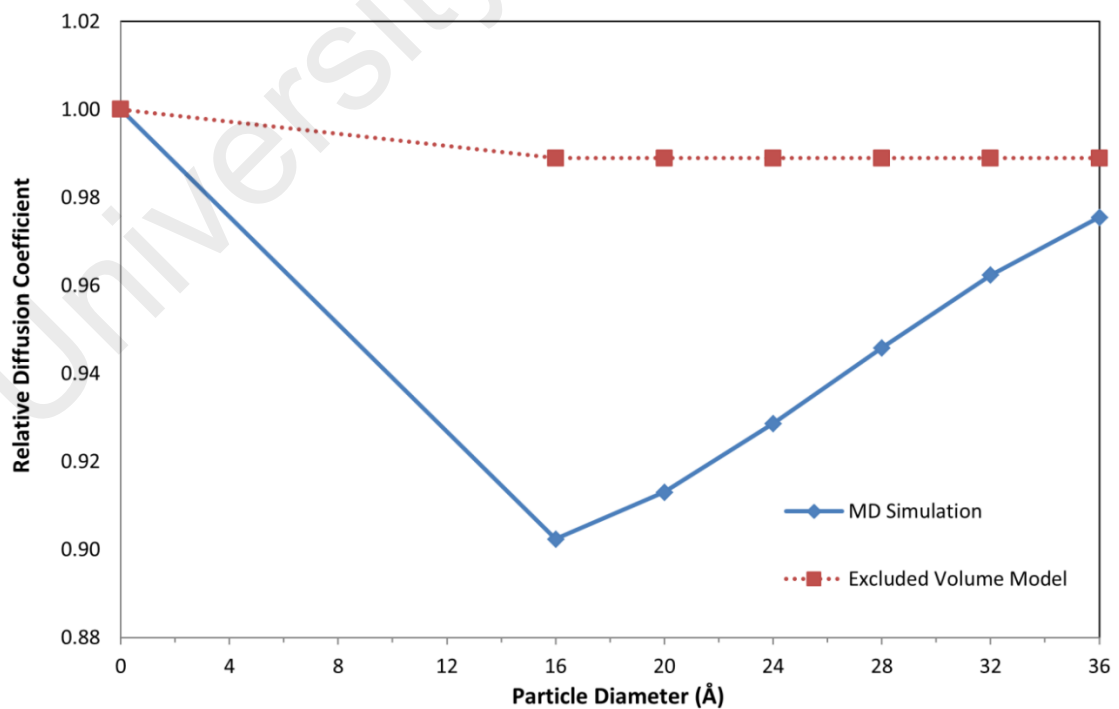


Figure 4.4: Relative diffusion coefficient of liquid in nanofluids with respect to particle diameter, comparing with prediction by excluded volume model.

excluded volume model is only close to the present simulation at higher particle diameter, for example 36 Å, which is a 2% reduction in MD simulation. Remarkably, the excluded volume model fails to account for the observed reduction in diffusion coefficient of nanofluids especially at smaller particle size.

The larger-than-predicted reduction in diffusion coefficient of liquid in nanofluids should be further analysed by investigating the second effect on diffusion coefficient reduction, which is the forming of an ordered liquid layer on the solid-liquid interface. The structure of liquid at the vicinity of nanoparticle can be studied by using radial distribution function (RDF). Details of RDF are given in Section 3.2.6.2. Figure 4.5 and Figure 4.6 display the liquid structure for the interaction between liquid-liquid and solid-liquid of 2.24 vol% nanofluids at 86 K, respectively. The RDF of liquid-liquid is similar for pure base fluid ($d = 0$ Å) and bulk liquid of 2.24 vol% nanofluids with particle diameters varying from 16 Å to 36 Å. However, it is interesting to note the RDF of solid-liquid, which is the liquid structure around the solid atom. The structure of liquid changes with the addition of nanoparticle – it apparently becomes more crystalline in the vicinity of nanoparticle compared with the surrounding bulk liquid such as RDF of the liquid-liquid. This RDF on solid-liquid profile is in good agreement with the profile reported in MD simulation on nanofluid systems (Sergis & Hardalupas, 2014). As the particle diameter decreases from 36 Å to 16 Å, the first peak becomes more pronounced in amplitude, indicating that the liquid atoms become more strongly attracted towards the nanoparticle, to form higher density of ordered interfacial liquid layer on the interface of the nanoparticle. For a nanoparticle diameter of 16 Å, the split of second peak into two clearly indicates that the liquid atoms packed themselves into random close packing which is a signature of amorphous atomic packing (Wendt & Abraham, 1978). This means that the addition of nanoparticle changes the structure of the neighbouring liquid atoms into an amorphous-like liquid structure, which is lesser in

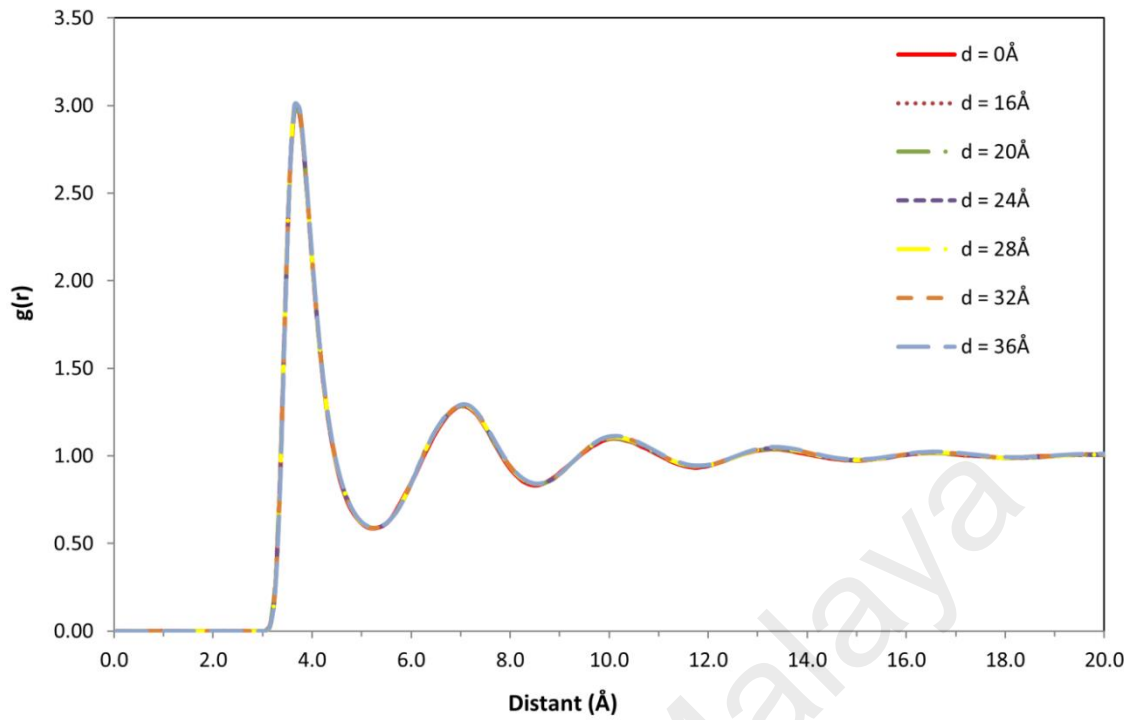


Figure 4.5: RDF of liquid structure for interaction between liquid-liquid in 2.24 vol% nanofluids as a function of radial distant from reference atom.

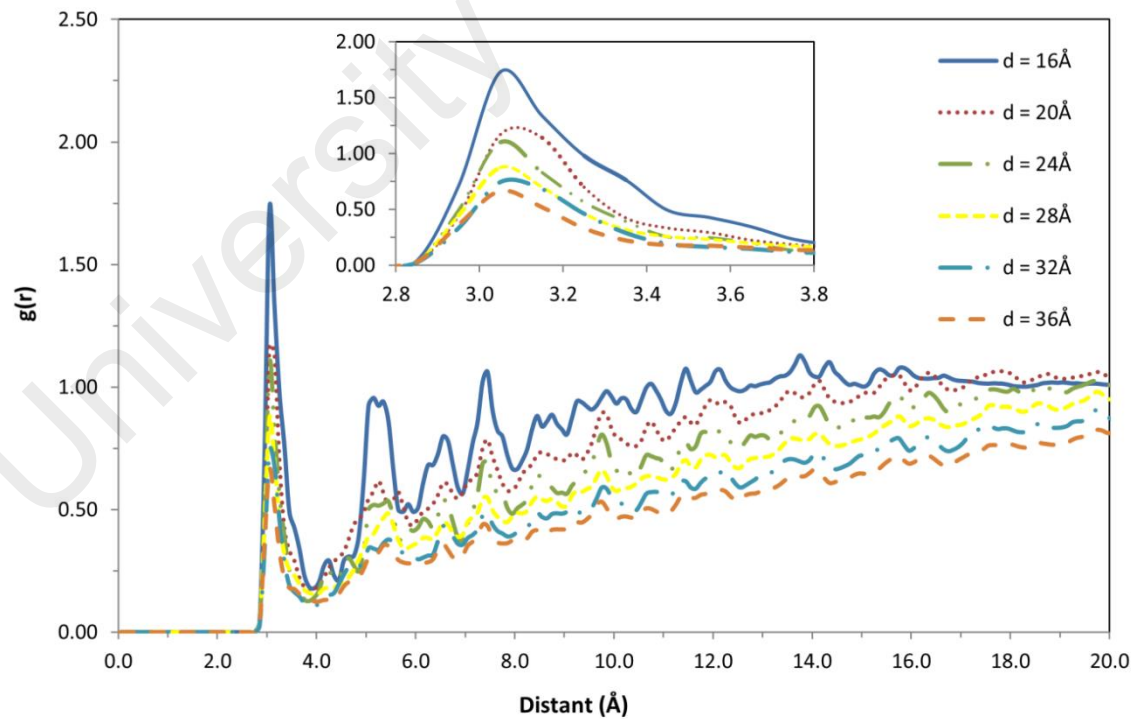


Figure 4.6: RDF of liquid structure for interaction between solid-liquid in 2.24 vol% nanofluids as a function of radial distant from reference atom.

density than the surrounding bulk liquid. The nanoparticle having higher specific surface area tends to “freeze” neighboring liquid atoms into a more ordered layer. The ordered liquid layer is absorbed on the solid-liquid interface and moves with the nanoparticle in the base fluid. Consequently, the formation of an amorphous-like interfacial liquid structure lowers the average diffusion coefficient compared to the free moving liquid atoms in pure base fluid. This reduction in the diffusion coefficient in nanofluids becomes more pronounced for smaller nanoparticle sizes, which has a higher specific surface area.

The formation of amorphous-like interfacial liquid structure can be further identified by examining the velocity autocorrelation function (VACF) of solid atoms in nanofluids. VACF represents the overview of the velocity of atom at current time ($t = t$) along the initial direction of its motion ($t = t^0$). The area under VACF represents the diffusion coefficient of the nanoparticle, as shown in Equation 3.18. Figure 4.7 demonstrates that VACF of solid atom in 2.24 vol% nanofluids against particle diameter varying from 16 Å to 36 Å at 86 K. It is clearly shown that the negative region in VACF becomes more prominent with decreasing particle diameter. For particle diameter of 36 Å, interfacial liquid layer with lower density is formed around the nanoparticles; the solid atoms tend to have many atoms transmission without reversing their direction, hence, the negative region of VACF is less and close to the positive region. Whereas for particle diameter of 16 Å, interfacial liquid layer with higher density is formed around the nanoparticle; many liquid atoms are closely packed, so the atoms backscattering are more than atoms transmission, hence, resulting in larger negative region (Haile, 1992). Similarly, the negative region is also known as cage effect where the solid atoms are trapped in temporary cage imposed by its interfacial liquid atoms (Mausbach & May, 2006). The observed negative region or cage effect in different particle diameters indicate that the nanoparticle confined in interfacial liquid layer has amorphous-like

characteristic. Therefore, based on the present microscopic analysis of RDF and VACF, this demonstrates that the Brownian motion of nanoparticle and its induced micro-convection in base fluid do not enhance thermal transport in nanofluids due to the hydrodynamic effect mediated by the amorphous-like interfacial liquid structure in the vicinity of nanoparticle.

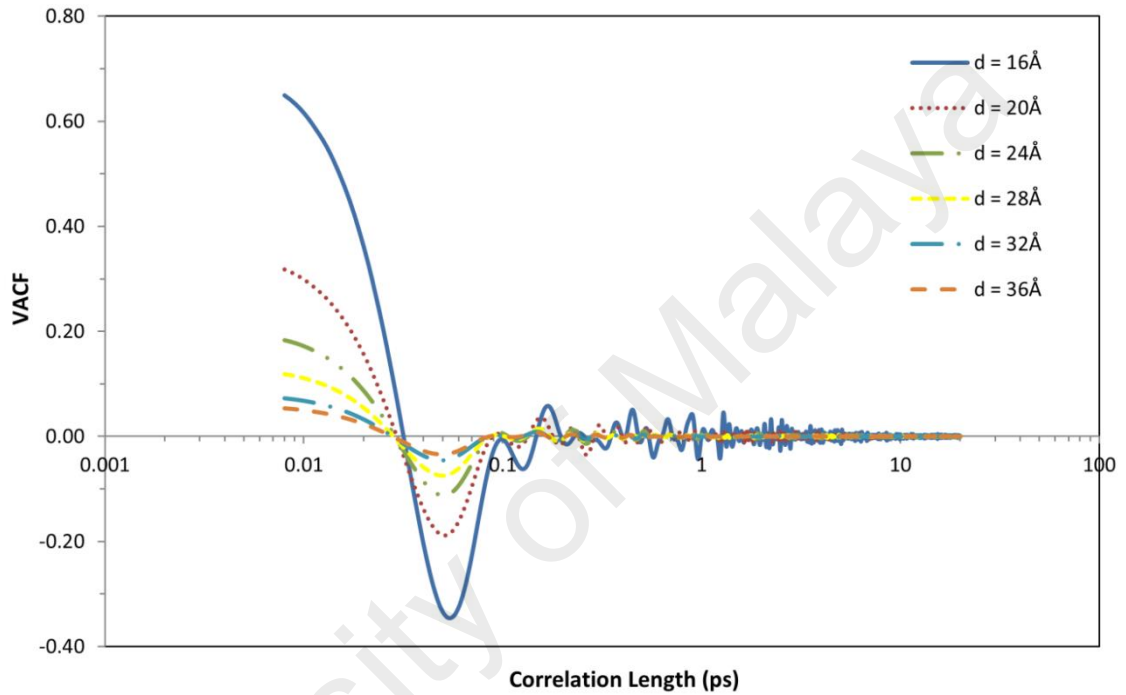


Figure 4.7: VACF of solid atom in 2.24 vol% nanofluids with particle diameter from 16 Å to 36 Å at 86 K.

Table 4.1: Analysis on Brownian motion and its induced micro-convection effects.

Parameters	Big particle size	Small particle size
Thermal conductivity	↑	↓
MSD/diffusion coefficient of base liquid in nanofluids	↑	↓
RDF - density of bulk liquid	□	□
RDF - ordering of interfacial liquid	↓	↑
VACF - cage effect in solid atoms	↓	↑

Symbol: ↑ - high at the particle size; ↓ - low at the particle size; □ - constant at the particle size

4.1.5 Summary

In Section 4.1, the roles of Brownian motion of nanoparticle and induced micro-convection in base fluid to enhance thermal conductivity in nanofluids were systematically investigated at the macroscopic and microscopic levels. These roles were identified by computing the thermal conductivity and diffusion coefficient of nanofluids with the effect of different nanoparticle sizes. The main findings of the present simulation are presented in Table 4.1 and the details are as follow:

- Larger nanoparticle size produces higher thermal conductivity compared to smaller nanoparticle size. The thermal conductivity enhancement is 13% for particle diameter of 16 Å compared to 31% for a particle diameter of 36 Å. Thus, Brownian motion of nanoparticle is not the key mechanism to enhance thermal conductivity in nanofluids.
- Diffusion coefficient of liquid in nanofluids increases with increasing nanoparticle size, but it is still lower than the diffusion coefficient of pure base fluid. Compared with that of pure base fluid, the diffusion coefficient reduction is 10% for a particle diameter of 16 Å and gradually reduces to 2% for a particle diameter of 36 Å. Significantly, the micro-convection effect is reduced instead of being enhanced with the presence of nanoparticle in base fluid. Therefore, the induced micro-convection has negligible effects in enhancing thermal conductivity in nanofluids.
- Based on the analysis on RDF of liquid-liquid, the density of bulk liquid in nanofluids is similar to pure base fluid. Thus, the density of bulk liquid in nanofluids shows no changes with the addition of nanoparticle. However, by studying RDF of solid-liquid, the addition of nanoparticle has changed the liquid structure of base fluid in the vicinity of nanoparticle into amorphous-like

interfacial liquid structure. The crystallinity or density of amorphous-like liquid structure increases with decreasing particle size from 36 Å to 16 Å due to its higher specific surface area. The formation of amorphous-like interfacial liquid structure is further confirmed by observing the cage effect in VACF of nanoparticle, in which the cage effect becomes more pronounced with decreasing particle size.

As a conclusion, the effects of Brownian motion of nanoparticle and induced micro-convection in base fluid are not responsible for thermal conductivity enhancement in nanofluids due to the hydrodynamic effect mediated by amorphous-like interfacial liquid structure in the vicinity of the nanoparticle.

4.2 Effects of Nanoparticle Aggregation in Thermal Conductivity of Nanofluids

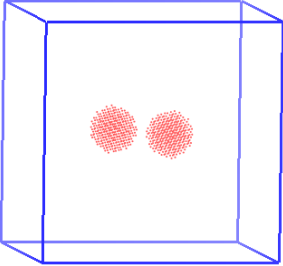
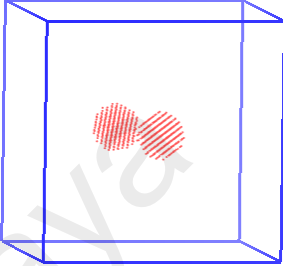
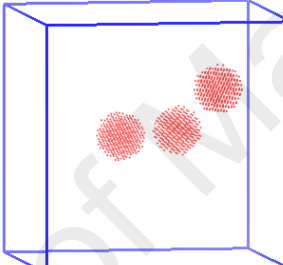
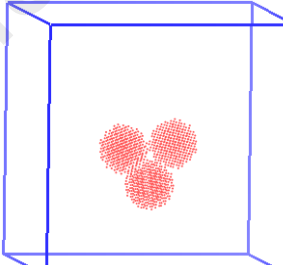
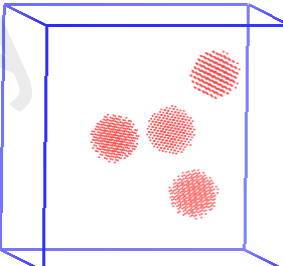
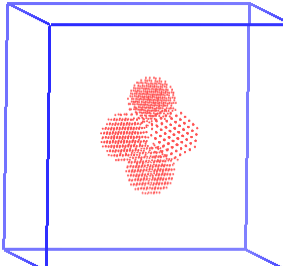
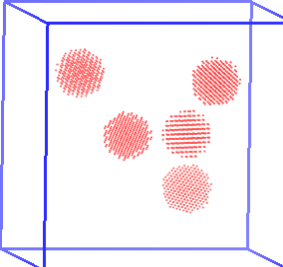
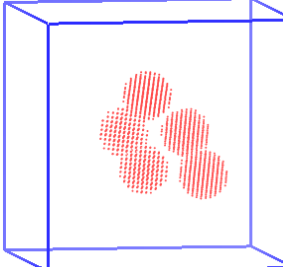
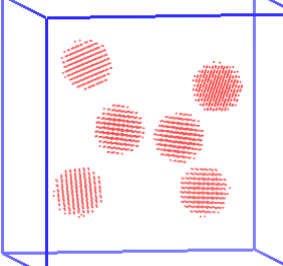
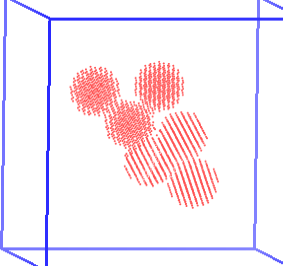
The objective of this section is to investigate the effects of nanoparticle aggregation on thermal conductivity of nanofluids. The effects of aggregation can be identified by comparing thermal conductivity enhancement of nanofluids in aggregated and non-aggregated (well-dispersed) states with the same particle volume fraction, temperature and particle size.

4.2.1 Design of Model

Aggregated and non-aggregated states in nanofluids were modelled by suspending multi-nanoparticle with particle diameter of 20 Å at temperature of 86 K. Both nanofluids system were modelled at five different particle volume fractions, namely 2.59 vol%, 3.89 vol%, 5.18 vol%, 6.48 vol% and 7.77 vol%. For better comparison, both systems have the same simulation cell but with different configuration of nanoparticles, as shown in Table 4.2 (liquid argon is excluded in the display in order to provide a clearer overview of nanoparticles configurations). The aggregated and non-

aggregated nanofluids system correspond to system #3 and system #4, respectively. The details of the systems are presented in Table 3.4.

Table 4.2: Configurations of aggregated and non-aggregated nanofluids.

Particle volume fraction (vol%)	Number of nanoparticles	Non-aggregated nanofluids	Aggregated nanofluids
2.59	2		
3.89	3		
5.18	4		
6.48	5		
7.77	6		

4.2.2 Calculation of Thermal Conductivity

Thermal conductivity of nanofluids in aggregated and non-aggregated states are summarised in Figure 4.8. The thermal conductivity according to the prediction of Maxwell model is also shown for comparison. The thermal conductivity of both states increases with increasing particle volume fraction and is higher than the prediction of Maxwell model. It is interesting to note that the thermal conductivity of aggregated nanofluids is significantly higher than non-aggregated nanofluids. For aggregated nanofluids, thermal conductivity increases from 0.185 W/m.K to 0.196 W/m.K, to 0.218 W/m.K, to 0.235 W/m.K, and then to 0.255 W/m.K for particle volume fraction increments from 2.59 vol% to 3.89 vol%, to 5.18 vol%, 6.48 vol%, and then to 7.77 vol%. Such behaviour also observed for non-aggregated nanofluids with thermal conductivity increasing from 0.172 W/m.K to 0.183 W/m.K, to 0.187 W/m.K, to 0.188 W/m.K and then to 0.213 W/m.K for particle volume fraction increments from 2.59 vol% to 3.89 vol%, to 5.18 vol%, 6.48 vol%, and then to 7.77 vol%. Such difference becomes more pronounced for a particle volume fraction higher than 3.89 vol%, and clearly demonstrates that the existence of nanoparticle aggregation enhances the thermal conductivity of base fluid, especially at a high particle volume fraction. This finding is in agreement with aggregation-based theoretical models (Evans et al., 2008; Feng et al., 2007; Keblinski et al., 2002; Pang et al., 2014; Pang et al., 2015; Prasher et al., 2006b; Prasher et al., 2006c; Wang, Zhou, & Peng, 2003), experimental studies (Angayarkanni & Philip, 2014; Gao et al., 2009; Hong & Kim, 2012; Liao et al., 2003; Philip et al., 2008; Shalkevich et al., 2010; Shima et al., 2010; Xuan et al., 2003; Zhu et al., 2006) and MD simulation studies (Kang et al., 2012; Vladkov & Barrat, 2008).

The thermal conductivity enhancements of simulation data is further compared to the Hashin-Shtrikman (HS) mean field theory, as shown in Figure 4.9. It is interesting to note that the simulation data are bounded by the upper and lower bounds of HS mean

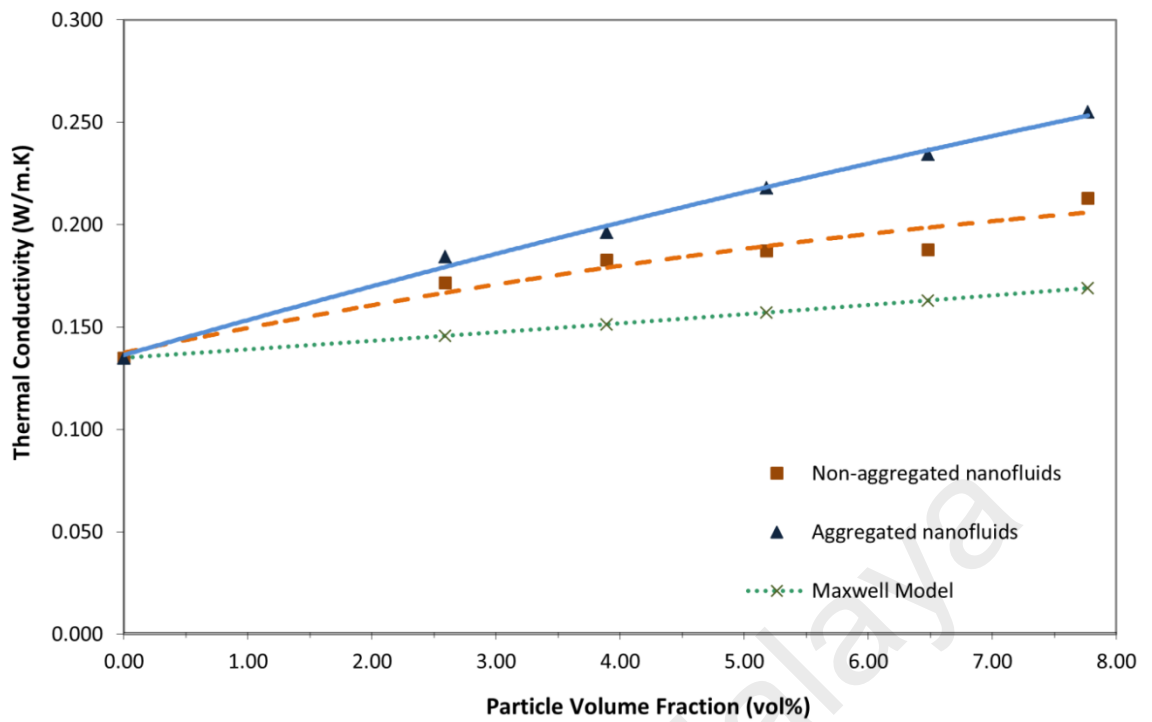


Figure 4.8: Thermal conductivity of non-aggregated and aggregated nanofluids as a function of particle volume fraction, comparing with prediction by Maxwell model.

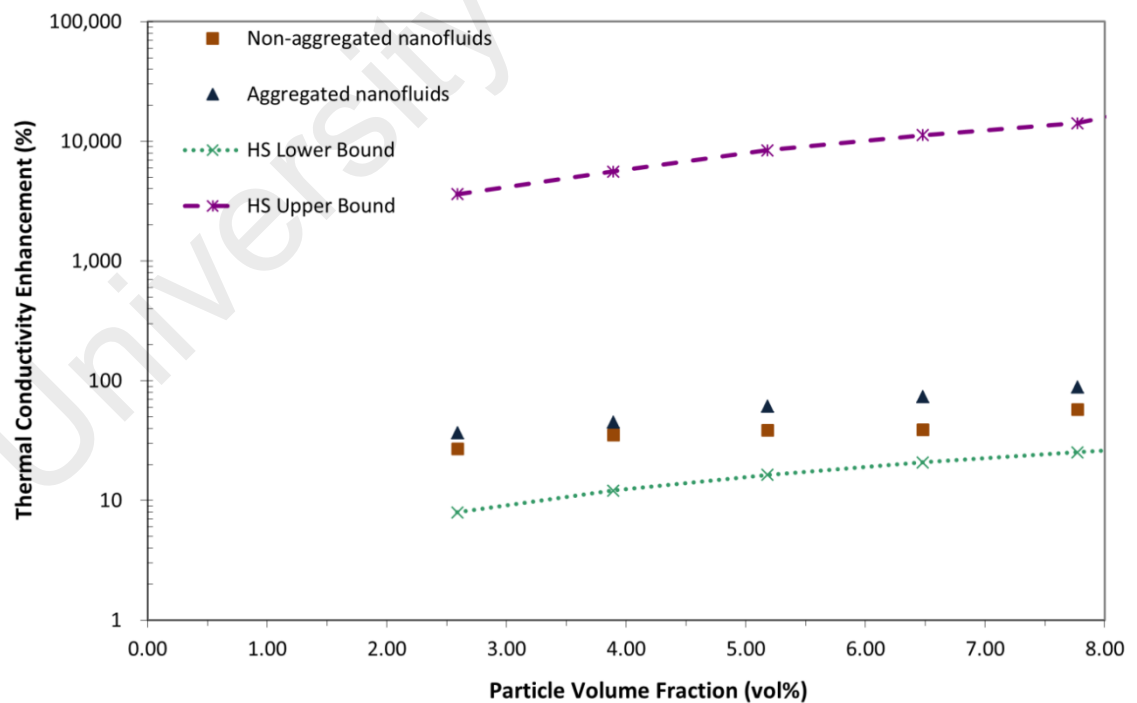


Figure 4.9: Comparison of thermal conductivity enhancement of nanofluids in aggregated and non-aggregated states with HS mean field theory.

field theory, expressed by (Hashin & Shtrikman, 1962):

$$k_f \left(1 + \frac{3\phi(k_p - k_f)}{3k_f + (1-\phi)(k_p - k_f)} \right) \leq k_{nf} \leq \left(1 - \frac{3(1-\phi)(k_p - k_f)}{3k_p - \phi(k_p - k_f)} \right) k_p \quad (4.2)$$

where k and ϕ are thermal conductivity and particle volume fraction, respectively. The subscripts nf , p and f , represent the nanofluid, nanoparticle and base fluid, respectively. With the assumption that $k_p > k_f$, the HS lower bound is identical to Maxwell model as shown in Equation 2.1. In dilute limit, the prediction of HS lower bound and Maxwell model becomes $k_{nf} = 1 + 3\phi$. Physically, HS lower bound corresponds to well-dispersed nanoparticles as shown in Figure 4.10a, whereas the thermal conduction is in series mode and biased conduction through base fluid. The HS upper bound refers to large pockets of fluid separated by chain formation or aggregated nanoparticles as shown in Figure 4.10b, whereas the thermal conduction path is in parallel mode and biased conduction through nanoparticles. HS bounds set a limit based on the knowledge of particle volume fraction and do not depend on any special mechanism of thermal conduction. It is clear that for nanofluids with low particle volume fraction, additional thermal conduction path can be created by having nanoparticles form linear chains or percolating network with embedding large volume

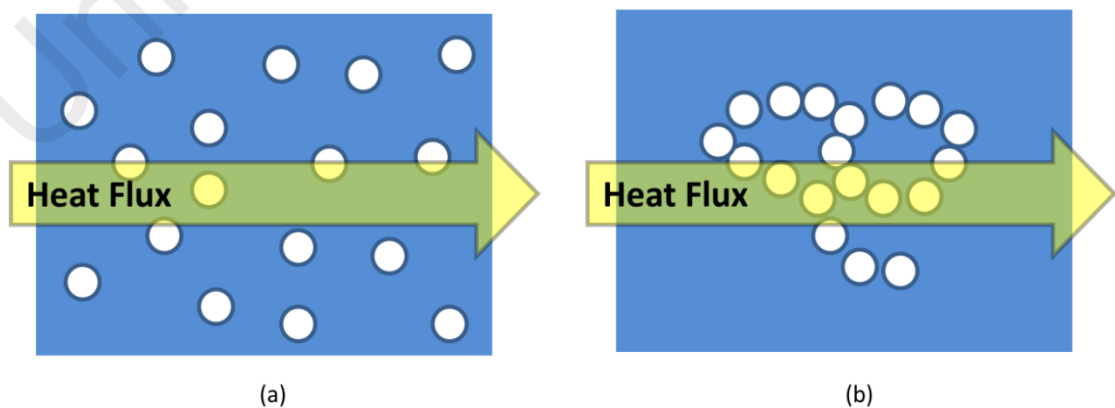


Figure 4.10: HS mean field theory: (a) lower bound corresponds to well-dispersed nanoparticles; (b) upper bound corresponds to large pockets of fluid separated by chain formation or aggregated nanoparticles.

of base fluids. This demonstrates the mean field theory, which is purely based on thermal conduction is obeyed by nanofluids. Again, the results in this particular simulation support observed results from other studies (Eapen et al., 2010; Koblinski, Prasher, & Eapen, 2008) that mean field theory can explain the marked thermal conductivity enhancement in experimental studies.

4.2.3 Decomposition of Thermal Conductivity

To further analyse the simulation data, further insight is gained on the molecular mechanism that govern the variation in thermal conductivity of nanofluids in aggregated and non-aggregated states. Equation 3.13 shows that the thermal conductivity is correlated with the integral of heat current autocorrelation function (HCACF). Self-correlation heat current in Equation 3.14 is decomposed into convective and collision terms, whereas the convective term consists of kinetic and potential energy. Collision or also known as virial term represents the virial interaction of work done by stress tensor. Kinetic term corresponds to energy transfer by the exchange kinetic energy amongst the atoms. Potential term refers to potential energy exchange amongst the atoms.

Figure 4.11 shows the contribution of convective and collision terms to overall thermal conductivity with respect to particle volume fraction. Figure 4.11b shows the thermal conductivity contributed by collision correlation of the aggregated and non-aggregated nanofluids remains more or less constant with increasing particle volume fractions. For pure base fluid (at particle volume fraction 0 vol%), the thermal conductivity is mainly contributed by a collision correlation about 82%, which agrees to the notion that collision correlation contributes most to the thermal conductivity of typical liquids (Eapen, Li, & Yip, 2007a). Although the collision correlation is almost constant against particle volume fraction, the collision correlation of aggregated nanofluids is obviously higher than non-aggregated nanofluids at an average of 18%.

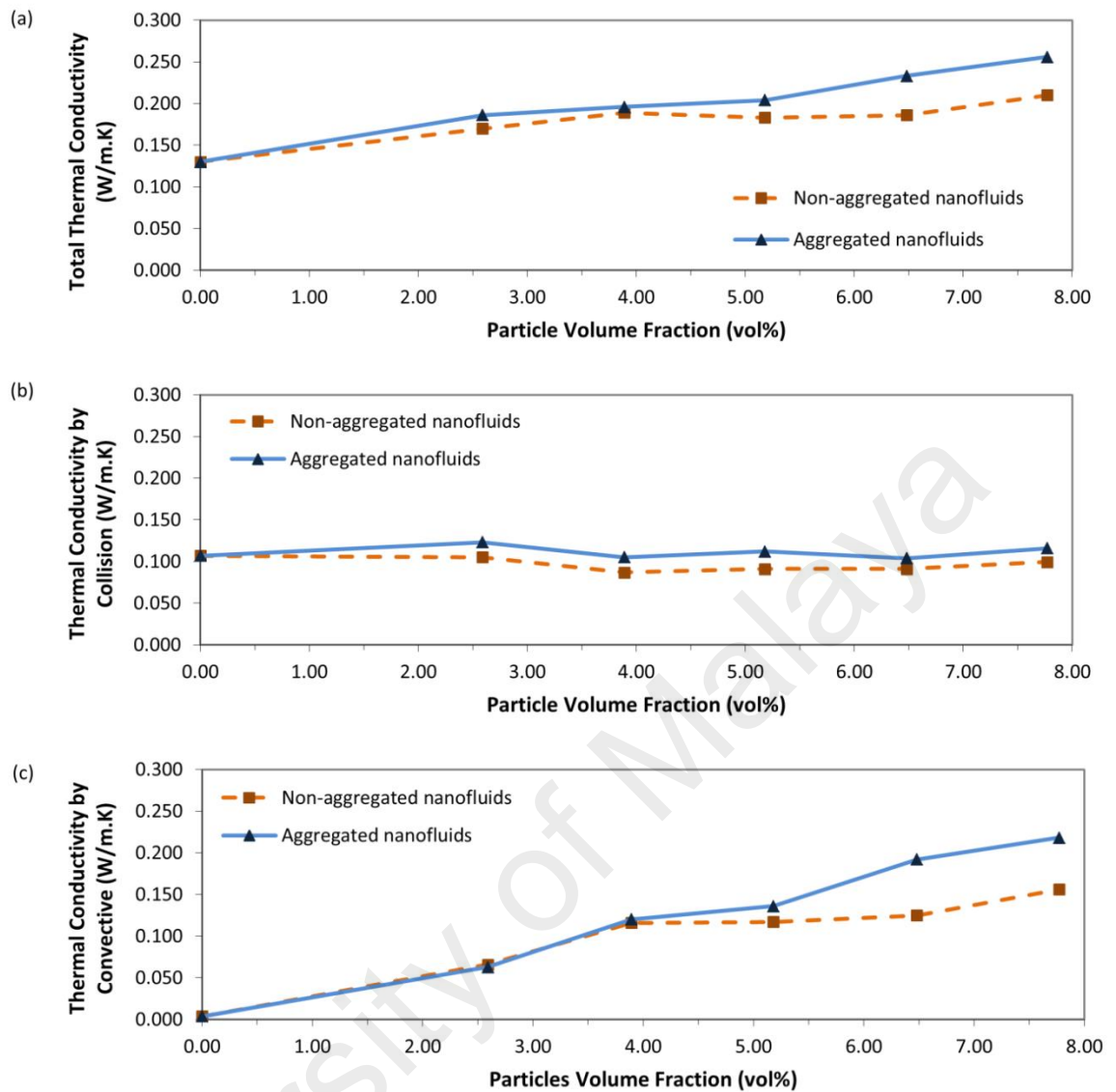


Figure 4.11: Thermal conductivity of nanofluids as a function of particle volume fraction. (a) Total thermal conductivity contributed by collision and convective correlations; (b) thermal conductivity contributed by collision correlation; (c) thermal conductivity contributed by convective correlation.

Figure 4.11c shows that the thermal conductivity contributed by the convective correlation clearly increases with increasing particle volume fraction, the trend is similar to the increase in overall thermal conductivity of nanofluids as shown in Figure 4.11a. The convective correlation of the aggregated nanofluids is higher than for the non-aggregated nanofluids, and such difference becomes more obvious for a high particle volume fraction for example 5.18 vol% and above. At low particle volume fraction of 2.59 vol% and 3.89 vol%, the convective correlation of aggregated nanofluids is close

to non-aggregated nanofluids. At high particle volume fraction of 6.48 vol% and 7.77 vol%, the convective correlation of the aggregated nanofluids is much higher than for the non-aggregated nanofluids by 40-50%. Based on Figure 4.11, two important implications can be made. First, the magnitudes of thermal conductivity of both systems are mainly governed by collision correlation while the enhancement is contributed by the convective correlation. Second, the higher thermal conductivity of aggregated nanofluids compared to non-aggregated nanofluids can be attributed to two regimes: at low particle volume fraction of 2.59 vol% and 3.89 vol%, collision correlation dominates thermal conductivity variation in both aggregated and non-aggregated nanofluids; however, at high particle volume fraction of 5.18 vol% and above, thermal conductivity variation is contributed by both collision and convective correlations, though more by the latter.

As the above results show that the convective term plays a major role in enhancing thermal conductivity with respect to particle volume fraction, it would be interesting to further analyse its decomposition into kinetic and potential energy. Figure 4.12a and 4.12b show the average kinetic energy of copper and argon, respectively, in both nanofluids as a function of particle volume fraction. It is worth to note that the average kinetic energy of copper and argon in both systems has similar values and is not influenced by the particle volume fraction. Furthermore, the average kinetic energy of argon shows insignificant changes before and after the addition of copper nanoparticles. Therefore, the contribution of kinetic energy to thermal conductivity of nanofluids is negligible. In other words, Brownian motion of nanoparticles or its induced micro-convection plays an insignificant role in thermal conductivity enhancement. Again, these findings are consistent with the conclusion drawn in Section 4.1. Figure 4.13a and Figure 4.13b display the average potential energy of copper and argon, respectively, in both systems with respect to particle volume fraction. Figure 4.13a indicates that the

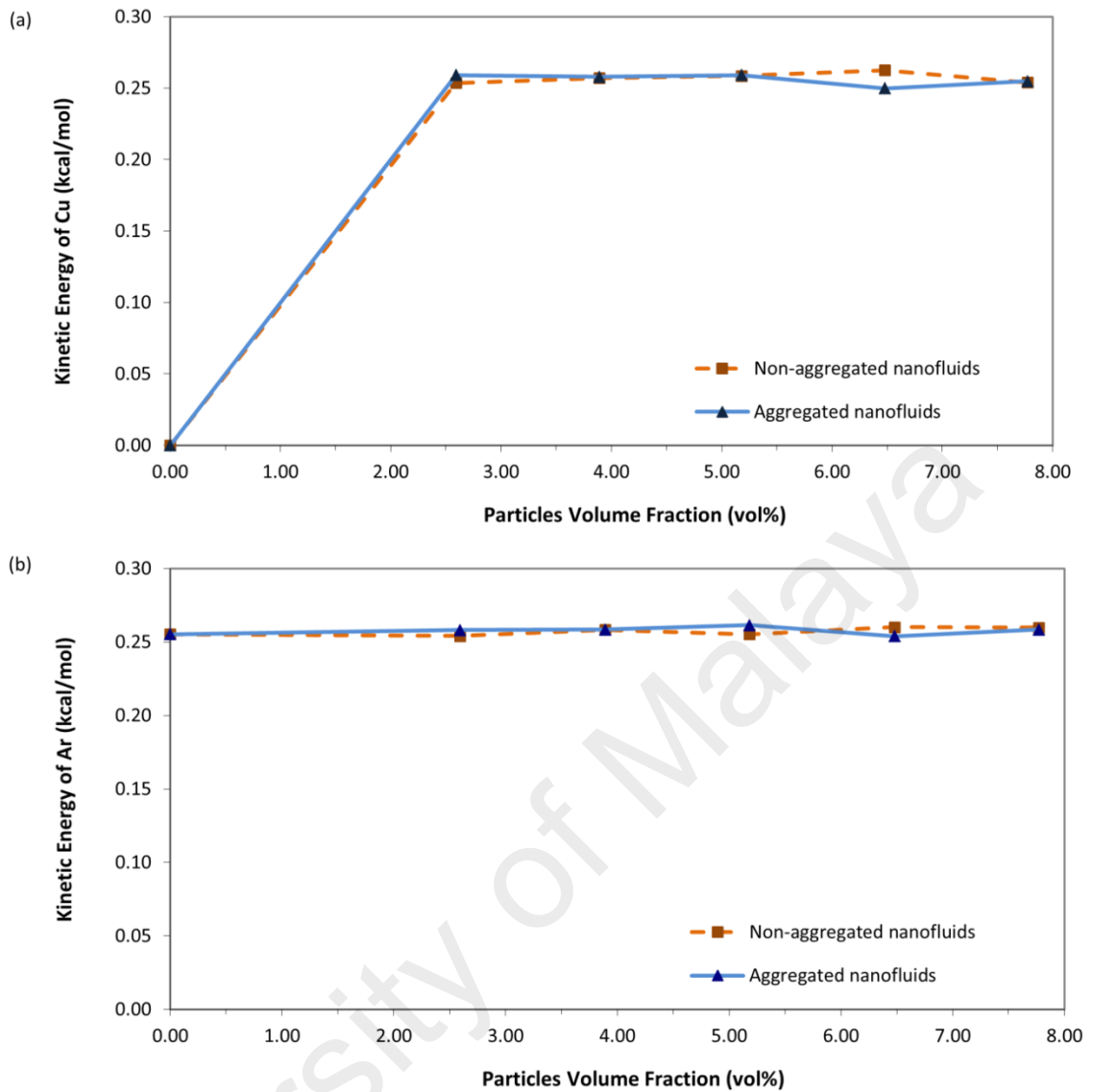


Figure 4.12: Decomposition of convective correlation into kinetic energy in aggregated and non-aggregated states as a function of particle volume fraction. (a) Average kinetic energy of Cu; (b) average kinetic energy of Ar.

average potential energy of copper in aggregated nanofluids is higher than non-aggregated nanofluids. The inset of Figure 4.13a shows that the potential energy in the non-aggregated nanofluids remains almost constant with increasing particle volume fraction. In contrast, the potential energy of copper in the aggregated nanofluids increases with increasing particle volume fraction. It can be hypothesised that the increase in potential is due to nanoparticle aggregation which induces higher potential interaction amongst atoms. Figure 4.13b demonstrates that the average potential energy

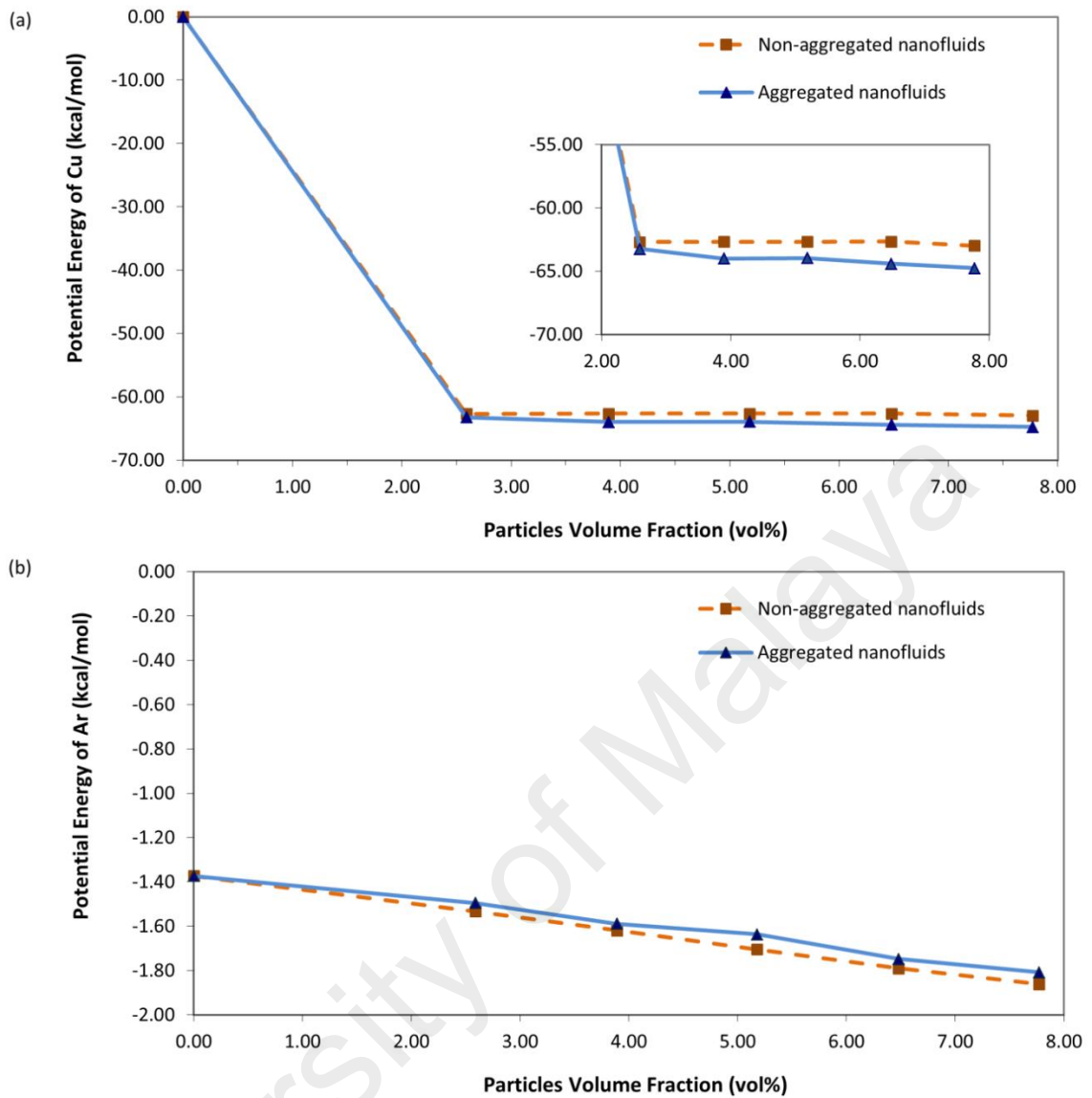


Figure 4.13: Decomposition of convective correlation into potential energy in aggregated and non-aggregated states as a function of particle volume fraction. (a) Average potential energy of Cu; (b) average potential energy of Ar.

of argon in both states increases with increasing particle volume fraction. The potential energy of argon in non-aggregated nanofluids is slightly higher than that in the aggregated nanofluids. In short, the presence of copper nanoparticles increases the initial potential energy of pure liquid argon. Based on overall analysis on the decomposition of the convective correlation into average kinetic and potential energy, it is notable that the thermal conductivity enhancement in nanofluids is mainly contributed by potential energy rather than kinetic energy, and it also dominated thermal

conductivity variation in both aggregated and non-aggregated nanofluids. For non-aggregated nanofluids, the increase in thermal conductivity is dominated by increasing potential energy of argon, whereas for aggregated nanofluids, the increase in thermal conductivity is dominated by the increasing potential energy of both argon and copper. As a result, thermal conductivity of the aggregated nanofluids is higher than that of the non-aggregated nanofluids.

Table 4.3: Summary on decomposition of thermal conductivity of nanofluids.

Decomposition of thermal conductivity	Aggregated nanofluids	Non-aggregated nanofluids	Remark
Overall thermal conductivity	↑	↑	aggregated > non-aggregated
Collision	□	□	aggregated > non-aggregated
Convective	↑	↑	aggregated > non-aggregated
Kinetic energy of copper	□	□	aggregated ≈ non-aggregated
Kinetic energy of argon	□	□	aggregated ≈ non-aggregated
Potential energy of copper	↑	□	aggregated > non-aggregated
Potential energy of argon	↑	↑	aggregated < non-aggregated

Symbol: ↑ - increase with increasing particle volume fraction; □ - independent with increasing particle volume fraction

4.2.4 Summary

In Section 4.2, the role of nanoparticle aggregation in governing the enhanced thermal conductivity of nanofluids was investigated by comparing thermal conductivity in both the aggregated and non-aggregated states. The thermal conductivity in both suspended states was further decomposed into collision correlation and convective correlation (kinetic energy and potential energy) for microscopic analysis. The main findings of the present simulation are presented in Table 4.3 and the details are as below:

- The thermal conductivity of the aggregated nanofluids is higher than that of the non-aggregated nanofluids by up to 35%. Thus, nanoparticle aggregation

induced higher thermal conductivity enhancement compared to non-aggregated nanofluids. However, thermal conductivities of both states are well enveloped by HS mean field bounds. It indicates that thermal conduction which is purely based on particle volume fraction and geometrical setup is well obeyed by nanofluids.

- Based on the decomposition of heat current into collision and convective correlations, thermal conductivity of both states is mainly governed by collision correlation while the enhancement is contributed by the convective correlation. The higher thermal conductivity of aggregated nanofluids compared to non-aggregated nanofluids can be attributed to two regimes: at low particle volume fraction of 2.59 vol% and 3.89 vol%, collision correlation dominated thermal conductivity variation in both aggregated and non-aggregated nanofluids; however, at high particle volume fraction of 5.18 vol% and above, thermal conductivity variation is contributed by both collision and convective correlations, though more by the latter.
- The convective correlation was further decomposed into average kinetic and potential energy. It was shown that thermal conductivity enhancement in nanofluids is mainly contributed by potential energy rather than kinetic energy, and the potential energy also dominates thermal conductivity variation in both aggregated and non-aggregated nanofluids. The average kinetic energy of argon and copper atoms is practically constant which implies that Brownian motion or its induced micro-convection has negligible effects on the thermal conductivity enhancement. For non-aggregated nanofluids, the increase in thermal conductivity is dominated by increasing potential energy of argon, whereas for aggregated nanofluids, the increase in thermal conductivity is dominated by the increasing potential energy of both argon and copper. As a result, thermal

conductivity of the aggregated nanofluids is higher than that of the non-aggregated nanofluids.

In conclusion, these findings ultimately prove that nanoparticle aggregation purely based on conduction is the key mechanism governing enhanced thermal conductivity. The collision and potential energy of copper nanoparticles are identified as inducing higher thermal conductivity in aggregated nanofluids than that in non-aggregated nanofluids. Aggregated nanoparticle with percolating network not only increases collision amongst particles but also induces higher potential energy amongst nanoparticles to allow effective heat conduction along the backbone of aggregation.

4.3 Effects of Particle Size and Temperature on Efficiency of Nanofluids

The objective in this section is to investigate the efficiency of nanofluids by comparing thermal conductivity enhancement and viscosity enhancement against the effects of particle size and temperature. As discussed in Section 2.3, the enhanced thermal conductivity in nanofluids is always accompanied by increased viscosity, leading to higher pumping energy in thermal system. Studying the effects of particle size and temperature on thermal conductivity and viscosity enhancement simultaneously on nanofluids can provide insights to develop efficient nanofluids with high thermal conductivity and low viscosity.

4.3.1 Design of Model

Well-dispersed nanofluids with suspension of multi-nanoparticle were modelled at particle volume fraction range from 2.19 vol% to 7.77 vol%. To study the particle size, nanofluids with two particle diameters of 15 Å and 20 Å were compared at temperature of 86 K. The temperature dependency was further investigated by varying the temperature from 86 K to 101 K for nanofluids with particle diameter of 20 Å. The well-dispersed nanofluids with particle diameter of 15 Å and 20 Å are represented by

system #2 and system #3, respectively. The details of simulation cell of system #2 and system #3 are presented in Table 3.3 and Table 3.4, respectively, and illustrated in Figure 3.4.

4.3.2 Effect of Particle Size on Thermal Conductivity

Figure 4.14 shows relative thermal conductivity (defined as the nanofluid-to-base fluid ratio of thermal conductivity) with respect to particle volume fraction for particle diameter of 20 Å and 15 Å at a temperature of 86 K. It is shown that the relative thermal conductivity for nanofluids for both particle diameters increase with the rise in particle volume fractions and it is significantly higher than the increase predicted by the Maxwell model. It is notable that the thermal conductivity enhancement of nanofluids with particle diameter of 20 Å and 15 Å are significantly different, in which the thermal conductivity enhancement for nanofluids with particle diameter of 20 Å is higher than those of particle diameter of 15 Å. At 7.65-7.77 vol% of nanofluids, the thermal conductivity is enhanced by 55% and 39% corresponding to particle diameter of 20 Å and 15 Å, respectively; while the Maxwell model only predicts an enhancement by 25%. Therefore, it can be concluded that the thermal conductivity enhancement increases with increasing particle size, and it is also in agreement with the reported experimental works (Angayarkanni et al., 2015; Beck et al., 2009; Chen et al., 2008a; Timofeeva et al., 2010; Warriar & Teja, 2011; Yu et al., 2008). However, the particle size dependency is not accounted for in the prediction of the Maxwell model.

The decrease in thermal conductivity with decreasing particle size may be attributed to interfacial thermal resistance between solid and liquid (Beck et al., 2009; Timofeeva, Routbort, & Singh, 2009; Timofeeva et al., 2010). It has been pointed out that the specific surface area of solid-liquid interface increases as the particle size decreases, hence smaller particle size tends to attract adjacent liquid to form more ordered layer

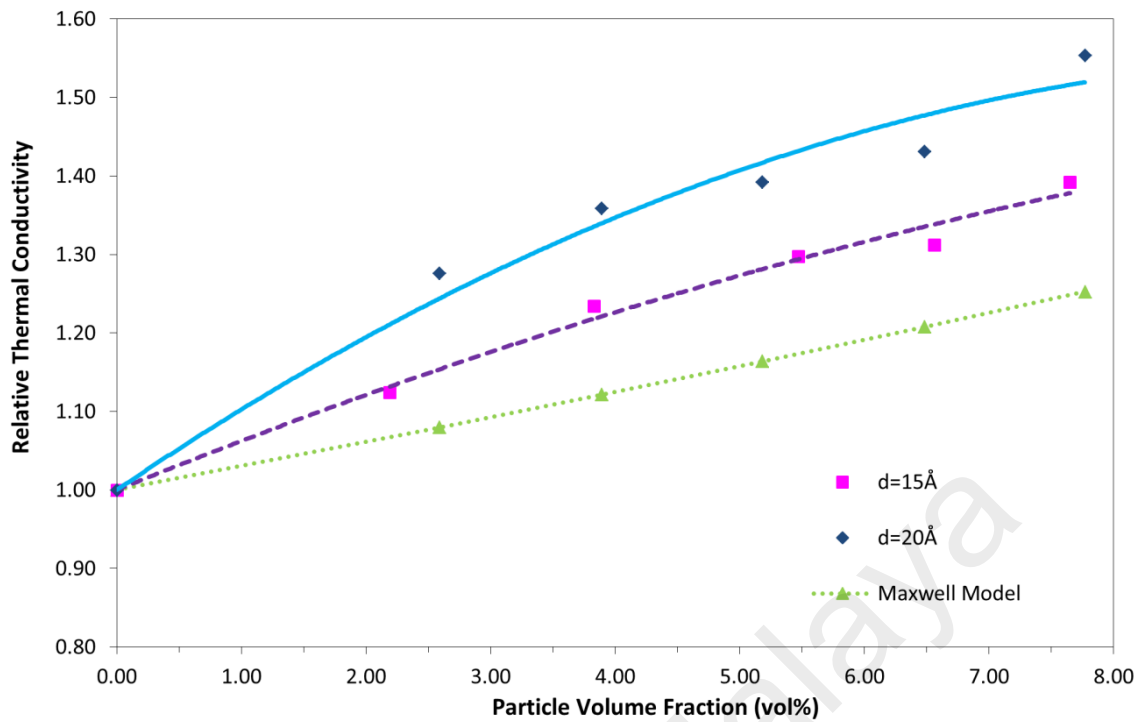


Figure 4.14: Relative thermal conductivity as a function of particle volume fraction for nanofluids with particle diameter of 15 Å and 20 Å at temperature 86 K, comparing with prediction by Maxwell model.

compared to bigger particle size. The effect of specific surface area was observed by studying radial distribution function (RDF) for solid-liquid interface in 7.65-7.77 vol% nanofluids with particle diameters of 15 Å and 20 Å, as shown in Figure 4.15. By comparing the RDF of bulk liquid, the structure of liquid changes with the addition of nanoparticle and it apparently becomes more crystalline in the vicinity of nanoparticle. The density of adjacent liquid to particle diameter of 15 Å is obviously higher than that of particle diameter of 20 Å. This ordered liquid layer on solid-liquid interface or amorphous-like interfacial liquid structure acts as an obstacle to heat flow (Barrat & Chiaruttini, 2003) which results in phonon scattering and abrupt temperature drop at the solid-liquid interface (Maruyama & Kimura, 1999; Xue, Koblinski, Phillpot, Choi, & Eastman, 2003). The resistance at solid-liquid interface is regarded as interfacial thermal resistance or Kapitza resistance (Maruyama & Kimura, 1999; Xue et al., 2003). The interfacial thermal resistance becomes more pronounced and critical for nanoscale

system due to the thickness of interfacial thermal resistance is comparable to the system size (Maruyama & Kimura, 1999). The existence of interfacial thermal resistance has been experimentally proven in carbon nanotube suspensions (Huxtable et al., 2003). In view of this, the decrease in thermal conductivity due to the increase in specific surface area of solid-liquid interface for smaller particle size indicates that the existence of interfacial thermal resistance in nanofluids is non-negligible.

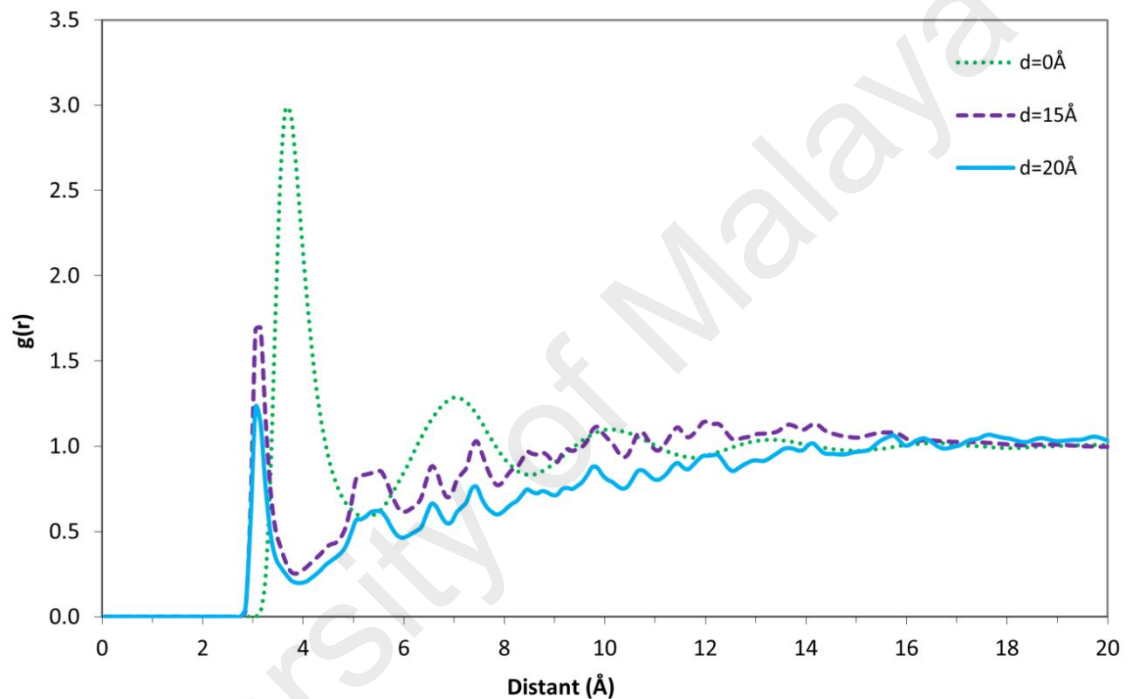


Figure 4.15: RDF for bulk liquid and 7.65-7.77 vol% nanofluids with particle diameter of 15 Å and 20 Å as a function of radial distant from reference atom.

4.3.3 Effect of Temperature on Thermal Conductivity

Thermal conductivity for nanofluids with particle diameter of 20 Å in different particle volume fractions was computed at temperatures that ranging from 86 K to 101 K. The results of thermal conductivity as well as the relative thermal conductivity are shown in Figure 4.16a and Figure 4.16b, respectively. Figure 4.16a shows that the thermal conductivity of nanofluids increases with increasing temperature. As for the temperature dependence, the slopes of nanofluids are approximately the same as that of

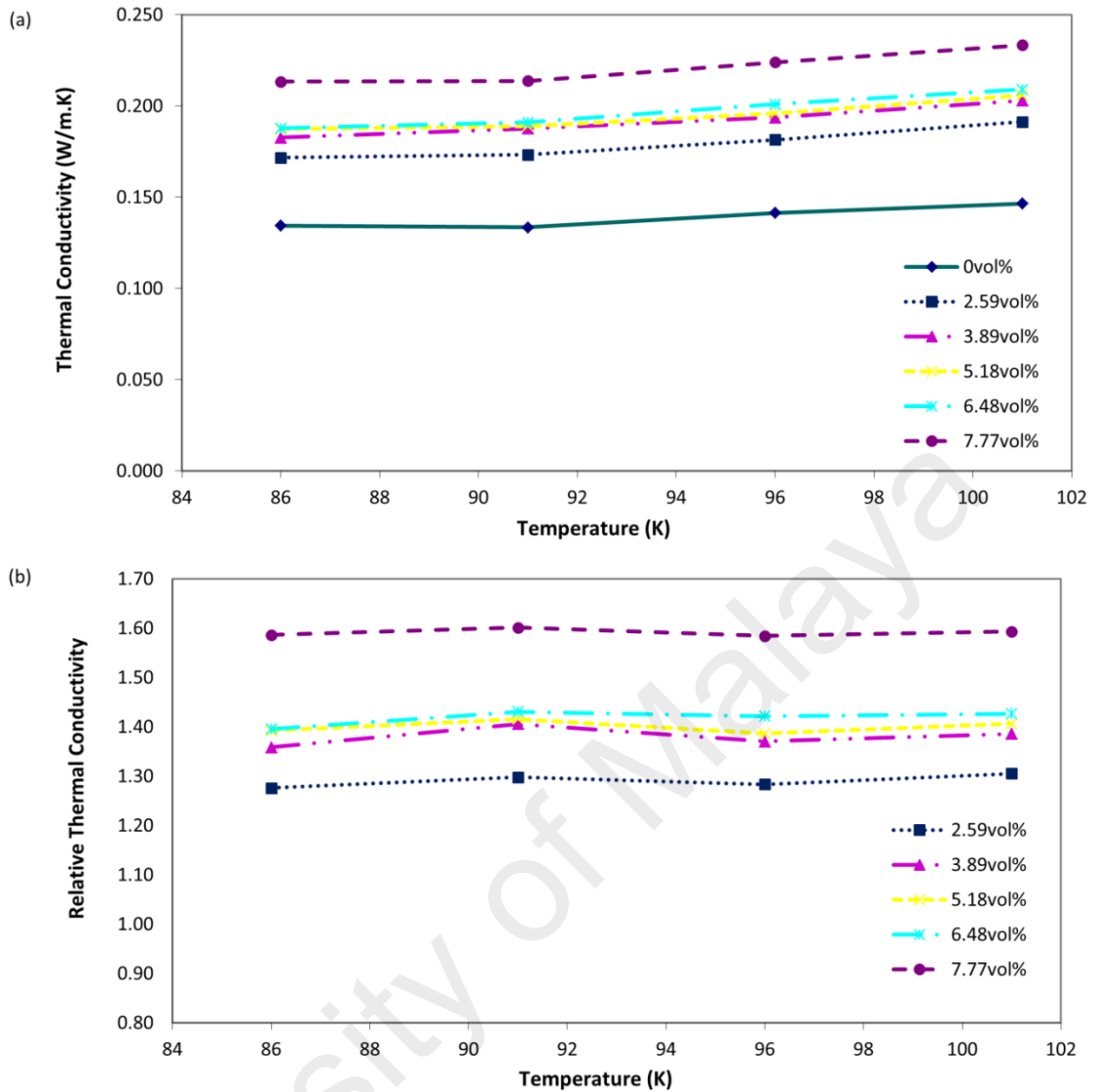


Figure 4.16: (a) Thermal conductivity and (b) relative thermal conductivity as a function of temperature for nanofluids with particle diameter of 20 Å.

pure base fluid. In Figure 4.16b, it is shown that the thermal conductivity enhancement does not vary significantly with the increasing temperature. When temperature rises from 86 K to 101 K, the thermal conductivity enhancement increases from 28% to 31% for 2.59 vol% nanofluids, whereas the thermal conductivity enhancement is maintained at 59% for 7.77 vol% nanofluids. Such weak temperature dependence indicates that the observed increase in thermal conductivity of nanofluids with increasing temperature originates from the base fluid rather than the addition of nanoparticles. Thus, it can be concluded that the thermal conductivity enhancement in nanofluids is independent of

temperature, which is consistent with Maxwell model. This finding is in excellent agreement with reported experimental works (Beck et al., 2007; Beck et al., 2010; Pastoriza-Gallego et al., 2011b; Peñas et al., 2008; Singh et al., 2009; Timofeeva et al., 2007; Venerus et al., 2006; Zhang et al., 2006b; Zhang et al., 2007).

4.3.4 Effect of Particle Size on Viscosity

Figure 4.17 shows relative viscosity (defined as the nanofluid-to-base fluid ratio of viscosity) as a function of particle volume fraction for nanofluids with particle diameter of 20 Å and 15 Å at a temperature of 86 K. It is shown that the viscosity increases with the rise in particle volume fractions and substantially higher than the prediction of Einstein and Batchelor models. The gap between the relative viscosity of MD simulation and prediction of classical theories becomes more pronounced with increasing particle volume fraction. This clearly indicates the strong interaction between particles in nanofluids. It is interesting to note that the viscosity of nanofluids with particle diameter of 20 Å and 15 Å significantly differ. The viscosity of nanofluids with particle diameter of 15 Å is higher than nanofluids with particle diameter of 20 Å. At high particle volume fraction 7.65-7.77 vol%, the viscosity increases by 148% and 104% corresponding to nanofluids with particle diameter of 15 Å and 20 Å, while the prediction by classical theories is only up to 23%. Therefore, it demonstrates that viscosity enhancement increases with decreasing particle size and its dependency is not accounted in classical theories for viscosity prediction. The observed trend of particle size dependency on viscosity is in good agreement with reported experimental works (Anoop et al., 2009b; Chang et al., 2005; Chevalier et al., 2007; Pastoriza-Gallego et al., 2011a; Rudyak, 2013; Timofeeva et al., 2010; Timofeeva et al., 2011a) and further supported by MD simulations (Lu & Fan, 2008; Rudyak et al., 2009; Rudyak & Krasnolutski, 2014).

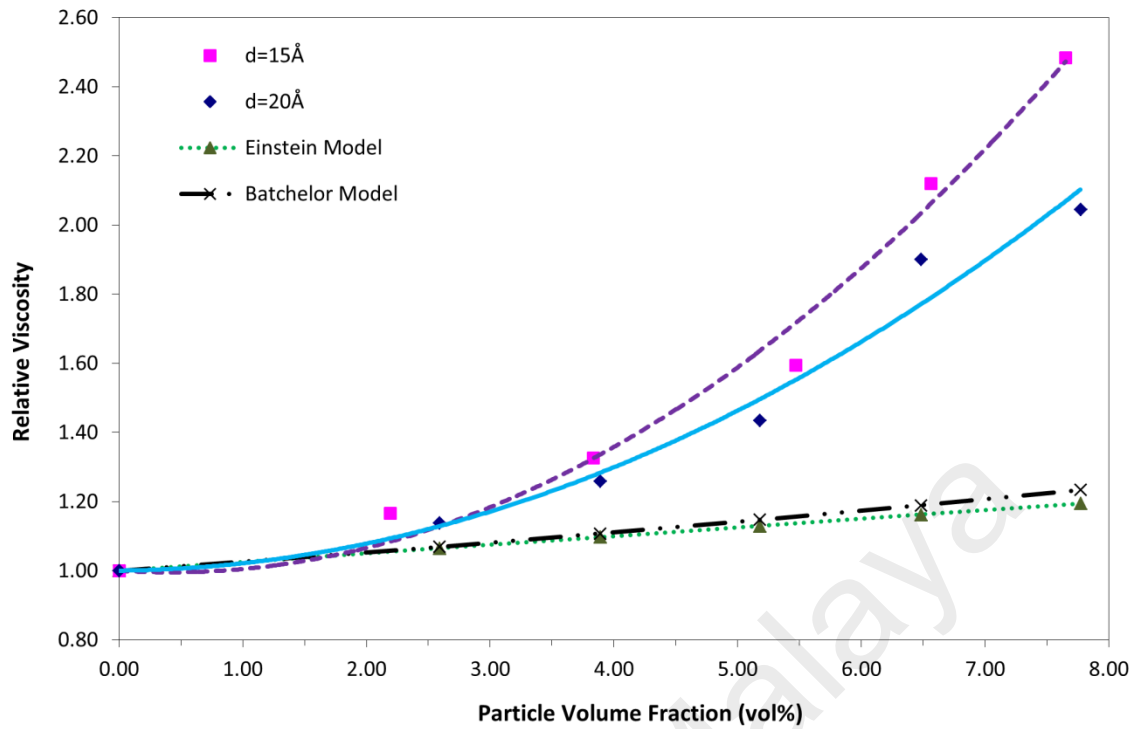


Figure 4.17: Relative viscosity as a function of particle volume fraction for nanofluids with particle diameter of 15 Å and 20 Å at temperature 86 K, comparing with prediction by Einstein model and Batchelor model.

The increase in viscosity of nanofluids is attributed to two effects (Timofeeva et al., 2010): (1) the electrostatic interaction between the nanoparticles and base fluid, which results in the formation of an ordered liquid layer on solid-liquid interface; and (2) the electrostatic interaction between the nanoparticles, which is related to the aggregation state of nanoparticles. As the present simulation controls the suspended nanoparticles in well-dispersed or non-aggregated state, the investigation on the second effect is ignored in the present analysis. The first effect of interaction between nanoparticle and base fluid is determined by referring the radial distribution function (RDF) for liquid around the nanoparticles, as shown in Figure 4.15. It indicates that an ordered liquid layer on solid-liquid interface is formed and its density increases with decreasing particle size. The ordered liquid layer or interfacial liquid structure is frozen at the solid-liquid interface and exhibits lower mobility compared to surrounding bulk liquid, hence reducing the overall mobility in nanofluids. Therefore, the increase in viscosity with

decreasing particle size was due to higher density of immobilised ordered liquid layer which is formed on solid-liquid interface for smaller particle size.

4.3.5 Effect of Temperature on Viscosity

The viscosity of nanofluids with particle diameter of 20 Å is computed at different particle volume fractions and temperature ranging from 86 K to 101 K. The results of viscosity as well as relative viscosity are shown in Figure 4.18a and Figure 4.18b, respectively. In Figure 4.18a, it is shown that the viscosity of nanofluids decreases with increasing temperature, and similar behaviour is also exhibited in the base fluid with minimal decreases. In Figure 4.18b, it is worth noting that the relative viscosity also decreases with increasing temperature. The temperature dependence on viscosity enhancement is more pronounced for high particle volume fraction, for example 6.48 vol% and 7.77 vol% but it appears weaker at low particle volume fraction. At temperature range from 86 K to 101 K, the viscosity enhancement is reduced from 104% to 84% for 7.77 vol% nanofluids, but the viscosity enhancement is only reduced from 14% to 6% for 2.59 vol% nanofluids. This result indicates that the temperature dependence on viscosity may be different for nanofluids with high and low particle volume fraction. The observed trend of temperature dependence on viscosity is in well agreement with mostly reported experimental works (Kole & Dey, 2013; Namburu et al., 2007; Nguyen et al., 2008; Nguyen et al., 2007; Pastoriza-Gallego et al., 2011b; Sundar et al., 2014; Tavman et al., 2008; Timofeeva et al., 2010; Timofeeva et al., 2011a).

The relationship between temperature and viscosity enhancement suggests that temperature dependence of nanofluids is dominated by the insertion of nanoparticles especially at high particle volume fraction. As liquid viscosity is usually temperature dependent, an increase in temperature will decrease the liquid viscosity. Therefore,

similar behaviour becomes more significant for nanofluids with higher particles interactions. From the molecular point of view, higher temperature increases velocities of atoms, hence reducing the interaction time between neighbouring atoms in nanofluids. As a result, the inter-particle force is weakened and this is followed by the decrease in viscosity.

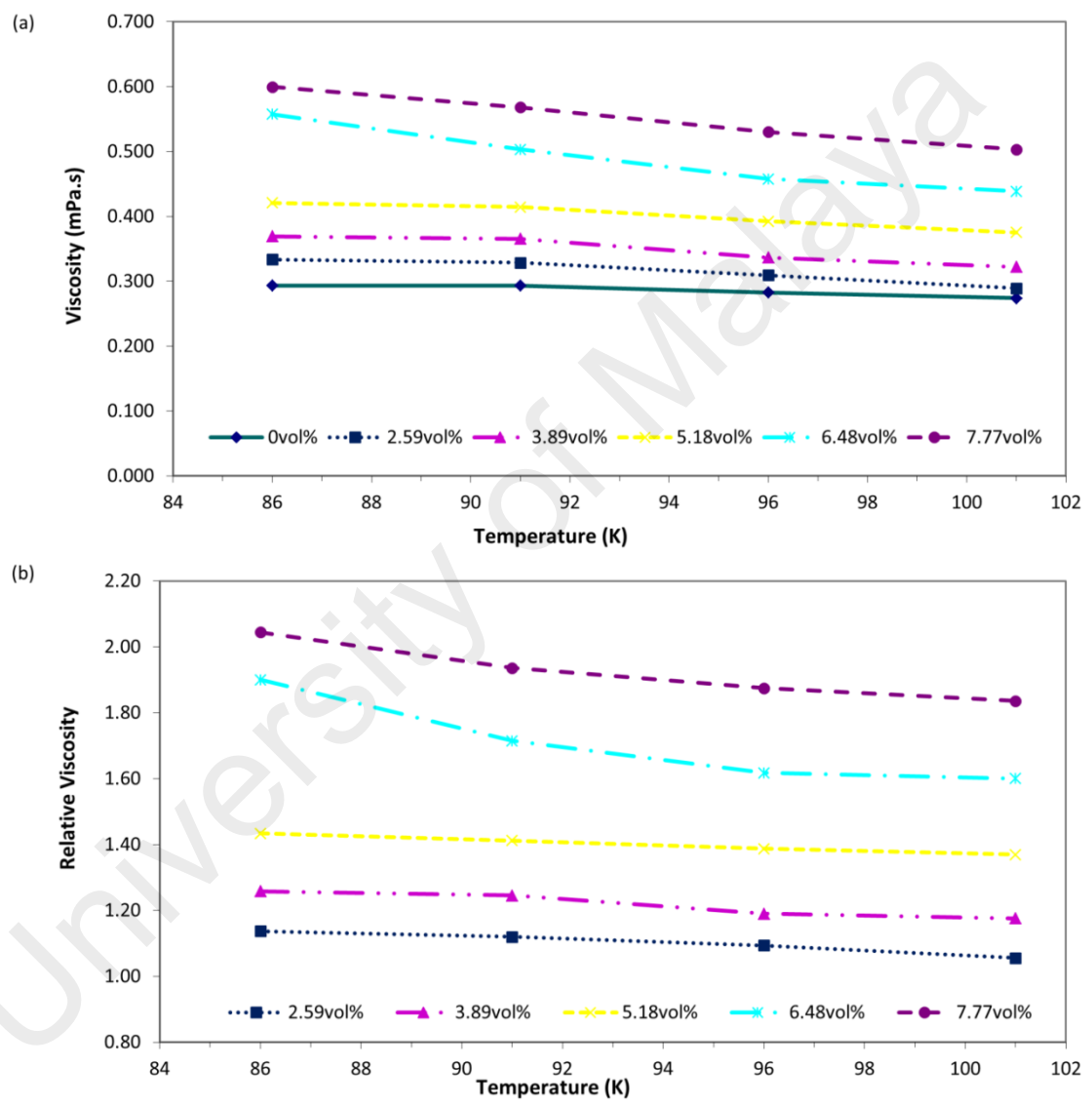


Figure 4.18: (a) Viscosity and (b) relative viscosity as a function of temperature for nanofluids with particle diameter of 20 Å.

4.3.6 Cooling Efficiency of Nanofluids

Based on the criterion discussed in Section 2.4, the efficiency of nanofluids can be evaluated by comparing the viscosity enhancement coefficient and the thermal conductivity enhancement coefficient. Figure 4.19a and Figure 4.19b show the relative thermal conductivity and viscosity with respect to particle volume fraction for nanofluids with particle diameter of 15 Å and 20 Å, respectively. Physically, the enhancement of thermal conductivity and viscosity increases with increasing particle

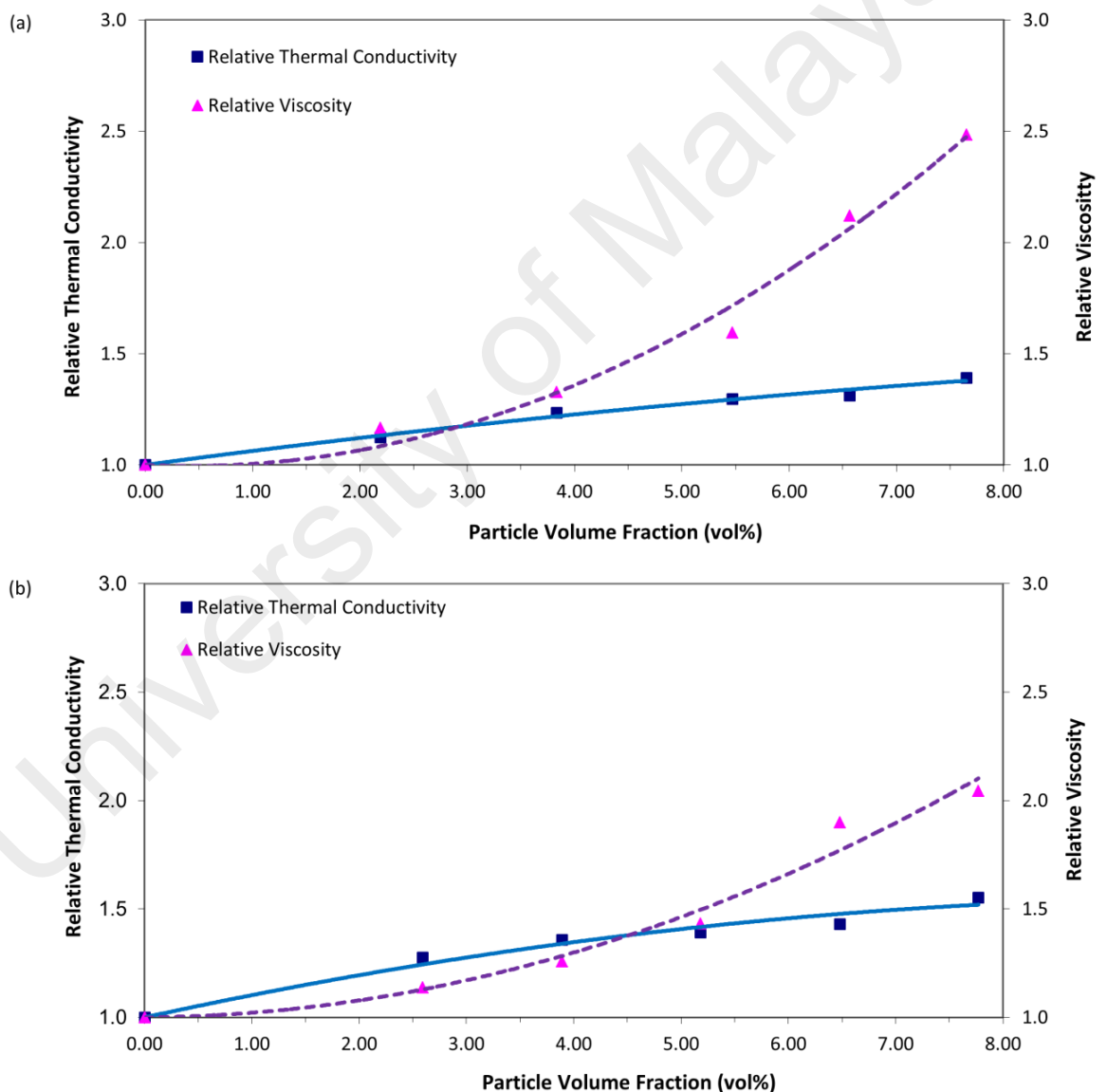


Figure 4.19: Relative thermal conductivity and viscosity as a function of particle volume fraction for (a) nanofluids with particle diameter of 15 Å and (b) nanofluids with particle diameter of 20 Å.

volume fraction. However, the enhancement in viscosity is even higher than that in thermal conductivity at high particle volume fraction and the difference is more pronounced for nanofluids with particle diameter of 15 Å than that of 20 Å. The efficiency of nanofluids with particle diameter of 15 Å and 20 Å with respect to particle volume fraction is analysed in Figure 4.20. It is shown that although the efficiency of nanofluids is reduced with increasing particle volume fraction, the efficiency can be improved significantly by increasing the particle diameter, as larger particle size produces higher thermal conductivity enhancement and lower viscosity enhancement.

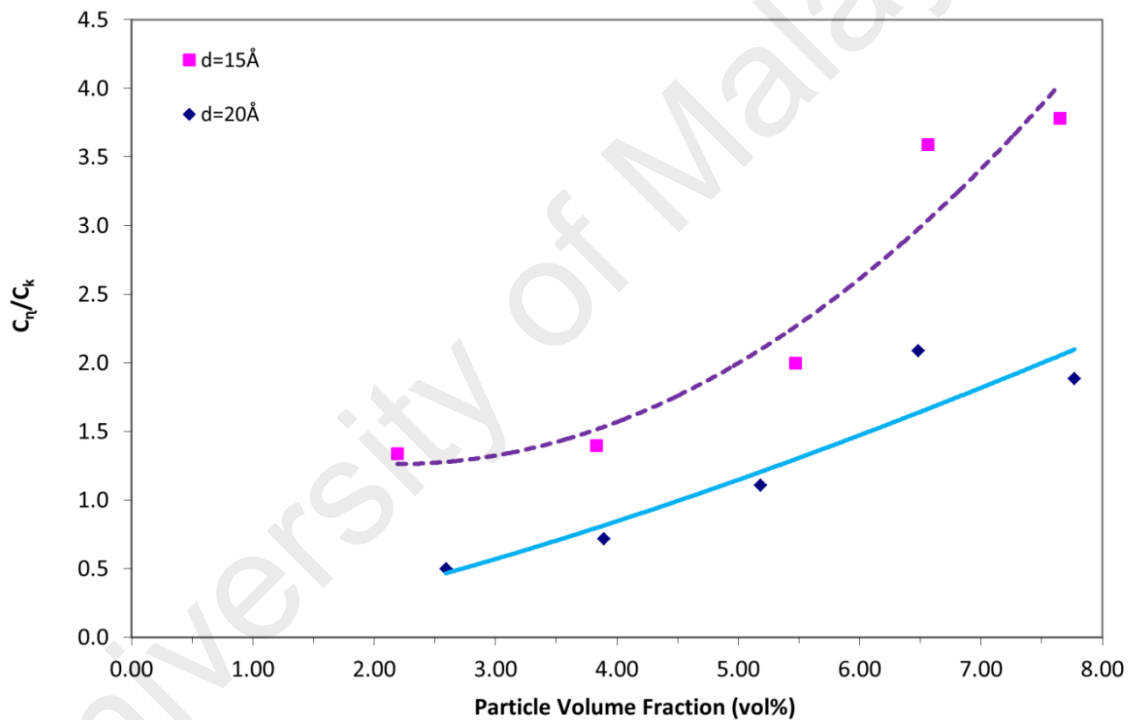


Figure 4.20: C_η/C_k as a function of particle size and particle volume fraction for nanofluids at 86 K.

Apart from the effects of particle size, the effect of temperature on efficiency of nanofluids is also studied. Figure 4.21a and Figure 4.21b depicts the relative thermal conductivity and viscosity with respect to temperature for 2.59 vol% and 7.77 vol% nanofluids, respectively, with particle diameter of 20 Å. By increasing the temperature from 86 K to 101 K, the thermal conductivity enhancement is significantly higher than

viscosity enhancement for 2.59 vol% nanofluids; whereas the thermal conductivity enhancement is obviously lower than the viscosity enhancement for 7.77 vol% nanofluids. The efficiency of nanofluids with respect to temperature is analysed in Figure 4.22. It is shown that the efficiency of nanofluids is improved by increasing the temperature. The improvement is mainly attributed to the decrease in viscosity enhancement but constant temperature enhancement at rising temperature.

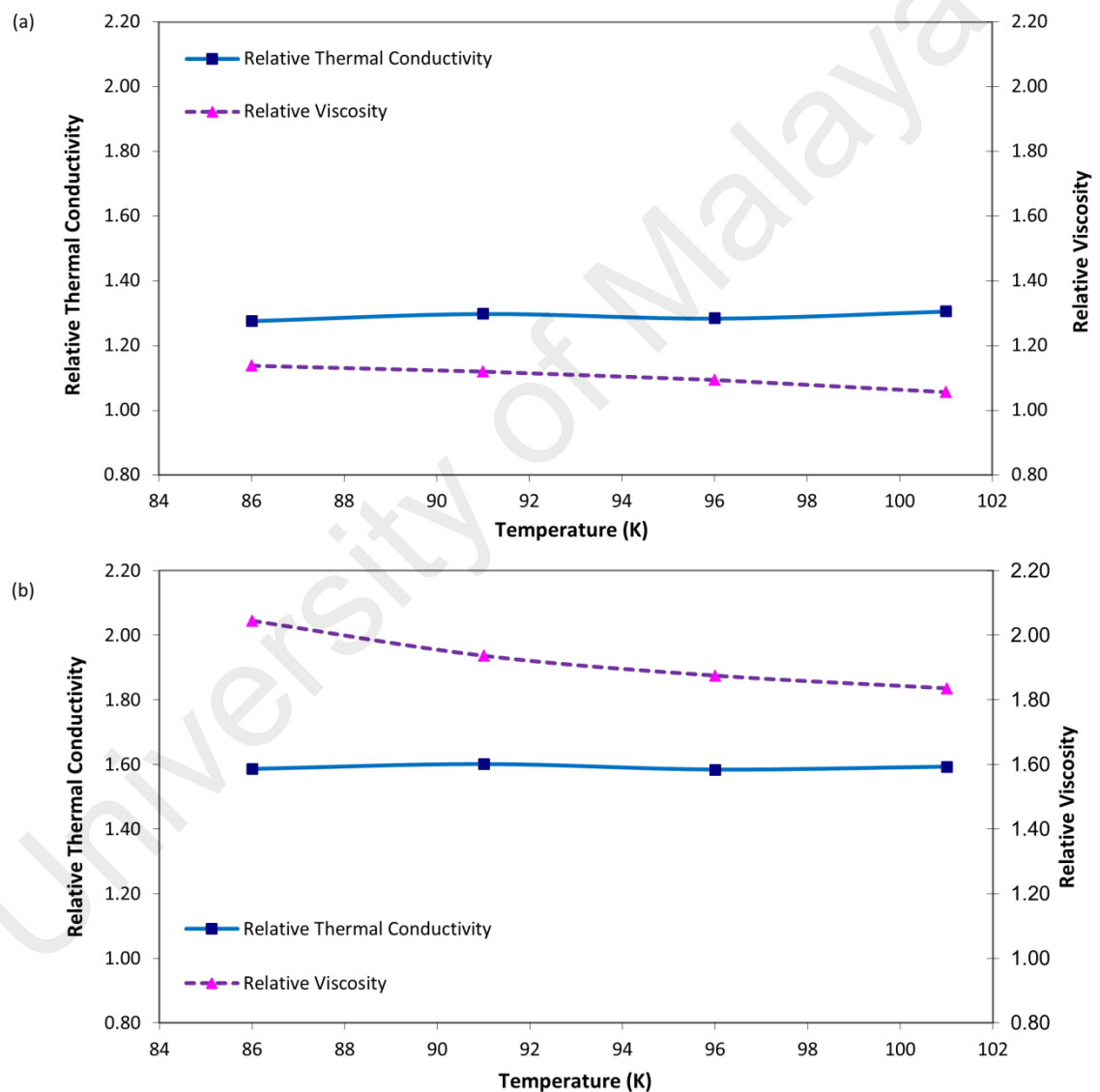


Figure 4.21: Relative thermal conductivity and viscosity as a function of temperature for (a) 2.59 vol% nanofluids and (b) 7.77 vol% nanofluids with particle diameter of 20 Å.

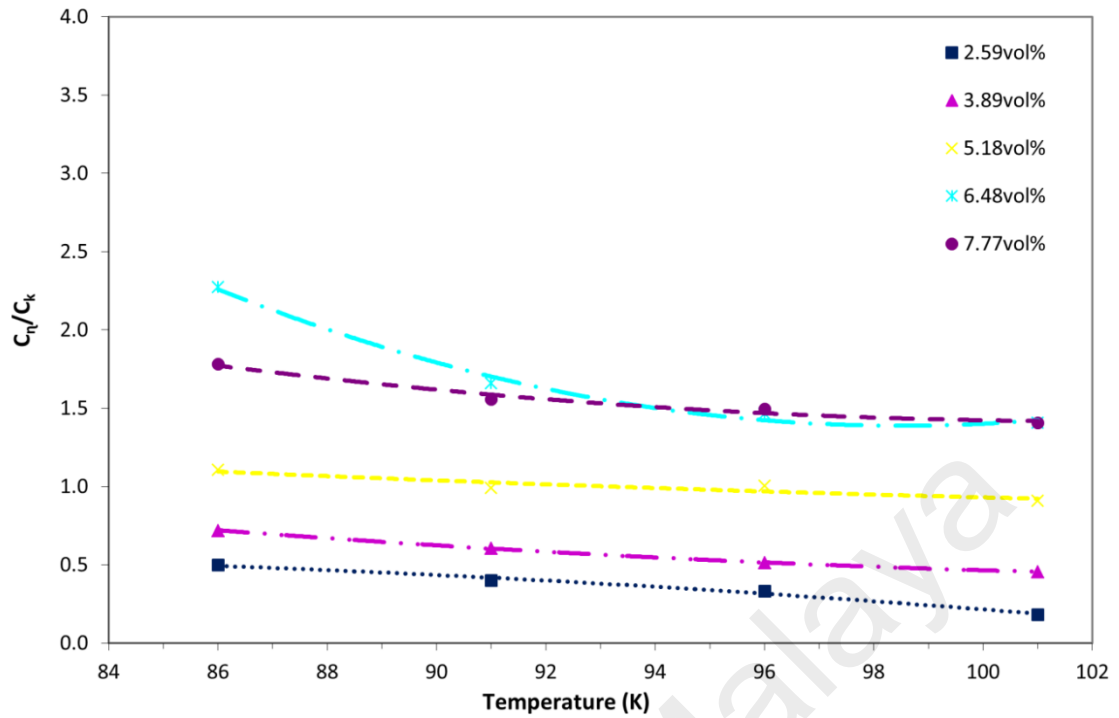


Figure 4.22: C_{η}/C_k as a function of temperature and particle volume fraction for nanofluids with particle diameter of 20 Å.

Based on the above examination on the efficiency of nanofluids with respect to particle size and temperature, it can be concluded that particle size and temperature are important parameters to improve the efficiency of nanofluids. The particle size variation is more effective than temperature control in producing highly efficient nanofluids. One has to keep in mind that, considerable particle size can lead to surface impact, erosion and stability problems. Therefore, it is necessary to quantify the behaviour which relates to particle size in the energy system.

Table 4.4: Effects of particle size and temperature on thermal conductivity enhancement, viscosity enhancement and efficiency of nanofluids.

	Particle Size	Temperature
Thermal conductivity enhancement	↑	□
Viscosity enhancement	↓	↓
Efficiency	↑	↑

Symbol: ↑ - increase with increasing parameter; ↓ - decrease with increasing parameter; □ - independent with increasing parameter

4.3.7 Summary

In Section 4.3, the effects of particle size and temperature on thermal conductivity and viscosity enhancement were investigated in order to determine the efficiency of nanofluids. The findings of the present investigation are presented in Table 4.4 and the details are as below:

- Effect of particle size on thermal conductivity - larger particle size produces higher thermal conductivity enhancement compared to smaller particle size. For 7.65-7.77 vol% of nanofluids, the thermal conductivity enhancement increases by 55% and 39% corresponding to nanofluids with particle diameter of 20 Å and 15 Å, respectively. The reduction in thermal conductivity enhancement with decreasing particle size and increasing specific surface area may be attributed to interfacial thermal resistance of the ordered liquid layer on the solid-liquid interface.
- Effect of temperature on thermal conductivity – the absolute thermal conductivity increases with the rise in temperature from 86 K to 101 K but the thermal conductivity enhancement is independent of temperature. This indicates that the temperature dependence on thermal conductivity of nanofluids is dominated by the base fluid itself instead of the addition of nanoparticles.
- Effect of particle size on viscosity – the viscosity enhancement is decreased by increasing particle size. For 7.65-7.77 vol%, the viscosity enhancement is increased by 104% and 148% corresponding to particle diameter of 20 Å and 15 Å, respectively. The viscosity enhancement variation is caused by the higher density of ordered liquid layer on the solid-liquid interface for smaller particle size compared to that larger particle size, hence reducing the overall mobility in nanofluids.

- Effect of temperature on viscosity – the viscosity and viscosity enhancement decreases with the rise in temperature, and its temperature dependency may be different for nanofluids with high and low particle volume fraction. At temperature range of 86 K to 101 K, the reduction in viscosity enhancement is up to 20% for 7.77 vol% nanofluids but only up to 8% for 2.59 vol% nanofluids. This demonstrates that the temperature dependence on viscosity enhancement is dominated by the insertion of nanoparticles especially at high particle volume fraction.

In conclusion, the efficiency of nanofluids can be improved by increasing the particle size and temperature in nanofluids. The thermal conductivity enhancement increases with increasing particle size but independent of temperature; whereas the viscosity enhancement decreases with increasing particle size and temperature. The particle size variation is therefore shown to be more effective than temperature control. As a result, the manipulation of particle size and temperature enables optimum directions in producing nanofluids that is more efficient than base fluid without being penalised by increases in pumping power.

CHAPTER 5: CONCLUSIONS

In this chapter, a summary of the works and findings described in this thesis are presented. This thesis is concerned with the investigation on the thermal transport of nanofluids at the molecular level, using the MD simulation. The objectives of this thesis as outlined in Chapter 1 are reviewed and the achievements are addressed. Finally, recommendations for future works are proposed.

5.1 Conclusions

Nanofluids have emerged as potential alternative for next generation of heat transfer fluids owing to its improved thermal conductivity. Nanofluids are engineered by suspending nanoparticles with the size of 1-100 nm into conventional heat transfer fluids to enhance its inherent poor thermal conductivity. Compared to microparticle suspension, the nanoparticle suspension in nanofluids behaved like molecules of liquid and has successfully avoided problems of clogging and erosion on thermal system and was compatible with existing heat exchanger system, for example microchannel heat exchanger. Thus, the exploitation of nanofluids brings about the possibilities to improve the efficiency of thermal system while maintaining the existing footprint, alternatively, provides the same efficiency of cooling system at smaller and lighter footprint as well as reduced inventory of heat transfer fluids. Nevertheless, the main concern of this novel exploitation is that there is no established physical fundamental to explain the observed enhanced thermal conductivity and results reported from different laboratories are controversial. To make the exploitation of nanofluids worse, the enhanced thermal conductivity in nanofluids is always accompanied by an increase in viscosity. The increase in viscosity leads to higher pumping power and this in turn increases operation cost. In order to fill the research gap, the goal of this thesis is to study the potential thermal conduction mechanisms in nanofluids, namely Brownian motion of

nanoparticles, Brownian motion induced micro-convection in base fluids and effects of nanoparticle aggregation. Apart from this, the efficiency of nanofluids in terms of thermal conductivity and viscosity enhancement against particle size and temperature effects is also investigated.

Based on the literatures, the inconsistent results of nanofluids are mainly attributed to poor characterisation of nanofluids especially sample polydispersity and hydrodynamic particle size distribution. Despite the increasing number of experimental works, the exploitation is still constrained by the high cost of nanofluids characterisation and difficulty to explore the enhanced thermal transport at nanoscale level. For this reason, MD simulation integrated with Green Kubo method was employed in this thesis to perform an ideal experiment and investigate the thermal transport at the molecular level. In the present work, nanofluids were modelled by suspending copper nanoparticles in liquid argon. Although liquid argon is not a real base fluid for nanofluids, it provides insightful information in an economic way. L-J potential was used to describe the three inter-atomic interactions in nanofluids, namely Ar-Ar, Cu-Cu and Ar-Cu. The employed potential and methodology in the present work were validated against previous experimental results; it has been shown that the present simulation is capable of providing good results with a maximum error of 5.9%.

The effect of Brownian motion of nanoparticles was identified to have negligible effects in enhancing thermal conductivity in nanofluids. It has been shown that thermal conductivity in nanofluids increased with increasing particle diameter from 16 Å to 36 Å, which was different with the Stokes-Einstein model which states that Brownian motion is inversely proportional to the particle size. Similarly, the effect of Brownian motion induced micro-convection in base fluids was also shown to be insignificant in enhancing thermal conductivity in nanofluids. It is interesting to note that the diffusion

coefficient of nanofluids was reduced instead of being enhanced by the addition of nanoparticles in base fluid. The reduction in diffusion coefficient was more pronounced for smaller particle size compared to that of larger particle size. Based on the analysis on RDF, the addition of nanoparticle changed the liquid structure of the base fluid in the vicinity of nanoparticle into an amorphous-like interfacial liquid structure. The crystallinity or density of the amorphous-like liquid structure increased with decreasing particle size due to its higher specific surface area. The formation of amorphous-like interfacial liquid structure was confirmed by observing the cage effect in VACF of nanoparticle, in which the cage effect became more pronounced with decreasing particle size. As a result, the effects of Brownian motion of nanoparticle and induced micro-convection in base fluid are not responsible for thermal conductivity enhancement in nanofluids owing to the hydrodynamic effect is mediated by amorphous-like interfacial liquid structure in the vicinity of nanoparticle.

The effect of nanoparticle aggregation was identified as the key mechanism to enhance thermal conductivity in nanofluids. The present simulation indicated that thermal conductivity enhancement of aggregated nanofluids was higher than non-aggregated nanofluids. The thermal conductivity of both states was beyond the prediction of the Maxwell model but was well enveloped by the lower and upper bounds of HS mean field theory. It is clear that the observed larger-than-predicted thermal conductivity enhancement in nanofluids is within the prediction of the mean field theory which sets the most restrictive limits based on the knowledge of particle volume fraction in different geometry. Based on the decomposition of thermal conductivity into collision and convective correlations, thermal conductivity of both systems was mainly governed by collision correlation while the enhancement was contributed by the convective correlation. The convective correlation was further decomposed into average kinetic and potential energy of atoms, it was seen that the enhancement was

significantly emanated from the potential energy amongst nanofluids rather than the kinetic energy. The higher thermal conductivity of aggregated nanofluids compared to non-aggregated nanofluids could be attributed to two regimes: at low particle volume fraction, collision correlation dominated the thermal conductivity variation in both aggregated and non-aggregated nanofluids; however, at high particle volume fraction for example 5.18 vol% and above, thermal conductivity variation was contributed by both collisions and potential correlations, though more by the latter. For non-aggregated nanofluids, enhancement in potential correlation was only dominated by argon atoms only; whereas for aggregated nanofluids, the enhancement from potential correlation was not only dominated by argon atoms but also by copper atoms. The result demonstrates that aggregated nanoparticles with percolating network not only increase collision amongst particles but also induce higher potential energy amongst nanoparticles to allow effective heat conduction along the backbone of aggregation.

Effects of particle size and temperature on the efficiency (ratio of thermal conductivity and viscosity enhancement) of nanofluids were also analysed. It was shown that thermal conductivity enhancement increased with increasing particle diameter from 15 Å to 20 Å. Based on RDF study on liquid structure at the immediate vicinity of nanoparticles, the ordering of interfacial liquid was improved with the addition of nanoparticles. The ordering improvement was more pronounced for smaller particle size compared to that of larger particle size owing to higher specific surface area for smaller particle size. Such ordered interfacial liquid structure may act as an obstacle to heat flow which is regarded as interfacial thermal resistance. Thus, it can be hypothesised that the reduction in thermal conductivity enhancement with decreasing particle size may be attributed to such interfacial thermal resistance. Apart from that, it has been shown that the absolute thermal conductivity increased with the rise in temperature from 86 K to 101 K but the thermal conductivity enhancement was

independent of temperature. Thus, it can be concluded that the temperature dependence on thermal conductivity of nanofluids is dominated by the base fluid itself instead of the addition of nanoparticles. On the other hand, it was observed that viscosity enhancement decreased by increasing particle diameter from 15 Å to 20 Å. Similar with thermal conductivity, such increase in viscosity was caused by the higher density of ordered interfacial liquid for smaller particle size compared to that of larger particle size, hence reducing the overall mobility in nanofluids. Additionally, viscosity and viscosity enhancement were shown to decrease with the rise in temperature from 86 K to 101 K, and the temperature dependency might be different for nanofluids with high and low particle volume fraction. Based on the above examination on thermal conductivity and viscosity enhancement, the efficiency of nanofluids could be improved by increasing the particle size and temperature. It clearly demonstrates that the thermal conductivity enhancement increases with increasing particle size but independent of temperature; whereas the viscosity enhancement decreases with increasing particle size and temperature. The particle size variation is therefore shown to be more effective than temperature control.

In conclusion, the three objectives of this thesis were achieved and provided comprehensive understanding on the potential thermal conduction mechanisms as well as optimum direction in producing efficient nanofluids. By employing MD simulation and theoretical analysis, this thesis has successfully identified the importance of nanoparticle aggregation in enhancing thermal conductivity of nanofluids and disqualified the contribution of hydrodynamics mechanisms, namely Brownian motion of nanoparticles and its induced micro-convection in base fluids. Regarding the efficiency of nanofluids, particle size and temperature are found to be important parameters to engineer nanofluids with the best combination of high thermal conductivity and low viscosity.

5.2 Recommendations

There are two possible extensions to the present investigation which should be pursued in order to shed more light on thermal transport of nanofluids:

- i. Nanoparticle aggregation is shown to enhance thermal conductivity in nanofluids. However, large aggregation of nanoparticles decreases the thermal conductivity enhancement as well as increases viscosity in nanofluids. Furthermore, such large nanoparticle aggregation may lead to abrasion and clogging to the existing thermal system. Thus, it is important to study the effects of geometry or fractal structure of nanoparticle aggregation on thermal conductivity enhancement in nanofluids. Simultaneously, its effect on viscosity enhancement should also be taken into consideration.
- ii. Approach to nanofluids as a three-phase system, namely solid phase (nanoparticle), liquid phase (base fluid) and interfacial phase (ordered interfacial liquid on the solid-liquid interface) should be considered in nanofluids studies (Timofeeva, Yu, France, Singh, & Routbort, 2011b). Due to higher specific surface area of nanoparticle, the interfacial phase is more significant for suspension of nanoparticles compared to those of microparticles. Such interfacial phase may reduce mobility of nanofluids and act as interfacial thermal resistance between solid and liquid to reduce the effective thermal conductivity in nanofluids. Thus, the interfacial phase with respect to the effects of particle size and shape, particle and base fluid materials should be given attention in future works.

REFERENCES

- Allen, M. P., & Tildesley, D. J. (1987). *Computer simulation of liquids*. Oxford, England: Oxford University Press.
- Angayarkanni, S., & Philip, J. (2014). Effect of nanoparticles aggregation on thermal and electrical conductivities of nanofluids. *Journal of Nanofluids*, 3(1), 17-25.
- Angayarkanni, S., Sunny, V., & Philip, J. (2015). Effect of nanoparticle size, morphology and concentration on specific heat capacity and thermal conductivity of nanofluids. *Journal of Nanofluids*, 4(3), 302-309.
- Anoop, K., Kabelac, S., Sundararajan, T., & Das, S. K. (2009a). Rheological and flow characteristics of nanofluids: influence of electroviscous effects and particle agglomeration. *Journal of Applied Physics*, 106(3), 034909.
- Anoop, K., Sundararajan, T., & Das, S. K. (2009b). Effect of particle size on the convective heat transfer in nanofluid in the developing region. *International Journal of Heat and Mass Transfer*, 52(9), 2189-2195.
- Assael, M. J., Chen, C. F., Metaxa, I., & Wakeham, W. A. (2004). Thermal conductivity of suspensions of carbon nanotubes in water. *International Journal of Thermophysics*, 25(4), 971-985.
- Assael, M. J., Metaxa, I. N., Kakosimos, K., & Constantinou, D. (2006). Thermal conductivity of nanofluids—experimental and theoretical. *International Journal of Thermophysics*, 27(4), 999-1017.
- Babaei, H., Keblinski, P., & Khodadadi, J. (2013). A proof for insignificant effect of Brownian motion-induced micro-convection on thermal conductivity of nanofluids by utilizing molecular dynamics simulations. *Journal of Applied Physics*, 113(8), 084302.
- Babaei, H., Keblinski, P., & Khodadadi, J. M. (2012). Equilibrium molecular dynamics determination of thermal conductivity for multi-component systems. *Journal of Applied Physics*, 112(5), 054310.
- Barrat, J. L., & Chiaruttini, F. (2003). Kapitza resistance at the liquid—solid interface. *Molecular Physics*, 101(11), 1605–1610.
- Bastea, S. (2005). Comment on “model for heat conduction in nanofluids”. *Physical Review Letters*, 95(1), 19401.

- Batchelor, G. (1977). The effect of Brownian motion on the bulk stress in a suspension of spherical particles. *Journal of Fluid Mechanics*, 83(01), 97–117.
- Beck, M. P., Sun, T., & Teja, A. S. (2007). The thermal conductivity of alumina nanoparticles dispersed in ethylene glycol. *Fluid Phase Equilibria*, 260(2), 275–278.
- Beck, M. P., Yuan, Y., Warriar, P., & Teja, A. S. (2009). The effect of particle size on the thermal conductivity of alumina nanofluids. *Journal of Nanoparticle Research*, 11(5), 1129–1136.
- Beck, M. P., Yuan, Y., Warriar, P., & Teja, A. S. (2010). The thermal conductivity of alumina nanofluids in water, ethylene glycol, and ethylene glycol+ water mixtures. *Journal of Nanoparticle Research*, 12(4), 1469-1477.
- Bhattacharya, P., Saha, S., Yadav, A., Phelan, P., & Prasher, R. (2004). Brownian dynamics simulation to determine the effective thermal conductivity of nanofluids. *Journal of Applied Physics*, 95(11), 6492–6494.
- Buongiorno, J., & Hu, L. W. (2010). Nanofluid heat transfer enhancement for nuclear reactor applications. *Proceedings of the ASME Micro/Nanoscale Heat and Mass Transfer International Conference 2009*, 3, 517-522, doi: 10.1115/MNHMT2009-18062.
- Buongiorno, J., Hu, L. W., Apostolakis, G., Hannink, R., Lucas, T., & Chupin, A. (2009). A feasibility assessment of the use of nanofluids to enhance the in-vessel retention capability in light-water reactors. *Nuclear Engineering and Design*, 239(5), 941-948.
- Buongiorno, J., Hu, L. W., Kim, S. J., Hannink, R., Truong, B., & Forrest, E. (2008). Nanofluids for enhanced economics and safety of nuclear reactors: an evaluation of the potential features, issues, and research gaps. *Nuclear Technology*, 162(1), 80-91.
- Chandrasekar, M., Suresh, S., & Chandra Bose, A. (2010). Experimental investigations and theoretical determination of thermal conductivity and viscosity of Al₂O₃ /water nanofluid. *Experimental Thermal and Fluid Science*, 34(2), 210-216.
- Chang, H., Jwo, C., Lo, C., Tsung, T., Kao, M., & Lin, H. (2005). Rheology of CuO nanoparticle suspension prepared by ASNSS. *Reviews on Advanced Materials Science*, 10(2), 128-132.

- Chen, G., Yu, W., Singh, D., Cookson, D., & Routbort, J. (2008a). Application of SAXS to the study of particle-size-dependent thermal conductivity in silica nanofluids. *Journal of Nanoparticle Research*, 10(7), 1109–1114.
- Chen, H., Ding, Y., He, Y., & Tan, C. (2007a). Rheological behaviour of ethylene glycol based titania nanofluids. *Chemical Physics Letters*, 444(4), 333-337.
- Chen, H., Ding, Y., Lapkin, A., & Fan, X. (2009a). Rheological behaviour of ethylene glycol-titanate nanotube nanofluids. *Journal of Nanoparticle Research*, 11(6), 1513-1520.
- Chen, H., Ding, Y., & Tan, C. (2007b). Rheological behaviour of nanofluids. *New Journal of Physics*, 9(10), 367.
- Chen, H., Witharana, S., Jin, Y., Kim, C., & Ding, Y. (2009b). Predicting thermal conductivity of liquid suspensions of nanoparticles (nanofluids) based on rheology. *Particuology*, 7(2), 151-157.
- Chen, H., Yang, W., He, Y., Ding, Y., Zhang, L., Tan, C., . . . Bavykin, D. V. (2008b). Heat transfer and flow behaviour of aqueous suspensions of titanate nanotubes (nanofluids). *Powder Technology*, 183(1), 63-72.
- Chevalier, J., Tillement, O., & Ayela, F. (2007). Rheological properties of nanofluids flowing through microchannels. *Applied Physics Letters*, 91(23), 233103.
- Choi, S. U. S. (1995). Enhancing thermal conductivity of fluids with nanoparticles. *American Society of Mechanical Engineers, Fluids Engineering Division (Publication) FED*, 231, 99-105.
- Choi, S. U. S., Zhang, Z. G., Yu, W., Lockwood, F. E., & Grulke, E. A. (2001). Anomalous thermal conductivity enhancement in nanotube suspensions. *Applied Physics Letters*, 79(14), 2252–2254.
- Chon, C. H., Kihm, K. D., Lee, S. P., & Choi, S. U. S. (2005). Empirical correlation finding the role of temperature and particle size for nanofluid (Al_2O_3) thermal conductivity enhancement. *Applied Physics Letters*, 87(15), 153107.
- Chopkar, M., Das, P. K., & Manna, I. (2006). Synthesis and characterization of nanofluid for advanced heat transfer applications. *Scripta Materialia*, 55(6), 549-552.

- Chopkar, M., Kumar, S., Bhandari, D., Das, P. K., & Manna, I. (2007). Development and characterization of Al_2Cu and Ag_2Al nanoparticle dispersed water and ethylene glycol based nanofluid. *Materials Science and Engineering: B*, 139(2), 141-148.
- Das, S. K., Putra, N., Thiesen, P., & Roetzel, W. (2003). Temperature dependence of thermal conductivity enhancement for nanofluids. *Journal of Heat Transfer*, 125(4), 567-574.
- Demas, N. G., Timofeeva, E. V., Routbort, J. L., & Fenske, G. R. (2012). Tribological effects of BN and MoS_2 nanoparticles added to polyalphaolefin oil in piston skirt/cylinder liner tests. *Tribology Letters*, 47(1), 91-102.
- Dileep, S., Timofeeva, E. V., Yu, W., & France, D. M. (2013). *Development of nanofluids for cooling power electronics for hybrid electric vehicles* (VSS112). Washington, DC: Argonne National Laboratory.
- Duangthongsuk, W., & Wongwises, S. (2009). Measurement of temperature-dependent thermal conductivity and viscosity of TiO_2 -water nanofluids. *Experimental Thermal and Fluid Science*, 33(4), 706-714.
- Eapen, J., Li, J., & Yip, S. (2007a). Mechanism of thermal transport in dilute nanocolloids. *Physical Review Letters*, 98(2), 028302.
- Eapen, J., Rusconi, R., Piazza, R., & Yip, S. (2010). The classical nature of thermal conduction in nanofluids. *Journal of Heat Transfer*, 132(10), 102402.
- Eapen, J., Williams, W. C., Buongiorno, J., Hu, L., Yip, S., Rusconi, R., & Piazza, R. (2007b). Mean-field versus microconvection effects in nanofluid thermal conduction. *Physical Review Letters*, 99(9), 095901.
- Eastman, J. A., Choi, S. U. S., Li, S., Yu, W., & Thompson, L. J. (2001). Anomalously increased effective thermal conductivities of ethylene glycol-based nanofluids containing copper nanoparticles. *Applied Physics Letters*, 78(6), 718-720.
- Eastman, J. A., Phillpot, S. R., Choi, S. U. S., & Keblinski, P. (2004). Thermal transport in nanofluids. *Annual Review of Materials Research*, 34(0), 219-246.
- Einstein, A. (1956). *Investigation of the Brownian theory of movement*. New York, NY: Dover Publication.

- Esfe, M. H., Saedodin, S., Akbari, M., Karimipour, A., Afrand, M., Wongwises, S., . . . Dahari, M. (2015). Experimental investigation and development of new correlations for thermal conductivity of CuO/EG–water nanofluid. *International Communications in Heat and Mass Transfer*, 65, 47-51.
- Evans, W., Fish, J., & Keblinski, P. (2006). Role of Brownian motion hydrodynamics on nanofluid thermal conductivity. *Applied Physics Letters*, 88(9), 093116.
- Evans, W., Prasher, R., Fish, J., Meakin, P., Phelan, P., & Keblinski, P. (2008). Effect of aggregation and interfacial thermal resistance on thermal conductivity of nanocomposites and colloidal nanofluids. *International Journal of Heat and Mass Transfer*, 51(5), 1431–1438.
- Feng, X., & Johnson, D. W. (2012). Mass transfer in SiO₂ nanofluids: A case against purported nanoparticle convection effects. *International Journal of Heat and Mass Transfer*, 55(13–14), 3447–3453.
- Feng, Y., Yu, B., Xu, P., & Zou, M. (2007). The effective thermal conductivity of nanofluids based on the nanolayer and the aggregation of nanoparticles. *Journal of Physics D: Applied Physics*, 40(10), 3164.
- Gao, J., Zheng, R., Ohtani, H., Zhu, D., & Chen, G. (2009). Experimental investigation of heat conduction mechanisms in nanofluids. Clue on clustering. *Nano Letters*, 9(12), 4128–4132.
- Garg, J., Poudel, B., Chiesa, M., Gordon, J., Ma, J., Wang, J., . . . Nanda, J. (2008). Enhanced thermal conductivity and viscosity of copper nanoparticles in ethylene glycol nanofluid. *Journal of Applied Physics*, 103(7), 074301.
- Gerardi, C., Cory, D., Buongiorno, J., Hu, L. W., & McKrell, T. (2009). Nuclear magnetic resonance-based study of ordered layering on the surface of alumina nanoparticles in water. *Applied Physics Letters*, 95(25), 253104.
- Gharagozloo, P. E., Eaton, J. K., & Goodson, K. E. (2008). Diffusion, aggregation, and the thermal conductivity of nanofluids. *Applied Physics Letters*, 93(10), 103110.
- Ghosh, M. M., Roy, S., Pabi, S. K., & Ghosh, S. (2011). A molecular dynamics-stochastic model for thermal conductivity of nanofluids and its experimental validation. *Journal of Nanoscience and Nanotechnology*, 11(3), 2196-2207.
- Haile, J. M. (1992). *Molecular dynamics simulation: elementary methods*. New York, NY: John Wiley & Sons, Inc.

- Hamilton, R., & Crosser, O. (1962). Thermal conductivity of heterogeneous two-component systems. *Industrial & Engineering Chemistry Fundamentals*, 1(3), 187-191.
- Hansen, J., & McDonald, I. (1986). *Theory of Simple Fluids*. New York, NY: Academic Press.
- Hashin, Z., & Shtrikman, S. (1962). A variational approach to the theory of the effective magnetic permeability of multiphase materials. *Journal of Applied Physics*, 33(10), 3125-3131.
- He, Y., Jin, Y., Chen, H., Ding, Y., Cang, D., & Lu, H. (2007). Heat transfer and flow behaviour of aqueous suspensions of TiO₂ nanoparticles (nanofluids) flowing upward through a vertical pipe. *International Journal of Heat and Mass Transfer*, 50(11), 2272–2281.
- Hess, B. (2002). Determining the shear viscosity of model liquids from molecular dynamics simulations. *The Journal of Chemical Physics*, 116(1), 209-217.
- Ho, C. J., Wei, L. C., & Li, Z. W. (2010). An experimental investigation of forced convective cooling performance of a microchannel heat sink with Al₂O₃/water nanofluid. *Applied Thermal Engineering*, 30(2), 96-103.
- Hong, J., & Kim, D. (2012). Effects of aggregation on the thermal conductivity of alumina/water nanofluids. *Thermochimica Acta*, 542, 28-32.
- Hong, K., Hong, T. K., & Yang, H. S. (2006). Thermal conductivity of Fe nanofluids depending on the cluster size of nanoparticles. *Applied Physics Letters*, 88(3), 031901.
- Hong, T. K., Yang, H. S., & Choi, C. J. (2005). Study of the enhanced thermal conductivity of Fe nanofluids. *Journal of Applied Physics*, 97(6), 064311.
- Humphrey, W., Dalke, A., & Schulten, K. (1996). Vmd: Visual Molecular Dynamics. *Journal of Molecular Graphics*, 14, 33–38.
- Huxtable, S. T., Cahill, D. G., Shenogin, S., Xue, L., Ozisik, R., Barone, P., . . . Shim, M. (2003). Interfacial heat flow in carbon nanotube suspensions. *Nature Materials*, 2(11), 731–734.

- Hwang, Y., Lee, J., Lee, C., Jung, Y., Cheong, S., Lee, C., . . . Jang, S. (2007). Stability and thermal conductivity characteristics of nanofluids. *Thermochimica Acta*, 455(1), 70-74.
- Hwang, Y., Park, H., Lee, J., & Jung, W. (2006). Thermal conductivity and lubrication characteristics of nanofluids. *Current Applied Physics*, 6, e67-e71.
- Jana, S., Salehi-Khojin, A., & Zhong, W. H. (2007). Enhancement of fluid thermal conductivity by the addition of single and hybrid nano-additives. *Thermochimica Acta*, 462(1), 45-55.
- Jang, S. P., & Choi, S. U. S. (2004). Role of Brownian motion in the enhanced thermal conductivity of nanofluids. *Applied Physics Letters*, 84(21), 4316-4318.
- Jang, S. P., & Choi, S. U. S. (2007). Effects of various parameters on nanofluid thermal conductivity. *Journal of Heat Transfer*, 129, 617-623.
- Jones, R. E., & Mandadapu, K. K. (2012). Adaptive Green-Kubo estimates of transport coefficients from molecular dynamics based on robust error analysis. *The Journal of Chemical Physics*, 136(15), 154102.
- Jönsson, B., Wennerström, H., Nilsson, P., & Linse, P. (1986). Self-diffusion of small molecules in colloidal systems. *Colloid and Polymer Science*, 264(1), 77-88.
- Kang, H., Zhang, Y., Yang, M., & Li, L. (2012). Molecular dynamics simulation on effect of nanoparticle aggregation on transport properties of a nanofluid. *Journal of Nanotechnology in Engineering and Medicine*, 3(2), 021001.
- Kang, H. U., Kim, S. H., & Oh, J. M. (2006). Estimation of thermal conductivity of nanofluid using experimental effective particle volume. *Experimental Heat Transfer*, 19(3), 181-191.
- Karthikeyan, N., Philip, J., & Raj, B. (2008). Effect of clustering on the thermal conductivity of nanofluids. *Materials Chemistry and Physics*, 109(1), 50-55.
- Kebllinski, P., & Cahill, D. G. (2005). Comment on "Model for Heat Conduction in Nanofluids". *Physical Review Letters*, 95(20), 209401.
- Kebllinski, P., Eastman, J. A., & Cahill, D. G. (2005). Nanofluids for thermal transport. *Materials Today*, 8(6), 36-44.

- Keblinski, P., Phillpot, S. R., Choi, S. U. S., & Eastman, J. A. (2002). Mechanisms of heat flow in suspensions of nano-sized particles (nanofluids). *International Journal of Heat and Mass Transfer*, 45(4), 855–863.
- Keblinski, P., Prasher, R., & Eapen, J. (2008). Thermal conductance of nanofluids: is the controversy over? *Journal of Nanoparticle Research*, 10(7), 1089-1097.
- Keblinski, P., & Thomin, J. (2006). Hydrodynamic field around a Brownian particle. *Physical Review E*, 73(1), 010502.
- Kim, S. H., Choi, S. R., & Kim, D. (2007). Thermal conductivity of metal-oxide nanofluids: particle size dependence and effect of laser irradiation. *Journal of Heat Transfer*, 129(3), 298-307.
- Kole, M., & Dey, T. (2010). Viscosity of alumina nanoparticles dispersed in car engine coolant. *Experimental Thermal and Fluid Science*, 34(6), 677-683.
- Kole, M., & Dey, T. (2013). Enhanced thermophysical properties of copper nanoparticles dispersed in gear oil. *Applied Thermal Engineering*, 56(1), 45–53.
- Koo, J., & Kleinstreuer, C. (2004). A new thermal conductivity model for nanofluids. *Journal of Nanoparticle Research*, 6(6), 577-588.
- Krishnamurthy, S., Bhattacharya, P., Phelan, P., & Prasher, R. (2006). Enhanced mass transport in nanofluids. *Nano Letters*, 6(3), 419–423.
- Kubo, R., Yokota, M., & Nakajima, S. (1957). Statistical-mechanical theory of irreversible processes. II. Response to thermal disturbance. *Journal of the Physical Society of Japan*, 12(11), 1203-1211.
- Kumar, D. H., Patel, H. E., Kumar, V. R. R., Sundararajan, T., Pradeep, T., & Das, S. K. (2004). Model for heat conduction in nanofluids. *Physical Review Letters*, 93(14), 144301.
- Kuppusamy, N. R., Mohammed, H., & Lim, C. (2014). Thermal and hydraulic characteristics of nanofluid in a triangular grooved microchannel heat sink (TGMCHS). *Applied Mathematics and Computation*, 246, 168-183.
- Lee, D., Kim, J. W., & Kim, B. G. (2006). A new parameter to control heat transport in nanofluids: surface charge state of the particle in suspension. *The Journal of Physical Chemistry B*, 110(9), 4323-4328.

- Lee, J. H., Lee, S. H., & Jang, S. P. (2014). Do temperature and nanoparticle size affect the thermal conductivity of alumina nanofluids? *Applied Physics Letters*, *104*(16), 161908.
- Lee, S., Choi, S. U. S., Li, S., and, & Eastman, J. A. (1999). Measuring thermal conductivity of fluids containing oxide nanoparticles. *Journal of Heat Transfer*, *121*(2), 280–289.
- Lee, S. W., Park, S. D., Kang, S., Bang, I. C., & Kim, J. H. (2011). Investigation of viscosity and thermal conductivity of SiC nanofluids for heat transfer applications. *International Journal of Heat and Mass Transfer*, *54*(1), 433-438.
- Lennard-Jones, J. E., & Devonshire, A. F. (1937). Critical phenomena in gases. I. *Proceedings of the Royal Society of London*, *163*, 53–70.
- Li, C. H., & Peterson, G. (2006). Experimental investigation of temperature and volume fraction variations on the effective thermal conductivity of nanoparticle suspensions (nanofluids). *Journal of Applied Physics*, *99*(8), 084314.
- Li, C. H., & Peterson, G. P. (2007a). The Effect of Particle Size on the Effective Thermal Conductivity of Al₂O₃-Water Nanofluids. *Journal of Applied Physics*, *101*(4), 044312.
- Li, C. H., & Peterson, G. P. (2007b). Mixing effect on the enhancement of the effective thermal conductivity of nanoparticle suspensions (nanofluids). *International Journal of Heat and Mass Transfer*, *50*(23), 4668-4677.
- Liao, J., Zhang, Y., Yu, W., Xu, L., Ge, C., Liu, J., & Gu, N. (2003). Linear aggregation of gold nanoparticles in ethanol. *Colloids and Surfaces A: Physicochemical and Engineering Aspects*, *223*(1), 177-183.
- Liu, M. S., Lin, M. C. C., Tsai, C. Y., & Wang, C. C. (2006). Enhancement of thermal conductivity with Cu for nanofluids using chemical reduction method. *International Journal of Heat and Mass Transfer*, *49*(17), 3028-3033.
- Lu, W. Q., & Fan, Q. M. (2008). Study for the particle's scale effect on some thermophysical properties of nanofluids by a simplified molecular dynamics method. *Engineering Analysis with Boundary Elements*, *32*(4), 282-289.
- Ma, H. B., Wilson, C., Borgmeyer, B., Park, K., Yu, Q., Choi, S. U. S., & Tirumala, M. (2006). Effect of nanofluid on the heat transport capability in an oscillating heat pipe. *Applied Physics Letters*, *88*(14), 143116.

- Mahbubul, I., Saidur, R., & Amalina, M. (2012). Latest developments on the viscosity of nanofluids. *International Journal of Heat and Mass Transfer*, 55(4), 874–885.
- Maruyama, S., & Kimura, T. (1999). A study on thermal resistance over a solid-liquid interface by the molecular dynamics method. *Thermal Science & Engineering*, 7(1), 63–68.
- Masuda, H., Ebata, A., Teramae, K., & Hishinuma, N. (1993). Alteration of thermal conductivity and viscosity of liquid by dispersing ultra-fine particles. *Netsu Bussei*, 7(2), 227–233.
- Mausbach, P., & May, H.-O. (2006). Static and dynamic anomalies in the Gaussian core model liquid. *Fluid Phase Equilibria*, 249(1), 17–23.
- Maxwell, J. (1954). *A Treatise on Electricity and Magnetism* (3rd ed.). New York, NY: Dover.
- McGaughey, A., & Kaviany, M. (2004). Thermal conductivity decomposition and analysis using molecular dynamics simulations. Part I. Lennard-Jones argon. *International Journal of Heat and Mass Transfer*, 47(8), 1783-1798.
- McQuarrie, D. A. (2000). *Statistical Mechanics* (2nd ed.). Sausalito, CA: University Science Books.
- Mehrali, M., Sadeghinezhad, E., Latibari, S. T., Mehrali, M., Togun, H., Zubir, M., . . . Metselaar, H. S. C. (2014). Preparation, characterization, viscosity, and thermal conductivity of nitrogen-doped graphene aqueous nanofluids. *Journal of Materials Science*, 49(20), 7156-7171.
- Mintsa, H. A., Roy, G., Nguyen, C. T., & Doucet, D. (2009). New temperature dependent thermal conductivity data for water-based nanofluids. *International Journal of Thermal Sciences*, 48(2), 363–371.
- Mohammed, H., Gunnasegaran, P., & Shuaib, N. (2011). The impact of various nanofluid types on triangular microchannels heat sink cooling performance. *International Communications in Heat and Mass Transfer*, 38(6), 767-773.
- Müller-Plathe, F. (1997). A simple nonequilibrium molecular dynamics method for calculating the thermal conductivity. *The Journal of Chemical Physics*, 106(14), 6082–6085.

- Murshed, S. M. S., Leong, K. C., & Yang, C. (2005). Enhanced thermal conductivity of TiO₂—water based nanofluids. *International Journal of Thermal Sciences*, 44(4), 367–373.
- Murshed, S. M. S., Leong, K. C., & Yang, C. (2008). Investigations of thermal conductivity and viscosity of nanofluids. *International Journal of Thermal Sciences*, 47(5), 560-568.
- Murshed, S. M. S., Leong, K. C., & Yang, C. (2009). A combined model for the effective thermal conductivity of nanofluids. *Applied Thermal Engineering*, 29(11), 2477–2483.
- Murshed, S. M. S., Santos, F. J. V., & Nieto de Castro, C. A. (2013). Rheology of nanofluids containing TiO₂ and SiO₂ nanoparticles. *Proc. 8th World Conference on Experimental Heat Transfer, Fluid Mechanics, and Thermodynamics*.
- Naghizadeh, J., & Rice, S. A. (1962). Kinetic theory of dense fluids. X. Measurement and interpretation of self-diffusion in liquid Ar, Kr, Xe, and CH₄. *The Journal of Chemical Physics*, 36(10), 2710-2720.
- Namburu, P. K., Kulkarni, D. P., Misra, D., & Das, D. K. (2007). Viscosity of copper oxide nanoparticles dispersed in ethylene glycol and water mixture. *Experimental Thermal and Fluid Science*, 32(2), 397–402.
- Nguyen, C. T., Desgranges, F., Galanis, N., Roy, G., Maré, T., Boucher, S., & Angue Mintsas, H. (2008). Viscosity data for Al₂O₃—water nanofluid—hysteresis: is heat transfer enhancement using nanofluids reliable? *International Journal of Thermal Sciences*, 47(2), 103–111.
- Nguyen, C. T., Desgranges, F., Roy, G., Galanis, N., Mare, T., Boucher, S., & Angue Mintsas, H. (2007). Temperature and particle-size dependent viscosity data for water-based nanofluids—Hysteresis phenomenon. *International Journal of Heat and Fluid Flow*, 28(6), 1492–1506.
- Nie, C., Marlow, W., & Hassan, Y. (2008). Discussion of proposed mechanisms of thermal conductivity enhancement in nanofluids. *International Journal of Heat and Mass Transfer*, 51(5), 1342-1348.
- Ozturk, S., Hassan, Y. A., & Ugaz, V. M. (2010). Interfacial complexation explains anomalous diffusion in nanofluids. *Nano Letters*, 10(2), 665–671.

- Pak, B. C., & Cho, Y. I. (1998). Hydrodynamic and heat transfer study of dispersed fluids with submicron metallic oxide particles. *Experimental Heat Transfer an International Journal*, 11(2), 151-170.
- Pang, C., Jung, J.-Y., & Kang, Y. T. (2014). Aggregation based model for heat conduction mechanism in nanofluids. *International Journal of Heat and Mass Transfer*, 72, 392-399.
- Pang, C., Lee, J. W., & Kang, Y. T. (2015). Enhanced thermal conductivity of nanofluids by nanoconvection and percolation network. *Heat and Mass Transfer*, 1-10.
- Pastoriza-Gallego, M. J., Casanova, C., Legido, J. L., & Piñeiro, M. M. (2011a). CuO in water nanofluid: influence of particle size and polydispersity on volumetric behaviour and viscosity. *Fluid Phase Equilibria*, 300(1), 188–196.
- Pastoriza-Gallego, M. J., Lugo, L., Legido, J. L., & Piñeiro, M. M. (2011b). Thermal conductivity and viscosity measurements of ethylene glycol-based Al₂O₃ nanofluids. *Nanoscale Research Letters*, 6(1), 1–11.
- Patel, H. E., Anoop, K., Sundararajan, T., & Das, S. K. (2006). A micro-convection model for thermal conductivity of nanofluids. *Pramana*, 65(5), 863-869.
- Patel, H. E., Das, S. K., Sundararajan, T., Sreekumaran Nair, A., George, B., & Pradeep, T. (2003). Thermal conductivities of naked and monolayer protected metal nanoparticle based nanofluids: Manifestation of anomalous enhancement and chemical effects. *Applied Physics Letters*, 83(14), 2931–2933.
- Patel, H. E., Sundararajan, T., & Das, S. K. (2008). A cell model approach for thermal conductivity of nanofluids. *Journal of Nanoparticle Research*, 10(1), 87–97.
- Peñas, J. R. V., de Zárata, J. M. O., & Khayet, M. (2008). Measurement of the thermal conductivity of nanofluids by the multicurrent hot-wire method. *Journal of Applied Physics*, 104(4), 044314.
- Philip, J., Shima, P., & Raj, B. (2007). Enhancement of thermal conductivity in magnetite based nanofluid due to chainlike structures. *Applied Physics Letters*, 91(20), 203108.
- Philip, J., Shima, P., & Raj, B. (2008). Evidence for enhanced thermal conduction through percolating structures in nanofluids. *Nanotechnology*, 19(30), 305706.

- Plimpton, S. (1995). Fast parallel algorithms for short-range molecular dynamics. *Journal of Computational Physics*, 117(1), 1-19.
- Prasher, R., Bhattacharya, P., & Phelan, P. E. (2005). Thermal conductivity of nanoscale colloidal solutions (nanofluids). *Physical Review Letters*, 94(2), 25901.
- Prasher, R., Bhattacharya, P., & Phelan, P. E. (2006a). Brownian-motion-based convective-conductive model for the effective thermal conductivity of nanofluids. *Journal of Heat Transfer*, 128(6), 588–595.
- Prasher, R., Evans, W., Meakin, P., Fish, J., Phelan, P., & Keblinski, P. (2006b). Effect of aggregation on thermal conduction in colloidal nanofluids. *Applied Physics Letters*, 89(14), 143119.
- Prasher, R., Phelan, P. E., & Bhattacharya, P. (2006c). Effect of aggregation kinetics on the thermal conductivity of nanoscale colloidal solutions (nanofluid). *Nano Letters*, 6(7), 1529–1534.
- Prasher, R., Song, D., Wang, J., & Phelan, P. (2006d). Measurements of nanofluid viscosity and its implications for thermal applications. *Applied Physics Letters*, 89(13), 133108.
- Putnam, S. A., Cahill, D. G., Braun, P. V., Ge, Z., & Shimmin, R. G. (2006). Thermal conductivity of nanoparticle suspensions. *Journal of Applied Physics*, 99(8), 084308.
- Ren, Y., Xie, H., & Cai, A. (2005). Effective thermal conductivity of nanofluids containing spherical nanoparticles. *Journal of Physics D: Applied Physics*, 38(21), 3958.
- Roberts, N. A., & Walker, D. (2010). Convective performance of nanofluids in commercial electronics cooling systems. *Applied Thermal Engineering*, 30(16), 2499-2504.
- Rudyak, V. Y. (2013). Viscosity of Nanofluids—Why It Is Not Described by the Classical Theories. *Advances in Nanoparticles*, 2(03), 266–279.
- Rudyak, V. Y., Belkin, A., & Egorov, V. (2009). On the effective viscosity of nanosuspensions. *Technical Physics*, 54(8), 1102-1109.

- Rudyak, V. Y., Dimov, S., Kuznetsov, V., & Bardakhanov, S. (2013). Measurement of the viscosity coefficient of an ethylene glycol-based nanofluid with silicon-dioxide particles. *Doklady Physics*, 58(5), 173-176.
- Rudyak, V. Y., & Krasnolutsii, S. (2014). Dependence of the viscosity of nanofluids on nanoparticle size and material. *Physics Letters A*, 378(26), 1845–1849.
- Saidur, R., Leong, K. Y., & Mohammad, H. A. (2011). A review on applications and challenges of nanofluids. *Renewable and Sustainable Energy Reviews*, 15(3), 1646–1668.
- Sankar, N., Mathew, N., & Sobhan, C. (2008). Molecular dynamics modeling of thermal conductivity enhancement in metal nanoparticle suspensions. *International Communications in Heat and Mass Transfer*, 35(7), 867-872.
- Sarkar, S., & Selvam, R. P. (2007). Molecular dynamics simulation of effective thermal conductivity and study of enhanced thermal transport mechanism in nanofluids. *Journal of Applied Physics*, 102(7), 074302.
- Sergis, A., & Hardalupas, Y. (2014). Molecular Dynamic Simulations of a Simplified Nanofluid. *Computational Methods in Science and Technology*, 20(4), 113–127.
- Shaikh, S., Lafdi, K., & Ponnappan, R. (2007). Thermal conductivity improvement in carbon nanoparticle doped PAO oil: An experimental study. *Journal of Applied Physics*, 101(6), 064302.
- Shalkevich, N., Shalkevich, A., & Bürgi, T. (2010). Thermal conductivity of concentrated colloids in different states. *The Journal of Physical Chemistry C*, 114(21), 9568-9572.
- Shima, P., Philip, J., & Raj, B. (2009). Role of microconvection induced by Brownian motion of nanoparticles in the enhanced thermal conductivity of stable nanofluids. *Applied Physics Letters*, 94(22), 223101.
- Shima, P., Philip, J., & Raj, B. (2010). Influence of aggregation on thermal conductivity in stable and unstable nanofluids. *Applied Physics Letters*, 97(15), 153113.
- Singh, D., Timofeeva, E., Yu, W., Routbort, J., France, D., Smith, D., & Lopez-Cepero, J. M. (2009). An investigation of silicon carbide-water nanofluid for heat transfer applications. *Journal of Applied Physics*, 105(6), 064306.

- Sundar, L. S., Ramana, E. V., Singh, M. K., & Sousa, A. C. (2014). Thermal conductivity and viscosity of stabilized ethylene glycol and water mixture Al_2O_3 nanofluids for heat transfer applications: An experimental study. *International Communications in Heat and Mass Transfer*, 56, 86-95.
- Tavman, I., Turgut, A., Chirtoc, M., Schuchmann, H., & Tavman, S. (2008). Experimental investigation of viscosity and thermal conductivity of suspensions containing nanosized ceramic particles. *Archives of Materials Science*, 34(2), 99–104.
- Taylor, R., Coulombe, S., Otanicar, T., Phelan, P., Gunawan, A., Lv, W., . . . Tyagi, H. (2013). Small particles, big impacts: a review of the diverse applications of nanofluids. *Journal of Applied Physics*, 113(1), 011301.
- Teng, T. P., Hung, Y. H., Teng, T. C., Mo, H. E., & Hsu, H. G. (2010). The effect of alumina/water nanofluid particle size on thermal conductivity. *Applied Thermal Engineering*, 30(14), 2213-2218.
- Timofeeva, E. V., Gavrilov, A. N., McCloskey, J. M., Tolmachev, Y. V., Sprunt, S., Lopatina, L. M., & Selinger, J. V. (2007). Thermal conductivity and particle agglomeration in alumina nanofluids: experiment and theory. *Physical Review E*, 76(6), 061203.
- Timofeeva, E. V., Routbort, J. L., & Singh, D. (2009). Particle shape effects on thermophysical properties of alumina nanofluids. *Journal of Applied Physics*, 106(1), 014304.
- Timofeeva, E. V., Smith, D. S., Yu, W., France, D. M., Singh, D., & Routbort, J. L. (2010). Particle size and interfacial effects on thermo-physical and heat transfer characteristics of water-based α -SiC nanofluids. *Nanotechnology*, 21(21), 215703.
- Timofeeva, E. V., Yu, W., France, D. M., Singh, D., & Routbort, J. L. (2011a). Base fluid and temperature effects on the heat transfer characteristics of SiC in ethylene glycol/ H_2O and H_2O nanofluids. *Journal of Applied Physics*, 109(1), 014914.
- Timofeeva, E. V., Yu, W., France, D. M., Singh, D., & Routbort, J. L. (2011b). Nanofluids for heat transfer: an engineering approach. *Nanoscale Research Letters*, 6(1), 1–7.

- Tsai, C., Chien, H., Ding, P., Chan, B., Luh, T., & Chen, P. (2004). Effect of structural character of gold nanoparticles in nanofluid on heat pipe thermal performance. *Materials Letters*, 58(9), 1461-1465.
- Turanov, A., & Tolmachev, Y. V. (2009). Heat-and mass-transport in aqueous silica nanofluids. *Heat and Mass Transfer*, 45(12), 1583-1588.
- Turgut, A., & Elbasan, E. (2014). Nanofluids for electronics cooling. *IEEE 20th International Symposium for Design and Technology of Electronics Packaging (SIITME)* 35-37, doi: 10.1109/SIITME.2014.6966989.
- Turgut, A., Tavman, I., Chirtoc, M., Schuchmann, H., Sauter, C., & Tavman, S. (2009). Thermal conductivity and viscosity measurements of water-based TiO₂ nanofluids. *International Journal of Thermophysics*, 30(4), 1213-1226.
- Venerus, D. C., Kabadi, M. S., Lee, S., & Perez-Luna, V. (2006). Study of thermal transport in nanoparticle suspensions using forced Rayleigh scattering. *Journal of Applied Physics*, 100(9), 094310.
- Vladkov, M., & Barrat, J.-L. (2006). Modeling transient absorption and thermal conductivity in a simple nanofluid. *Nano Letters*, 6(6), 1224-1228.
- Vladkov, M., & Barrat, J.-L. (2008). Modeling thermal conductivity and collective effects in a simple nanofluid. *Journal of Computational and Theoretical Nanoscience*, 5(2), 187-193.
- Vogelsang, R., Hoheisel, C., & Ciccotti, G. (1987). Thermal conductivity of the Lennard-Jones liquid by molecular dynamics calculations. *The Journal of Chemical Physics*, 86(11), 6371-6375.
- Wang, B. X., Zhou, L. P., & Peng, X. F. (2003). A fractal model for predicting the effective thermal conductivity of liquid with suspension of nanoparticles. *International Journal of Heat and Mass Transfer*, 46(14), 2665-2672.
- Wang, T., Wang, X., Luo, Z., & Cen, K. (2008). Physics behind the oscillation of pressure tensor autocorrelation function for nanocolloidal dispersions. *Journal of Nanoscience and Nanotechnology*, 8(8), 3990-3994.
- Wang, X., Xu, X., & Choi, S. U. S. (1999). Thermal conductivity of nanoparticle-fluid mixture. *Journal of Thermophysics and Heat Transfer*, 13(4), 474-480.

- Warrier, P., & Teja, A. (2011). Effect of particle size on the thermal conductivity of nanofluids containing metallic nanoparticles. *Nanoscale Research Letters*, 6(1), 1-6.
- Wen, D., & Ding, Y. (2004). Effective thermal conductivity of aqueous suspensions of carbon nanotubes (carbon nanotube nanofluids). *Journal of Thermophysics and Heat Transfer*, 18(4), 481-485.
- Wendt, H., & Abraham, F. F. (1978). Empirical criterion for the glass transition region based on Monte Carlo simulations. *Physical Review Letters*, 41(18), 1244–1246.
- Xie, H., Fujii, M., & Zhang, X. (2005). Effect of interfacial nanolayer on the effective thermal conductivity of nanoparticle-fluid mixture. *International Journal of Heat and Mass Transfer*, 48(14), 2926–2932.
- Xie, H., Lee, H., Youn, W., & Choi, M. (2003). Nanofluids containing multiwalled carbon nanotubes and their enhanced thermal conductivities. *Journal of Applied Physics*, 94(8), 4967-4971.
- Xie, H., Wang, J., Xi, T., Liu, Y., Ai, F., & Wu, Q. (2002). Thermal conductivity enhancement of suspensions containing nanosized alumina particles. *Journal of Applied Physics*, 91(7), 4568-4572.
- Xuan, Y., & Li, Q. (2000). Heat transfer enhancement of nanofluids. *International Journal of Heat and Fluid Flow*, 21(1), 58-64.
- Xuan, Y., Li, Q., & Hu, W. (2003). Aggregation structure and thermal conductivity of nanofluids. *AIChE Journal*, 49(4), 1038-1043.
- Xuan, Y., Li, Q., Zhang, X., & Fujii, M. (2006). Stochastic thermal transport of nanoparticle suspensions. *Journal of Applied Physics*, 100(4), 043507.
- Xue, L., Keblinski, P., Phillpot, S. R., Choi, S. U. S., & Eastman, J. A. (2003). Two regimes of thermal resistance at a liquid–solid interface. *The Journal of Chemical Physics*, 118, 337–339.
- Xue, Q. Z. (2003). Model for effective thermal conductivity of nanofluids. *Physics Letters A*, 307(5), 313-317.
- Yarnell, J., Katz, M., Wenzel, R. G., & Koenig, S. (1973). Structure factor and radial distribution function for liquid argon at 85 K. *Physical Review A*, 7(6), 2130.

- You, S., Kim, J., & Kim, K. (2003). Effect of nanoparticles on critical heat flux of water in pool boiling heat transfer. *Applied Physics Letters*, 83(16), 3374-3376.
- Yu, J., & Amar, J. G. (2002). Effects of short-range attraction in metal epitaxial growth. *Physical Review Letters*, 89(28), 286103.
- Yu, W., France, D. M., Routbort, J. L., & Choi, S. U. S. (2008). Review and comparison of nanofluid thermal conductivity and heat transfer enhancements. *Heat Transfer Engineering*, 29(5), 432-460.
- Zhang, X., Gu, H., & Fujii, M. (2006a). Effective thermal conductivity and thermal diffusivity of nanofluids containing spherical and cylindrical nanoparticles. *Journal of Applied Physics*, 100(4), 044325.
- Zhang, X., Gu, H., & Fujii, M. (2006b). Experimental study on the effective thermal conductivity and thermal diffusivity of nanofluids. *International Journal of Thermophysics*, 27(2), 569-580.
- Zhang, X., Gu, H., & Fujii, M. (2007). Effective thermal conductivity and thermal diffusivity of nanofluids containing spherical and cylindrical nanoparticles. *Experimental Thermal and Fluid Science*, 31(6), 593-599.
- Zhu, H., Zhang, C., Liu, S., Tang, Y., & Yin, Y. (2006). Effects of nanoparticle clustering and alignment on thermal conductivities of Fe₃O₄ aqueous nanofluids. *Applied Physics Letters*, 89(2), 23123.
- Zhu, H. T., Li, C. J., Wu, D. X., Zhang, C. Y., & Yin, Y. S. (2010). Preparation, characterization, viscosity and thermal conductivity of CaCO₃ aqueous nanofluids. *Science China Technological Sciences*, 53(2), 360-368.

LIST OF PUBLICATIONS AND PAPERS PRESENTED

- Lee, S. L., Saidur, R., Sabri, M. F. M., & Min, T. K. (2016). Molecular dynamic simulation: studying the effects of Brownian motion and induced micro-convection in nanofluids, *Numerical Heat Transfer, Part A: Application*, 69(6), 643-658. (ISI/SCOPUS Cited Publication – 1.975IF – Q1)
- Lee, S. L., Saidur, R., Sabri, M. F. M., & Min, T. K. (2015). Molecular dynamic simulation on the thermal conductivity of nanofluids in aggregated and non-aggregated states. *Numerical Heat Transfer, Part A: Applications*, 68(4), 432-453. (ISI/SCOPUS Cited Publication – 1.975IF – Q1)
- Lee, S. L., Saidur, R., Sabri, M. F. M., & Min, T. K. (2016). Effects of particle size and temperature on the efficiency of nanofluids using molecular dynamic simulation, *Numerical Heat Transfer, Part A: Applications*, 69(9), 996-1013. (ISI/SCOPUS Cited Publication – 1.975IF – Q1)

University of Malaysia